

SOME SPECTROSCOPIC STUDIES WITH CIRCULARLY POLARIZED LIGHT

MAGNETIC CIRCULAR DICHROISM  
OPTICAL ACTIVITY IN ABSORPTION AND EMISSION

H. P. J. M. DEKKERS

BIBLIOTHECA

GORLAEUS LABORATORIA DER R.U.

Wassenaarseweg 76

Postbus 75 - LEIDEN

## S T E L L I N G E N

### I

Het door Klingbiel en Eyring gebruikte model om de optische activiteit in de langgolvlige overgang van norbornanonon te beschrijven is daartoe minder geschikt.

R.T. Klingbiel en H. Eyring, 1970, J.Phys.Chem. 74, 4543

### II

De wijze waarop Rassing et al. de Langmuir adsorptietheorie toepassen op de kinetiek van micelvorming is aanvechtbaar.

J. Rassing, P.J. Sams en E. Wyn-Jones, 1974, J.C.S.Faraday II 70, 1247

### III

De interpretatie die Courtot en Rumin geven van het verschil in product-samenstelling als 2,6-dimethylhepta-1,(Z)3,5-trieen bestraald wordt met 254 nm-licht en met licht waarvan de golflengte groter is dan 280 nm, is aan bedenkingen onderhevig.

P. Courtot en R. Rumin, 1974, J.C.S.Chem.Comm., 168

### IV

Bij de simulatie van een experimenteel spectrum door een som van overlappende banden wordt de fysische relevantie in het bijzonder van zwakke banden niet zozeer bepaald door de kwaliteit van de overeenkomst tussen experimenteel en gesimuleerd spectrum als wel door de juistheid van de aangenomen bandvormen.

B. Klabuhn, D. Spindler en H. Goetz, 1973, Spectrochimica Acta 29A, 1283

### V

De door Weigang voorspelde tweede-orde effecten in de optische activiteit van ketonen zullen het best aangetoond kunnen worden in ketonen die  $C_2$ -symmetrie hebben, rigide zijn en een kleine statische rotatiesterkte bezitten.

O.E. Weigang, Jr, 1965, J.Chem.Phys., 42, 2244; 43, 3609

Dit proefschrift, hoofdstuk V

## VI

Op grond van het door Martin et al. voorgestelde mechanisme is het te verwachten dat de zuurgekatalyseerde reactie van optisch zuiver 1-hydroxymethyl[6]heliceen zal leiden tot optisch zuiver 5-H-benzo[c,d]pyreen-5-spiro-1'-indeen.

R.H. Martin, J. Jespers en N. Defay, 1975, Tetrahedron Letters, 1093

## VII

Het overzichtsartikel van Liptay wordt ernstig ontsierd door niet gedocumenteerde kritiek op werk van anderen.

W. Liptay in E.C. Lim, Excited States I  
(Academic Press, New York, 1974) p.206

## VIII

In het artikel van Gillard en Mitchell is de "Conclusion" helaas een rijke bron van goed verdedigbare stellingen.

R.D. Gillard en P.R. Mitchell, 1969, Trans.Farad.Soc. 65, 2611

H.P.J.M. Dekkers

Leiden, 4 juni 1975

SOME SOME SPECTROSCOPIC STUDIES WITH CIRCULARLY POLARIZED LIGHT LIGHT

MAGNETIC CIRCULAR DICHROISM  
OPTICAL ACTIVITY IN ABSORPTION AND EMISSION  
OPTICAL ACTIVITY IN ABSORPTION AND EMISSION

PROEFDEELT

DE VERHAALING VAN DE GRAD VAN DOCTOR  
IN DE WISSENSCHAP EN NATUURKUNDE  
VAN DE RIJKSUNIVERSITEIT TE LEIDEN,  
DE GRAD VAN DE SECTOR WISSENSCHAPEN EN A.B. LEIDEN,  
BETREFFENDE DE FACULTEIT DER LETTEREN,  
VULGENS BESLUIT VAN HET COLLEGE VAN GEWONEN  
TE VERDIENEN OP WOENSDAG 6 JUNI 1972  
TE RIJCKE 14.15 UUR

door

RECHTEREN PETER  
JOSEPHUS MARIA DEWINDT

gelezen te Hilburg in 1940

Kalpa Inge 21 - Pappel

THEORY OF CIRCULARLY POLARIZED LIGHT

in the case of uniaxial crystals. It is assumed that the wave vector is parallel to the optical axis.

The wave vector is assumed to be parallel to the optical axis. The wave vector is assumed to be parallel to the optical axis. The wave vector is assumed to be parallel to the optical axis.

R. E. HARRIS, J. JACOB, and S. HOFFER, 1973, *Tetrahedron Letters*, 14, 1001.

VII

The wave vector is assumed to be parallel to the optical axis. The wave vector is assumed to be parallel to the optical axis. The wave vector is assumed to be parallel to the optical axis.

W. HOFFER in *S. S. Liu, United States I*  
Gordon and Breach, New York, 1973, p. 201.

VIII

The wave vector is assumed to be parallel to the optical axis. The wave vector is assumed to be parallel to the optical axis. The wave vector is assumed to be parallel to the optical axis.

R. E. HARRIS and R. E. MITCHELL, 1969, *Trans. Faraday Soc.*, 65, 1011.

R. E. HARRIS

London, 4 July 1973

# SOME SPECTROSCOPIC STUDIES WITH CIRCULARLY POLARIZED LIGHT

MAGNETIC CIRCULAR DICHROISM  
OPTICAL ACTIVITY IN ABSORPTION AND EMISSION

PROEFSCHRIFT

TER VERKRIJGING VAN DE GRAAD VAN DOCTOR  
IN DE WISKUNDE EN NATUURWETENSCHAPPEN  
AAN DE RIJKSUNIVERSITEIT TE LEIDEN,  
OP GEZAG VAN DE RECTOR MAGNIFICUS DR. A.E. COHEN,  
HOGLERAAR IN DE FACULTEIT DER LETTEREN,  
VOLGENS BESLUIT VAN HET COLLEGE VAN DEKANEN  
TE VERDEDIGEN OP WOENSDAG 4 JUNI 1975  
TE KLOKKE 14.15 UUR

door

HENRICUS PETRUS  
JOSEPHUS MARIA DEKKERS

geboren te Tilburg in 1940

Krips Repro BV - Meppel

SOME SPECTROSCOPIC STUDIES WITH CIRCULARLY POLARIZED LIGHT

MAGNETIC CIRCULAR DICHROISM  
OPTICAL ACTIVITY IN ABSORPTION AND EMISSION

PROMOTOR: PROF. DR. J.H. VAN DER WAALS

Het onderzoek werd uitgevoerd onder leiding van PROF. DR. L.J. OOSTERHOFF<sup>†</sup>

PROEFSCHRIFT

VOOR DE VERLENING VAN DE GRADE VAN DOCTOR  
IN DE WISSENSCHAPPEN VAN NATHUURKUNDE  
AAN DE RIJKSUNIVERSITEIT TE LEIDEN  
OP GAARDEN VAN DE RECTOR-MAGISTRUS DR. A.E. OUDER  
DOOR DE HEER J.H. VAN DER WAALS  
WEGENS BEZIT VAN HET COLLEGE VAN DE RECTOR  
TE LEIDEN OP WOENSDAG 4 JUNI 1912  
TE RIJKE 14.12.12

1912

WILHELMUS FRANK  
JONKVROU MARIA HEEREN

Gezeten te Tilburg in 1912

Erste druk bij de uitgeverij



33	Further discussion of transition	55
34	The O-C transition	58
35	Origin dependence	61
36	The O-H band of acetone	62
37	Introduction	63
38	Vibronic coupling	63
39	Introduction	63
40	The role of non-totally symmetric vibrations	63
41	2-Formyl	63
42	Vibronic coupling via totally symmetric modes	64
43	In the presence of an acceptor	64
44	Energy levels of the acceptor	64
45	2-Formyl	64
46	Introduction	64
47	Formal theory	64
48	2-Formyl	64
49	Electronic absorption bands	64
50	Concluding remarks	64
51	Introduction	64
52	Introduction	64
53	Relatively low energy bands	64
54	Assignment and emission spectra of 2-Formyl	64
55	Assignment and IR spectra of 2-Formyl and related compounds	64
56	Analysis of the spectra	64
57	Calculations	64
58	Low-symmetry modes	64
59	Calculations	64
60	Conclusions	64
61	Conclusions	64
62	Dipole strengths	64
63	Magnetic moments	64
64	Comparison of theory and experiment	64
65	Conclusions	64
66	Conclusions	64
67	Conclusions	64
68	Conclusions	64
69	Conclusions	64
70	Conclusions	64
71	Conclusions	64
72	Conclusions	64
73	Conclusions	64
74	Conclusions	64
75	Conclusions	64
76	Conclusions	64
77	Conclusions	64
78	Conclusions	64
79	Conclusions	64
80	Conclusions	64
81	Conclusions	64
82	Conclusions	64
83	Conclusions	64
84	Conclusions	64
85	Conclusions	64
86	Conclusions	64
87	Conclusions	64
88	Conclusions	64
89	Conclusions	64
90	Conclusions	64
91	Conclusions	64
92	Conclusions	64
93	Conclusions	64
94	Conclusions	64
95	Conclusions	64
96	Conclusions	64
97	Conclusions	64
98	Conclusions	64
99	Conclusions	64
100	Conclusions	64

Aan mijn ouders  
Voor Anneke

## CONTENTS

INTRODUCTION	9
CHAPTER I    MAGNETIC CIRCULAR DICHROISM	
1. Introduction	10
2. A-terms	11
2a The Zeeman effect in an atom	11
2b A-terms in molecules	12
3. B-terms	14
4. Pseudo A-terms	17
5. Formel theory	20
5a General	20
5b Electronic absorption bands	21
6. Concluding remarks	22
CHAPTER II    MCD OF THE TRIPHENYLCARBENIUM ION AND SOME SYMMETRICALLY PARASUBSTITUTED DERIVATIVES	
1. Introduction	23
2. Absorption and emission spectra of $\phi_3C^+$	24
3. Absorption and MCD spectra of $\phi_3C^+$ and related compounds	26
Analysis of the spectra	26
4. Calculations	34
Wavefunctions	34
Configuration interaction	37
Dipole strengths	39
Magnetic moments	40
5. Comparison of theory and experiment	41
6. The sign of $(E_S   H   E_A)$	42
7. Discussion	45
CHAPTER III    MAGNETIC CIRCULAR DICHROISM OF AZULENE	
1. Introduction	49
2. MO calculations	51
3. The MCD in the O→A and O→C transitions	53
3a The O→A transition	53
3b Numerical calculations	55

3c	Further discussion of equation (4)	56
3d	The O→C transition	59
3e	Origin dependence	61
4	The O→B band of azulene	62
4a	Introduction	62
4b	Vibronic coupling	63
4c	The role of non-totally symmetric vibrations	65
4d	Vibronic coupling via totally symmetric modes	66
4e	Lacey's interpretation of the azulene O→B spectrum	72

CHAPTER IV MCD OF THE TRANSITION TO THE  $^3_{n\pi^*}$ -STATE IN THIOKETONES

1	Introduction	76
2	Optical activity	77
3	MCD in singlet-triplet transitions	79
4	Discussion	85
5	Conclusion	87

CHAPTER V THE OPTICAL ACTIVITY OF LOW-SYMMETRY KETONES

1	Introduction	88
2	Relationship between rotational strength and structure	92
3	Circular Polarization of Luminescence	95
3a	General	95
3b	Hydrindanone	96
3c	Low-symmetry ketones	99
4	Optical activity of ketones in absorption	104
4a	Theory of Moffitt and Moscovitz	104
4b	Theory of Weigang	108
5	Band shapes of CD and CPL	110
5a	General	110
5b	The rotational strength in vibronic transitions	114
5c	Band shapes of CD and CPL	116
5d	Discussion	119
6	Conclusion	121

APPENDIX APPARATUS

SUMMARY		124
SAMENVATTING		128
		130

36	Further discussion of equation (2)	1
37	The O-D transition	1
38	Origin dependence	1
39	The O-B band of acetone	1
40	Introduction	1
41	Vibronic coupling	1
42	The role of non-totally symmetric vibrations	1
43	Vibronic coupling via totally symmetric modes	1
44	Role of the totally symmetric modes	1
45	Lacey's investigation of the acetone O-D spectrum	1
46	Conclusion	1
47	CHAPTER IV THE O-D BAND OF THE TRANSITION TO THE $v_2$ -STATE IN DIMETHYL	1
48	Introduction	1
49	Optical activity	1
50	MD in single-vibron transitions	1
51	Discussion	1
52	Conclusion	1
53	CHAPTER V THE OPTICAL ACTIVITY OF LOW-FREQUENCY VIBRATIONS	1
54	Introduction	1
55	Relationship between vibrational strength and activity	1
56	Circular dichroism of amide I	1
57	General	1
58	Optical activity of amides in absorption	1
59	Theory of Heller and Herzberg	1
60	Theory of helicity	1
61	Good shape of CD and CPL	1
62	The rotational strength in vibrational transitions	1
63	Good shape of CD and CPL	1
64	Discussion	1
65	Conclusion	1
66	APPENDIX A	1
67	APPENDIX B	1
68	APPENDIX C	1
69	APPENDIX D	1
70	APPENDIX E	1

The excellent reviews of Buckingham and Stephens<sup>11</sup> and of Tatarski and McCallum<sup>12</sup>.

## 1. INTRODUCTION

The Zeeman effect is an effect

For a start we consider the Zeeman effect of a  $^1S_0$  transition in an atom. In the absence of a magnetic field the  $^1S_0$  state is threefold degenerate and it is immaterial whether we describe the state by the wave functions  $(\psi_x, \psi_y, \psi_z)$  or by the set  $(\psi_0, \psi_{\pm 1})$ . Upon the application of a magnetic field in the z-direction the degeneracy is removed and the latter set of eigenfunctions of the Hamiltonian (1)

### INTRODUCTION

Molecules that are chiral, i.e. are not superimposable on their mirror-images, absorb right- and left-handed circularly polarized light differently: they exhibit circular dichroism (CD). The same phenomenon may be observed with all molecules when they are influenced by a magnetic field parallel to the light beam: magnetic circular dichroism (MCD). Whereas the different responses to left and right circularly polarized light with chiral molecules originate in molecular architecture, a non-vanishing MCD is imposed by an external field. Therefore both phenomena, although closely related from a measuring point of view, yield quite different molecular information.

This thesis deals with both effects. The part pertaining to MCD (Chapters I-IV) is organized as follows. After a qualitative discussion on some general aspects of MCD spectroscopy (Chapter I), the MCD spectra of some specific organic molecules are presented and discussed in Chapters II-IV.

Chapter V of this thesis is concerned with the natural optical activity of ketones in absorption and emission. In the Appendix a short description is given of the apparatus which was constructed to measure the circular anisotropies.

The work described in this thesis has been carried out under the guidance of Professor L.J.Oosterhoff as a continuation of a series of impressive studies on optical activity accomplished in his Department. His premature death prevented him to see its completion. I here want to express my gratitude for having had the privilege to cooperate with him.

## CHAPTER I

### MAGNETIC CIRCULAR DICHROISM

#### 1. Introduction

Magnetic circular dichroism (MCD) is a form of spectroscopy in which one measures the difference in absorption of left and right circularly polarized light which arises when a sample is placed in a magnetic field that is parallel to the direction of propagation of the light beam. In the customary terminology of MCD spectroscopy one distinguishes three "terms" which, as we shall see, are characterized by differences in behaviour of the signal as a function of wave length or temperature.

A magnetic field can influence the light absorption of a molecular system in three different ways. Firstly, the magnetic field can change the energy of the initial and (or) final state of the transition. This effect gives rise to the so-called A-terms in the MCD, which can only arise if the lower and (or) upper state possess a permanent magnetic dipole moment. Secondly, the magnetic field affects the wave functions of the system, thereby changing the probability for the light absorption to occur. From this effect MCD B-terms originate. Lastly, if the external magnetic field can affect the population of the initial state, temperature dependent C-terms occur in the MCD.

In this chapter we shall discuss in a qualitative way A- and B-type MCD (we shall not be concerned with C-terms since the compounds we have studied did not exhibit temperature dependent MCD). For a more extensive treatment of the theory of magnetic optical activity and its applications we refer to

the excellent reviews of Buckingham and Stephens<sup>1)</sup> and of Schatz and McCaffery<sup>2)</sup>.

## 2. A-terms

### 2a. The Zeeman effect in an atom

For a start we consider the Zeeman effect of a  $^1S \rightarrow ^1P$  transition in an atom. In the absence of a magnetic field the  $^1P$ -state is threefold degenerate and it is immaterial whether we describe the state by the wave functions  $(p_x, p_y, p_z)$  or by the set  $(p_1 = \frac{p_x + ip_y}{\sqrt{2}}; p_0 = p_z; p_{-1} = \frac{p_x - ip_y}{\sqrt{2}})$ . Upon the application of a magnetic field in the z-direction the degeneracy is removed and the latter set of functions are the eigen functions of the Hamiltonian (1).

$$H = H^0 - \mu_z H_z = H^0 + \frac{\beta}{\hbar} (L_z + 2S_z) H_z \quad (1)$$

Here  $H^0$  is the Hamiltonian in the absence of the field and  $\mu_z$  is the magnetic dipole moment operator;  $L_z$  is the orbital and  $S_z$  the spin angular momentum and  $\beta$  is Bohr's magneton  $(\frac{e\hbar}{2mc})$ . Throughout this chapter we shall, considering only singlet-singlet transitions, neglect the contribution of spin to the magnetic moment. The energies of the three states  $p_m$  ( $m = +1, 0, -1$ ) are then given by

$$(p_m | H | p_m) = E_0 + \frac{\beta}{\hbar} H_z (p_m | L_z | p_m) = E_0 + \beta H_z M_z \quad (2)$$

where  $M_z = +1, 0, -1$  for  $m = +1, 0, -1$  respectively (See figure 1).

In the electric dipole approximation the probability  $W$  for the transition  $s \rightarrow p_m$  to occur is equal to

$$\left| (s | \vec{r} | p_m) \cdot \vec{e}_A \right|^2 \quad (3)$$

where  $\vec{r}$  is the electric dipole moment operator and  $\vec{e}_A$  the direction of the vector potential of the excitation light. Since the functions  $p_{+1}$  and  $p_{-1}$  transform like  $x+iy$  and  $x-iy$  and the unit vector  $\vec{e}_A$  is  $\frac{1}{\sqrt{2}}(\vec{i} + i\vec{j})$  and  $\frac{1}{\sqrt{2}}(\vec{i} - i\vec{j})$  for right and left circularly polarized light propagating in the z-direction, it follows from (3) that the transitions  $s \rightarrow p_{+1}$  and  $s \rightarrow p_{-1}$  are left- and right-circularly polarized, respectively. The transition  $s \rightarrow p_0$  is forbidden if the propagation direction of the light coincides with that of the magnetic field. It is clear that from the spectrum in R-light and that in

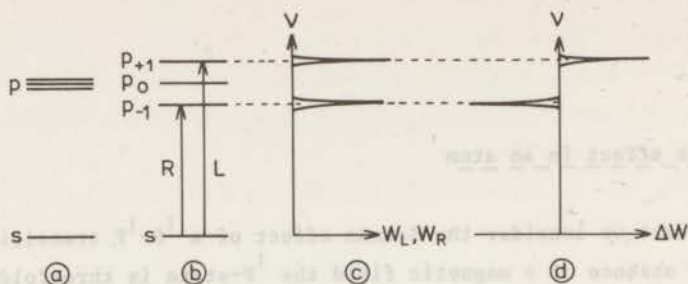


Figure 1. (a) Energy of an atomic p-state in the absence of a magnetic field.

(b) Splitting when a magnetic field  $H_z$  is applied. The symbols R and L mark the polarization of the transitions.

(c) Zeeman spectra.

(d) MCD spectrum.

L-light (cf. figure 1) the magnitude of the Zeeman splitting can be read off directly.

When measuring the magnetic circular dichroism  $\Delta W$ , i.e. the transition probability in L-light minus that in R-light ( $W_L - W_R$ ), we obtain a spectrum as shown in figure 1. It is obvious that for obtaining the magnetic splitting, MCD and Zeeman experiment are equivalent. Note, however, that all the information from a Zeeman experiment cannot be gained from a MCD measurement alone: one also needs the average transition probability  $\frac{1}{2}(W_L + W_R)$  in the magnetic field in order to obtain  $W_L$  and  $W_R$  separately. Later on it will be shown that MCD- and Zeeman spectra no longer yield the same information if the band width of the transitions is large in comparison with the Zeeman energy.

## 2b. A-terms in molecules

With the exception of diatomic molecules, where the component of  $\vec{L}$  along the molecular axis commutes with the Hamiltonian, the expectation value of the orbital angular momentum operator in molecules no longer is a good quantum number and its value in a particular state  $\Psi$  may be non-integral<sup>3)</sup>.



$$\langle \Psi | L_z | \Psi \rangle = M_z \quad (4)$$

In (4)  $L_z$  denotes one of the components of  $\vec{L}$ . However, for a non-degenerate state, which can always be described by a real wave function  $\Psi$ ,  $M_z$  is zero since the expectation value of the imaginary operator  $L_z$  vanishes unless  $\Psi$  is essentially complex. Therefore the occurrence of orbital magnetic moment in polyatomic molecules is restricted to those molecules which belong to point groups with degenerate representations, i.e. to molecules having an  $n$ -fold rotation axis  $C_n^z$ , where  $n \geq 3$ .

Consider now in such a molecule an electric dipole allowed transition between the non-degenerate ground state 0 and a doubly degenerate excited state E which we assume to carry a magnetic moment. When applying a magnetic field along the symmetry axis of the molecule ( $z$ -axis), we encounter a situation which in many respects is analogous to that described in §2a: The E state splits (cf. figure 2) and of the two states, which are described by wave functions which are conjugate to each other, one state is accessible only by L-light, the other one by R-light. If the Zeeman splitting  $|2\beta H M_z|$  is much smaller than the band width  $\Gamma$  of the transitions, both Zeeman components

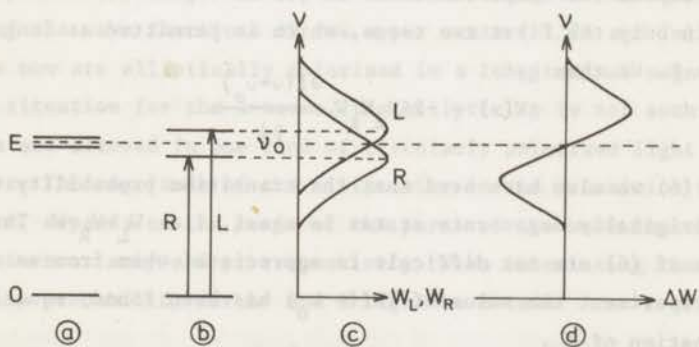


Figure 2. Energy scheme without (a) and with (b) a magnetic field  $H_z$ .

In (c) are plotted the Zeeman spectra and in (d) is given

the MCD. Note that the scale factors for  $W$  and  $\Delta W$  in

(c) and (d) of course are different.

overlap severely and a reliable value of the Zeeman shift cannot be obtained from the separation of the  $W_L$  and  $W_R$  curves. This situation by no means is exceptional: for large organic molecules in solution one may have band widths up to  $5000 \text{ cm}^{-1}$ , say, whereas Zeeman splittings are in the order  $1-10 \text{ cm}^{-1}$ . Since with the MCD apparatus presently available one can detect  $\frac{\Delta W}{W}$  values of  $10^{-5}$ , it is conceivable that MCD is superior to Zeeman spectroscopy for measuring shifts which are much smaller than  $\Gamma$ .

We now shall calculate the MCD, assuming that the lowest Zeeman level is accessible with R-light. (This is the normal situation with molecules approaching axial symmetry. In Chapter II we shall discuss an exception.) The spectral broadening is taken into account by introducing a normalized shape function  $f(\nu-\nu_j)$  which describes both the shape of the original absorption in zero field and that of the Zeeman transitions ( $\nu_j$  denotes the central frequency of the transition). This implies that the magnetic field does not change the form of the band, only its position on the frequency scale (rigid shift approximation). The function  $f(\nu-\nu_j)$  mostly is taken to be Gaussian or Lorentzian<sup>2)</sup>. The MCD as a function of frequency is then given by (compare figure 2)

$$\Delta W(\nu) = W_L f \left[ \nu - (\nu_0 + \beta H_z M_z) \right] - W_R f \left[ \nu - (\nu_0 - \beta H_z M_z) \right] \quad (5)$$

We now expand the shape functions in (5) as Taylor series in the point  $\nu_0$  and retain only the first two terms, which is permitted as long as  $|\beta H_z M_z| \ll \Gamma$ . We then get

$$\Delta W(\nu) = -2\beta H_z M_z W \frac{\partial f(\nu-\nu_0)}{\partial \nu} \quad (6)$$

In deriving (6) we also have used that the transition probability to either one of the originally degenerate states is equal, i.e.  $W_L = W_R = W$ . The implications of (6) are not difficult to appreciate: when from an unpolarized absorption experiment the value of  $2Wf(\nu-\nu_0)$  has been found, equation 6 allows the determination of  $M_z$ .

### 3. B-terms

As mentioned in §1 circular dichroism not only results from the effect of the magnetic field on the energies (A-terms) but also from the influence on the transition probabilities. The latter effect, which gives rise to the so-called B-type MCD, can be demonstrated as follows. We consider a molecule

with states  $|o\rangle$ ,  $|x\rangle$  and  $|y\rangle$ , where  $|o\rangle$  is the totally symmetric ground state and  $|x\rangle$  and  $|y\rangle$  denote non-degenerate excited states which transform as  $x$  and  $y$  in the molecular point group. Whereas  $|o\rangle$ ,  $|x\rangle$  and  $|y\rangle$  are correct eigen functions in the absence of a magnetic field, they are not when  $H_z \neq 0$ , since they do not form a basis which diagonalizes the Hamiltonian (1). We can improve them by first order perturbation theory

$$|o'\rangle = |o\rangle \quad (7a)$$

$$|x'\rangle = |x\rangle + \frac{\beta H_z}{\hbar} \frac{(y|L_z|x)}{E_x - E_y} |y\rangle = |x\rangle + i\lambda |y\rangle \quad (7b)$$

$$|y'\rangle = |y\rangle + \frac{\beta H_z}{\hbar} \frac{(x|L_z|y)}{E_y - E_x} |x\rangle = |y\rangle + i\lambda |x\rangle \quad (7c)$$

where we have assumed that the magnetic field does not affect the wave function for the ground state. The RHS of (7b) and (7c) obtain since the wave functions  $|x\rangle$  and  $|y\rangle$  are real and the operator  $L_z$  is imaginary. When  $E_x - E_y = \Delta E$  is large as compared to the magnetic interaction terms, perturbation theory applies and the energies of the transitions  $o \rightarrow x$  and  $o \rightarrow y$  are not affected by the magnetic field in first order. In the absence of the field both transitions are linearly polarized (the molecule is considered not to be optically active) in the  $x$  and  $y$  directions. Owing to the complex character of the wave functions of the upper state (cf. 7b and 7c) the transitions now are elliptically polarized in a longitudinal magnetic field. Unlike the situation for the A-terms, the ellipticity is not such that the transitions are allowed in one kind of circularly polarized light and forbidden in the other. The magnitude of the ellipticity in the transition to  $|y'\rangle$  for instance, depends on the ratio of the parts of the wave function  $|y'\rangle$  which transform as  $x-iy$  and  $y$ , respectively. When calculating the difference in transition probability for L- and R-light we obtain

$$\Delta W(o \rightarrow y') = \left| (o|\vec{r}|y') \cdot \left( \frac{\hat{i}-i\hat{j}}{\sqrt{2}} \right) \right|^2 - \left| (o|\vec{r}|y') \cdot \left( \frac{\hat{i}+i\hat{j}}{\sqrt{2}} \right) \right|^2 \quad (8a)$$

$$= -2\lambda (o|x|x)(y|y|o)$$

and

$$\Delta W(o \rightarrow x') = -\Delta W(o \rightarrow y') \quad (8b)$$

The MCD as a function of frequency is given by  $\Delta W(o \rightarrow y') f(\nu - \nu_y)$  and

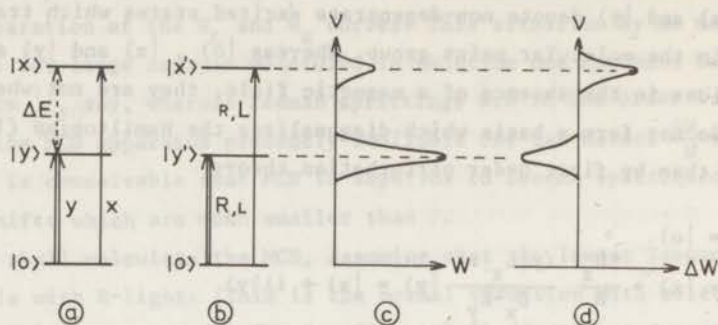


Figure 3. States and polarization characteristics of the transition without (a) and with (b) a magnetic field  $H_z$ . In (c) the unpolarized absorption  $W = \frac{1}{2}(W_L + W_R)$  is shown and in (d) the MCD.

$\Delta W(0 \rightarrow x')$   $f(\nu - \nu_x)$  for the transitions  $0 \rightarrow y'$  and  $0 \rightarrow x'$ , respectively. The shape functions of the MCD are taken equal to those of the unpolarized absorption, but  $f(\nu - \nu_y)$  and  $f(\nu - \nu_x)$  may have different forms. These data have been used in constructing figure 3. From (8) one notes that the MCD is larger, the larger the matrix element  $\langle x | L_z | y \rangle$  and the smaller the energy separation of the excited states. We note that  $\Delta W$  depends linearly on the transition moments  $\langle 0 | x | x \rangle$  and  $\langle 0 | y | y \rangle$ , which offers the interesting possibility to find from the MCD the relative signs of these moments. Another consequence of (8) may be visualized when we assume that  $|\langle 0 | x | x \rangle| \ll |\langle 0 | y | y \rangle|$ . Then the unpolarized absorption in the transition to  $|x\rangle$  will be much smaller than that in  $0 \rightarrow y'$ . The absolute magnitude of the MCD, however, is equal in both bands. Therefore one can expect the study of MCD to be particularly useful in the tracing of weak absorption bands nearby strong (and perpendicularly polarized) ones. In various ways this, indeed, is one of the most spectacular applications of the study of B-terms.

#### 4. Pseudo A-terms

So far we have discussed the circular dichroism induced by the magnetic field in a pair of degenerate transitions and in two transitions which are far apart on the frequency scale. Now we shall consider an intermediate situation.

Suppose the energy separation  $\Delta E$  in the two-level system of the preceding paragraph (cf. figure 3) is small as compared with the band width  $\Gamma$  of the transitions, but still large in comparison with  $\beta H(y|L_z|x)$ . Since the latter condition ensures that the effect of  $H_z$  on the transition energies again may be neglected, the MCD is given by (8). The general appearance of the MCD spectrum however, will be quite different from that in figure 3 since both transitions now overlap strongly and the MCD one observes is the sum of two contributions.

$$\begin{aligned} \Delta W(\nu) &= \Delta W(o \rightarrow y') f(\nu - \nu_y) + \Delta W(o \rightarrow x') f(\nu - \nu_x) \\ &= -2\lambda (o|x|x)(y|y|o)(E_x - E_y) \frac{\partial f(\nu, \nu_o)}{\partial \nu} \end{aligned} \quad (9)$$

In obtaining (9) we have again expanded both shape functions, which we take to be identical, as a power series (of which we have kept only the first two terms) in the point  $\frac{1}{2h}(E_x + E_y)$ . We have also used that  $\Delta W(o \rightarrow y') = -\Delta W(o \rightarrow x')$ . Inserting in (9) the value of  $\lambda$  (cf. (7)) we obtain

$$\Delta W(\nu) = \frac{-2i\beta H_z}{h} (x|L_z|y)(o|x|x)(y|y|o) \frac{\partial f(\nu, \nu_o)}{\partial \nu} \quad (10)$$

and it follows that the frequency dependence of the MCD as given by (10) is identical to that of a genuine A-term. Since, however, the MCD in (10) does not arise from the Zeeman splitting of a degenerate state, we might call it a pseudo A-term. In the derivation of (10) we have not assumed any relation between the wave functions  $|x\rangle$  and  $|y\rangle$ . It is true,  $|x\rangle$  transforms as  $x$  and  $|y\rangle$  as  $y$  in the point group of the molecule, but the functional forms of  $|x\rangle$  and  $|y\rangle$  may be quite different.

It is physically illuminating to consider the MCD in a transition to a doubly degenerate state  $E$  that is split in zero field by an (unspecified) interaction. Without the zero field splitting (and in the absence of a magnetic field)  $E$  may be represented by the state vectors  $|x\rangle$  and  $|y\rangle$  and one has  $|(o|x|x)|^2 = |(o|y|y)|^2$  since the two states are indistinguishable. We here

assume  $\langle 0|x|x\rangle = +\langle 0|y|y\rangle$ . The angular momentum in the state which becomes lowest in energy on applying a magnetic field  $H_z$  is

$$\left( \frac{x-iy}{\sqrt{2}} \middle| L_z \middle| \frac{x-iy}{\sqrt{2}} \right) = -i \langle x|L_z|y\rangle = M_z \hbar \quad (11)$$

Upon the introduction of the zero field interaction, two new states emerge at energies  $E_x$  and  $E_y$  ( $E_x > E_y$ ), which we assume to be described by the original wave functions  $|x\rangle$  and  $|y\rangle$ . If the zero field splitting  $E_x - E_y = \Delta E$  is large as compared to the magnetic interaction, but still small in comparison with the band width, the MCD is given by (10), which for this situation may be rewritten as

$$\Delta W(\nu) = -2\beta H_z M_z W \frac{\partial f(\nu - \nu_0)}{\partial \nu} \quad (12)$$

where  $W = |\langle 0|x|x\rangle|^2 = |\langle 0|y|y\rangle|^2$ . The pseudo A-term (12) is completely identical to the genuine A-term (6). Unlike in (6), where  $M_z$  denotes the orbital angular momentum in the degenerate upper state,  $M_z$  in (12) of course refers to an off-diagonal matrix element of  $L_z$ . Both values are equal however. This implies that via an MCD experiment one may detect excited state magnetic moments, as if there were no zero field splittings present. A rather trivial corollary of the above result is, of course, that the MCD technique is not particularly suited to detect zero field splittings. This job much better can be done by using Zeeman experiments, as we shall now demonstrate.

We compare the Zeeman spectra of the degenerate system of §2b and the near-degenerate case just discussed. Since with exact degeneracy a Zeeman level only can be populated by irradiation with either left or right circularly polarized light, the Zeeman spectra in L- and R-light will be identical, except for a shift in frequency. Moreover, their shape will be equal to the unpolarized absorption in zero field (see figure 2).

If the upper states are near-degenerate, however, they still are accessible by both R- and L-light in the presence of a field, although  $W_L \neq W_R$ . We thus have a situation as in figure 4. When measuring now the Zeeman spectra, the absorption curves in L- and R-light no longer are identical and both differ from the unpolarized absorption. So the fact that the Zeeman spectra have different band shapes here is not a consequence of the breakdown of the rigid shift approximation, but merely a manifestation of the absence of degeneracy (which could not be detected in the MCD). In our example the deviations in band form are relatively small. However, when dropping the condition that

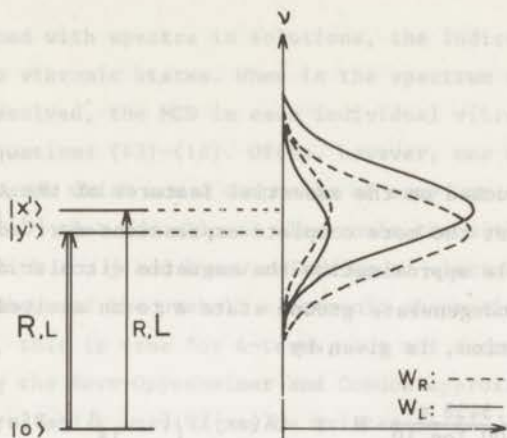


Figure 4. Left side. Energies and polarizations of the transitions in the presence of a magnetic field  $H_z$ .

Right side. Transition probabilities in L and R-light for both transitions. The shape function of all individual bands is equal to that of the unpolarized absorption. When summing the full (broken) curves in the figure, the Zeeman spectrum in L (R) light is obtained. Notice that the band shapes of both Zeeman spectra and of the unpolarized absorption will all be different.

$|\langle 0|x|x\rangle|^2 = |\langle 0|y|y\rangle|^2$ , which is not unrealistic since after the zero field interaction  $|x\rangle$  and  $|y\rangle$  no longer need to have the same functional forms, more drastic effects can be expected.

Until now we have assumed that  $|\beta H M_z| \ll \Delta E \ll \Gamma$ . When  $|\beta H M_z| \approx \Delta E \ll \Gamma$  the magnetic field influences both frequencies and wave functions. Then the MCD no longer can be described in terms of first order perturbation theory, but instead the energies and wave functions of the system in the magnetic field must be calculated by variational methods. When this is done, it follows that the MCD still has the form (10), provided the total energy splitting in the magnetic field (i.e. zero field splitting + Zeeman splitting) is small in comparison with  $\Gamma$ . The various Zeeman and MCD spectra which can be

expected as a function of the ratio  $\frac{\beta H M_z}{\Delta E}$  have recently been given<sup>4)</sup>.

## 5. Formal theory

### 5a. General

After having touched on the essential features of the A and B terms in the MCD we now present the more complete expressions derived by Stephens<sup>5)</sup>. In the electric dipole approximation the magnetic circular dichroism in a transition from a nondegenerate ground state a to an excited state j, measured in an isotropic solution, is given by

$$\Delta \epsilon(a \rightarrow j) = -\frac{21.3458 \pi}{4500 \log_e 10} H \sum_{a \rightarrow j} \{A(a \rightarrow j) f_1(\nu, \nu; j_a) + B(a \rightarrow j) f_2(\nu, \nu; j_a)\} \quad (13)$$

where  $\epsilon$  is in (liter Mole<sup>-1</sup> cm<sup>-1</sup>), the magnetic field strength H in Gauss, A in (Bohr magneton x square Debye) and B in (Bohr magneton x square Debye x cm). The MCD parameters A and B have the forms

$$A(a \rightarrow j) = \frac{1}{2} \vec{\mu}_{jj} \cdot \text{Im} \vec{r}_{aj} \wedge \vec{r}_{ja} \quad (14a)$$

$$B(a \rightarrow j) = \text{Im} \left\{ \sum_{k \neq a} \frac{\vec{\mu}_{ka}}{E_{ka}} \cdot \vec{r}_{aj} \wedge \vec{r}_{jk} + \sum_{k \neq j} \frac{\vec{\mu}_{jk}}{E_{kj}} \cdot \vec{r}_{aj} \wedge \vec{r}_{ka} \right\} \quad (14b)$$

In these equations  $\vec{r}_{pq}$  and  $\vec{\mu}_{pq}$  denote the matrix elements of the electric and magnetic dipole operator (cf. (1)) and  $E_{pq} = E_p - E_q$  is the energy separation of the states p and q. All wave functions involved in (14) are eigen functions in zero magnetic field; when evaluating (14a) for a degenerate state j one has to use the representation of j that diagonalizes  $\vec{\mu} \cdot \vec{H}$ .

The shape function for the B-term,  $f_2(\nu, \nu; j_a)$ , which is often taken equal to that of the unpolarized absorption<sup>2)</sup>, reads

$$f_2(\nu, \nu; j_a) = \frac{\pi}{2} \nu f(\nu, \nu; j_a) \quad (15)$$

while that of the A-term is given by

$$f_1(\nu, \nu; j_a) = \frac{\pi}{2} \nu \frac{\partial f(\nu, \nu; j_a)}{h \partial \nu} \quad (16)$$



## 5b. Electronic absorption bands

Being concerned with spectra in solutions, the indices  $a$ ,  $j$  and  $k$  in (13)-(16) refer to vibronic states. When in the spectrum all vibronic transitions are resolved, the MCD in each individual vibronic transition can be described by equations (13)-(16). Often, however, one observes in solution broad absorption bands which are a composite of many unresolved vibronic bands. Then it is argued<sup>1)2)</sup> that for allowed electronic transitions (13)-(16) again may be used, but with  $a$ ,  $j$  and  $k$  now referring to electronic states and  $f_2(v, v_j, a)$  to the shape of the overall electronic absorption band. As we shall indicate, however, this is true for A-terms, but not necessarily for B-terms.

When adopting the Born-Oppenheimer and Condon approximations the vibronic wave functions  $a$ ,  $j$  and  $k$  in (14) may be written as  $Aa$ ,  $Jj$  and  $Kk$ . Capital letters here denote electronic wave functions (evaluated at the ground state's equilibrium geometry) and lower case letters vibrational wave functions which belong to the corresponding electronic states. Then the A-term in a transition  $Aa \rightarrow Jj$  equals

$$A(Aa \rightarrow Jj) = \frac{1}{2} \vec{\mu}_{JJ} \cdot \text{Im} \vec{r}_{AJ} \wedge \vec{r}_{JA} (j|j)(a|j)(j|a) \quad (17)$$

Assuming that of the electronic ground state only the vibrational level  $a$  is populated, we obtain by summing over all vibrational structure  $j$

$$A(A \rightarrow J) = \sum_j A(Aa \rightarrow Jj) = \frac{1}{2} \vec{\mu}_{JJ} \cdot \text{Im} \vec{r}_{AJ} \wedge \vec{r}_{JA} \quad (18)$$

From (17) and (18) it follows that  $A(Aa \rightarrow Jj)$  is a product of an electronic A-term  $A(A \rightarrow J)$  and a Franck-Condon factor  $(a|j)(j|a)$ . Since this, mutatis mutandis, also holds for the unpolarized absorption, equations (13)-(16) may be used to describe A-terms with the understanding that in these equations  $a$  and  $j$  represent electronic states.

With the same approximations, however,  $B(Aa \rightarrow Jj)$  cannot be written as a product of an electronic part and a Franck-Condon factor. This is due to the presence of vibrational energies in the denominators in (14b), which prevents the application of the sum rule. Anticipating a discussion in Chapter III we shall not consider this point here.

## 6. Concluding remarks

Having available the quantities which allow the extraction of  $A(a \rightarrow j)$  and  $B(a \rightarrow j)$  from the observed MCD in an isolated absorption band  $a \rightarrow j$ , the question remains what information can be gained from these MCD parameters. As will be clear from the preceding discussions, a non-zero value of  $A$  proves degeneracy (or, what is more probable: near degeneracy, since one hardly expects exact degeneracy with molecules in solution). Unfortunately, the zero field splitting cannot be determined by the MCD. On the other hand, the favourable circumstance that the value of  $A$  yields the numerical value of the angular momentum  $M_z$ , allows a comparison with the calculated expectation value of  $L_z$  and thus offers the possibility to test the quality of calculated wave functions (Chapter II can be considered as an example for this).

In principle the interpretation of B-terms presents a more complicated problem owing to the fact that  $B(a \rightarrow j)$  contains contributions of all excited states. If, however, only a few transitions happen to mix appreciably under the influence of the magnetic field (that is: the summations over  $k$  in (14b) are restricted to one or two states), the interpretation of B-terms becomes feasible which often offers the possibility to obtain valuable spectroscopic information (cf. Chapter III).

## References

1. A.D. Buckingham and P.J. Stephens, 1966, *Ann. Rev. Phys. Chem.* **17**, 399
2. P.N. Schatz and A.J. McCaffery, 1969, *Quarterly Reviews* **23**, 552
3. G. Herzberg, *Electronic Spectra and Electronic Structure of Polyatomic Molecules* (D. van Nostrand Co., Inc., Princeton, New Jersey, 1966)
4. J.C. Sutherland, D. Axelrod and M.P. Klein, 1971, *J. Chem. Phys.* **54**, 2888
5. P.J. Stephens, 1964, Thesis Oxford

CHAPTER II  
MCD OF THE TRIPHENYLCARBENIUM ION AND SOME SYMMETRICALLY  
PARASUBSTITUTED DERIVATIVES

1. Introduction

Upon dissolving the colourless triphenylmethanol in sulphuric acid a yellow solution is obtained. It is now known that the colour is due to the triphenylcarbenium ion (trityl cation) which is formed by abstraction of  $\text{OH}^-$ . The delocalization of the positive unit charge in the cation would be maximum if all phenyl rings were coplanar (molecular symmetry  $D_{3h}$ ), but this is not possible because of steric hindrance between the rings. More likely, therefore, is a structure where two or three rings are forced out of the central plane (i.e. the plane through the three central bonds) by rotation about the central bonds<sup>1)</sup>. If all rings are rotated in the same sense over an angle  $\theta$ , the nuclear configuration of the cation has  $D_3$  symmetry and resembles a propeller. Although other, less symmetrical, configurations also might be possible<sup>2)</sup>, i.r. studies on various trityl salts<sup>3)4)</sup> indicate and an X-ray diffraction study of  $\phi_3\text{C}^+\text{ClO}_4^-$  establishes<sup>5)</sup> that in the solid state  $\phi_3\text{C}^+$  has  $D_3$  symmetry (angle of twist  $\theta \sim 32^\circ$ ). But also in solution the shape of triphenylcarbenium ions is that of a symmetrical propeller, as revealed by various nmr experiments<sup>6)</sup> on substituted trityl cations. Although a particular molecular symmetry on the nmr time scale not automatically implies that light absorption also may be described in terms of the same molecular symmetry, the assumption of  $D_3$  symmetry for the trityl cations seems a useful starting point for the description of

some of their spectroscopic properties.

## 2. Absorption and emission spectra of $\phi_3C^+$

Molecular orbital theory predicts for the trityl cation in  $D_3$  symmetry three nearby singlet-singlet transitions in the visible part of the spectrum: two of these involve (x,y)-polarized transitions to states with E-symmetry; the third transition - forbidden in the planar molecule - is weak and z-polarized. (See for the definition of the molecular axes figure 1.) The observed absorption spectrum of  $\phi_3C^+$ , depicted in figure 2, seems to confirm this prediction as it consists of at least two strongly overlapping bands.

Upon irradiating a cooled solution of  $\phi_3C^+$  in  $H_2SO_4$  a bright green emission is observed (full curve in figure 2). The emission consists of two parts: an intense band at  $\sim 18kK$  and a weaker one at  $\sim 20kK$ . As the excitation spectra of both emissions are very similar to the absorption spectrum they are attributed to  $\phi_3C^+$ . The 18kK emission decays exponentially with a time constant of .19 sec while that at 20kK decays much faster; they can be assigned as phosphorescence and fluorescence, respectively.

In figure 2 are also given the polarization P of the emission (EP) and of the absorption as measured with respect to either fluorescence (APF) or phosphorescence (APP). In fluorescence as well as in absorption (APF curve)  $P = 1/7$ , with the exception of a dip in the APF curve at 23kK. For  $\phi_3C^+$  this indicates that large parts of the absorption are (x,y)-polarized, while the polarization of the fluorescence is either (x,y) or  $x'$ , where  $x'$  is some direction in the x,y-plane. The drop in the APF curve could result from the

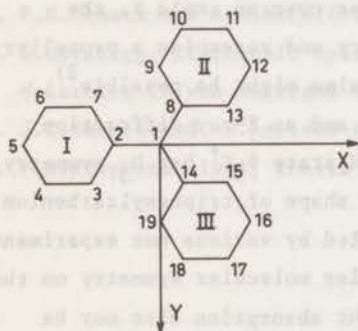


Figure 1. Molecular reference frame for  $\phi_3C^+$ , and numbering of the atoms and rings.

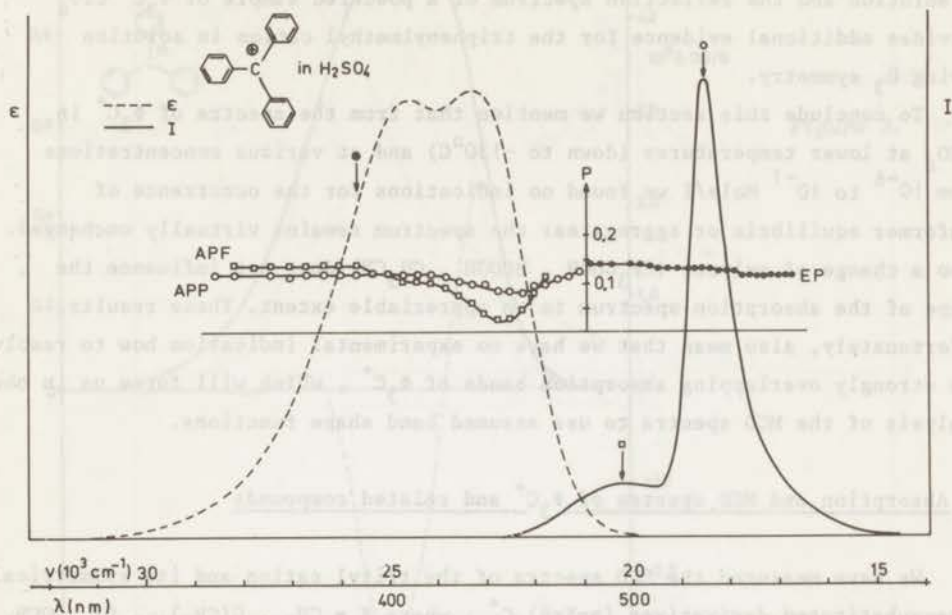


Figure 2. Absorption ( - - - - ) and emission of  $\phi_3C^+$  in  $H_2SO_4$  at  $-110^\circ C$  ( ——— ). Degree of polarization of absorption with respect to the fluorescence ( at a frequency denoted by  $\square$  ) and phosphorescence ( in the point marked by  $\circ$  ), and of the emission when excited by light of a frequency denoted by  $\bullet$  .

presence of z-polarized intensity in the absorption, which would tend to bring the value of P towards  $-1/3$ . We might ascribe this effect to the weak z-polarized transition predicted for a non-planar triphenylcarbenium ion. A great deal of what is said about the direction of the transition moments in absorption and fluorescence equally well applies when considering the polarization of the phosphorescence and the APP curve. But here it may be concluded that presumably the polarization of the emission is not (x,y), but linear (along a yet unspecified direction in the x,y-plane of the absorbent molecule) since it is found from triplet ESR measurements<sup>7)</sup> that in its lowest triplet state  $\phi_3C^+$  no longer has trigonal symmetry. So although no definite conclusions can be drawn about the symmetry of the fluorescent state of the trityl cation, the results of the polarization measurements are perfectly compatible with  $D_3$  symmetry of the species in its ground state.

The large similarity we observed between the absorption spectrum of  $\phi_3C^+$  in solution and the reflection spectrum of a powdered sample of  $\phi_3C^+ ClO_4^-$  provides additional evidence for the triphenylmethyl cation in solution having  $D_3$  symmetry.

To conclude this section we mention that from the spectra of  $\phi_3C^+$  in  $H_2SO_4$  at lower temperatures (down to  $-130^\circ C$ ) and at various concentrations from  $10^{-6}$  to  $10^{-1}$  Mole/l we found no indications for the occurrence of conformer equilibria or aggregates: the spectrum remains virtually unchanged. Also a change of solvent ( $CF_3COOH$ ,  $HCOOH$ ,  $CH_3CN$ ) does not influence the shape of the absorption spectrum to an appreciable extent. These results, unfortunately, also mean that we have no experimental indication how to resolve the strongly overlapping absorption bands of  $\phi_3C^+$ , which will force us in the analysis of the MCD spectra to use assumed band shape functions.

### 3. Absorption and MCD spectra of $\phi_3C^+$ and related compounds

We have measured the MCD spectra of the trityl cation and its symmetrically para-substituted derivatives  $(p-X-\phi)_3C^+$ , where  $X = CH_3$ ,  $C(CH_3)_3$ ,  $Cl$ ,  $OCH_3$  and  $N(CH_3)_2$ . The ions were prepared by dissolving the corresponding chlorides or carbinols in trifluoroacetic acid, except for the carbenium ion with  $X = N(CH_3)_2$  which is readily available as a salt (crystalviolet) and which was measured in water. In figure 3-8 we show the observed absorption and MCD spectra. The absorption (full lines) is displayed as absorbance  $OD (= \epsilon cd)$ , the MCD as differential absorbance  $\Delta OD (= \Delta \epsilon cd)$  per Gauss. The pathlength invariably was 1 cm, the concentrations (in  $10^{-5}$  Mole/l) were 2.3 ( $X=H$ ), .84 ( $X=CH_3$ ), 1.12 ( $X=C(CH_3)_3$ ), .90 ( $X=Cl$ ), .78 ( $X=OCH_3$ ) and 1.30 ( $X=N(CH_3)_2$ ).

#### Analysis of the spectra

It is well known<sup>8)9)</sup> that in the MCD of an isolated vibronic transition  $a \rightarrow j$  ( $a$  represents a non-degenerate ground state) one can distinguish the so-called A and B terms. The A-term, given in (1), only arises when the upper state is degenerate and carries a magnetic moment (or near degenerate as we shall see later) whereas the B-term, also given in (1), results from the mixing of the states  $a$  and  $j$  by the external field.

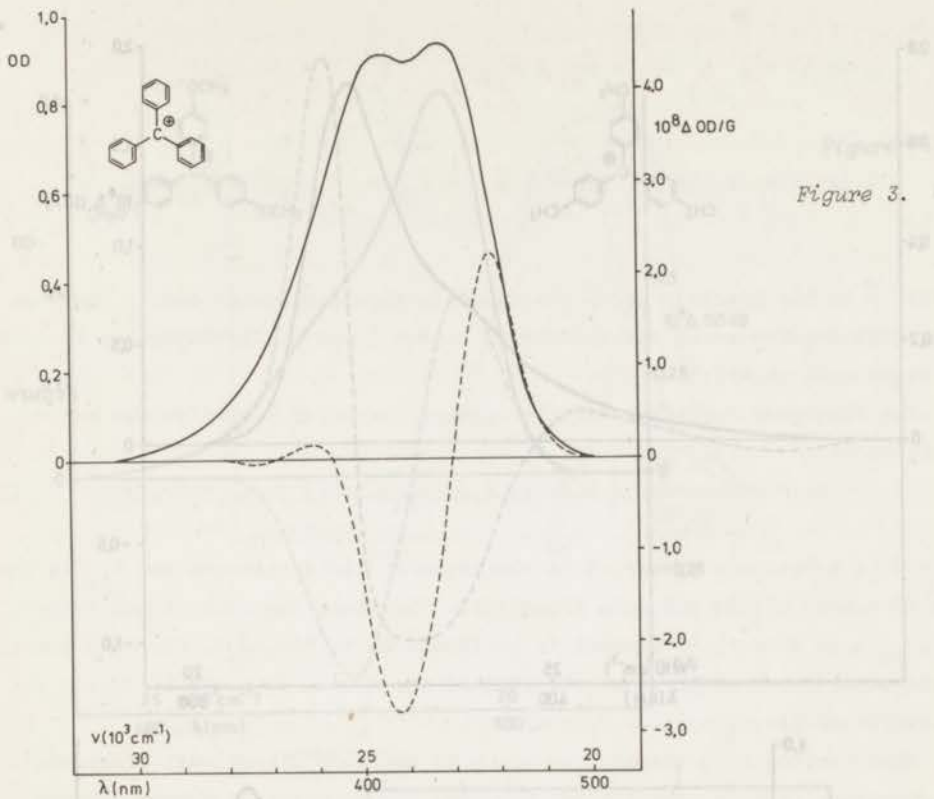
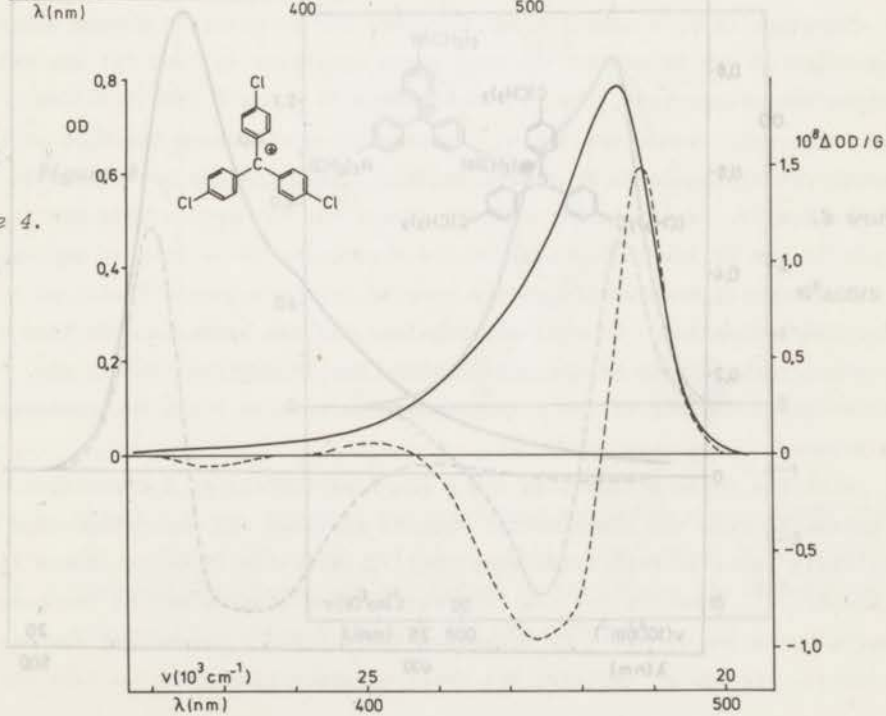


Figure 4.



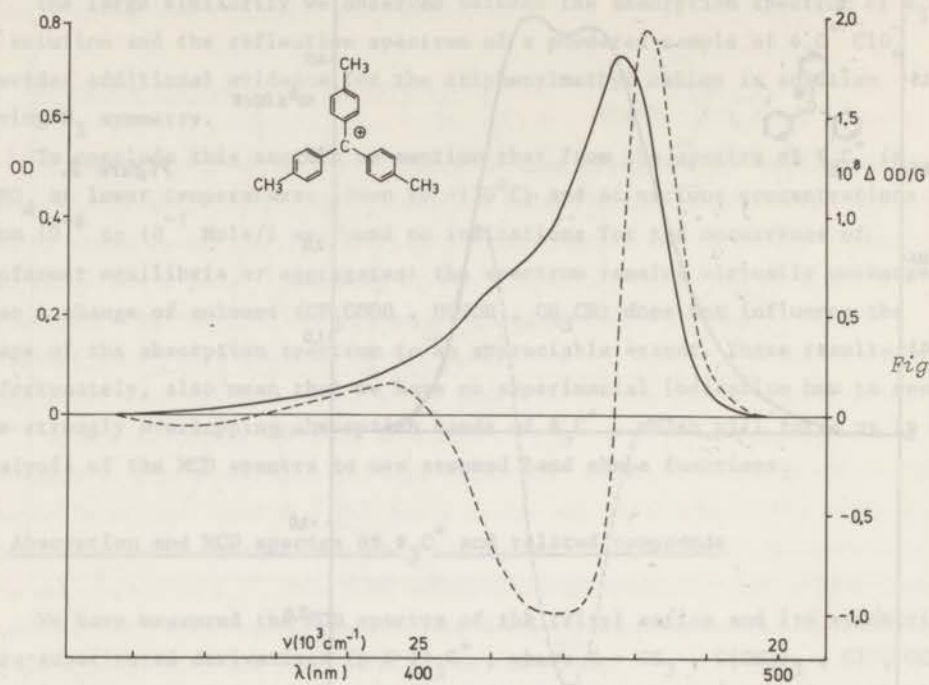


Figure 5.

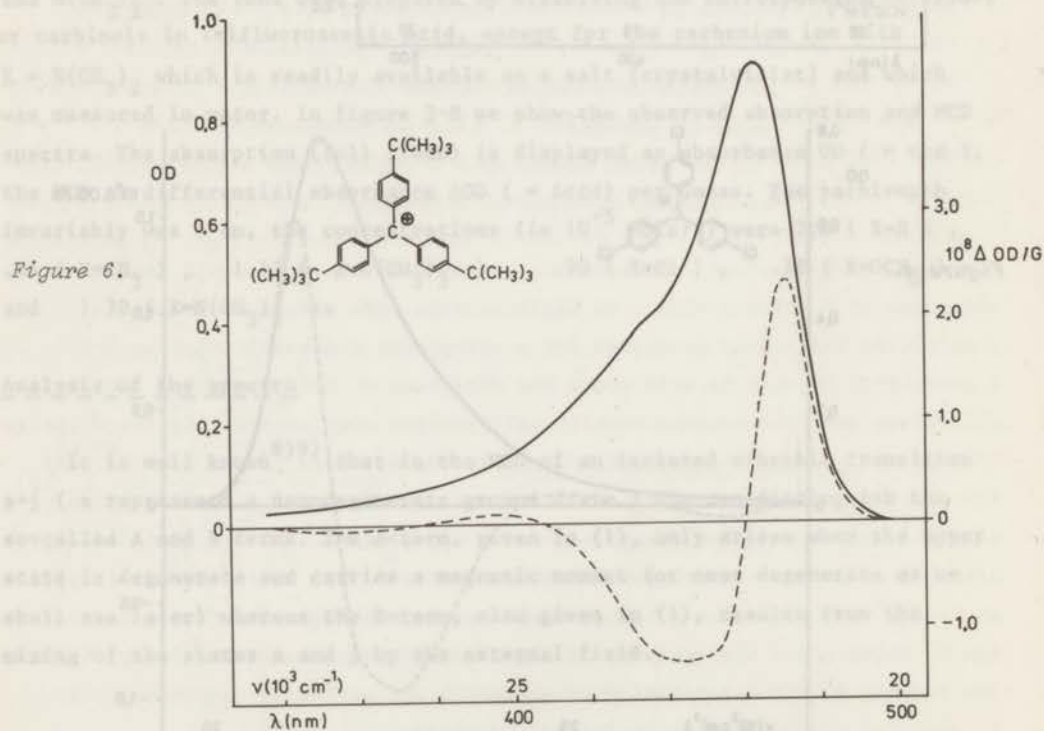


Figure 6.



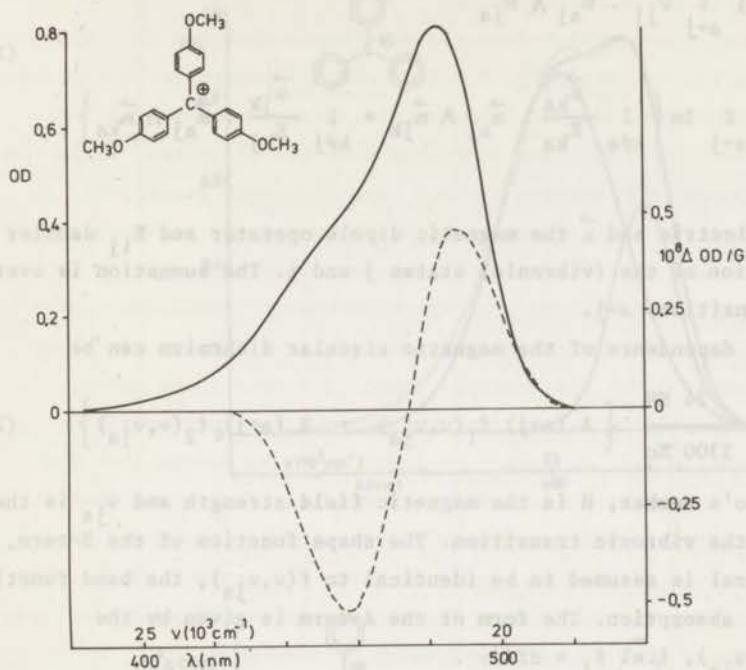


Figure 7.

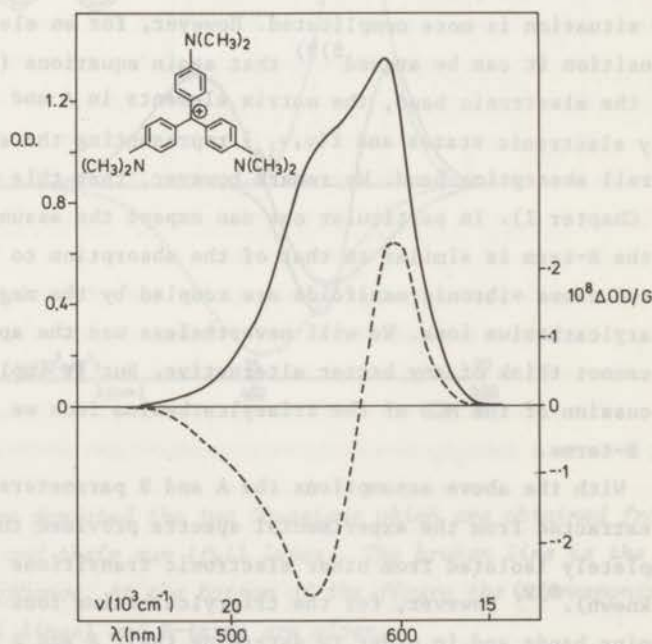


Figure 8.

$$A(a \rightarrow j) = \frac{1}{2} \sum_{a \rightarrow j} \vec{\mu}_{jj} \cdot \vec{m}_{aj} \wedge \vec{m}_{ja} \quad (1)$$

$$B(a \rightarrow j) = \sum_{a \rightarrow j} \text{Im} \left\{ \sum_{k \neq a} \frac{\vec{\mu}_{ka}}{E_{ka}} \cdot \vec{m}_{aj} \wedge \vec{m}_{jk} + \sum_{k \neq j} \frac{\vec{\mu}_{jk}}{E_{kj}} \cdot \vec{m}_{aj} \wedge \vec{m}_{ka} \right\}$$

In (1)  $\vec{m}$  is the electric and  $\vec{\mu}$  the magnetic dipole operator and  $E_{ij}$  denotes the energy separation of the (vibronic) states  $j$  and  $i$ . The summation is over all degenerate transitions  $a \rightarrow j$ .

The frequency dependence of the magnetic circular dichroism can be described by

$$\Delta \epsilon = - \frac{24 NH}{3300 \pi c} \left\{ A(a \rightarrow j) f_1(\nu, \nu_{ja}) + B(a \rightarrow j) f_2(\nu, \nu_{ja}) \right\} \quad (2)$$

where  $N$  is Avogadro's number,  $H$  is the magnetic field strength and  $\nu_{ja}$  is the peak frequency of the vibronic transition. The shape function of the B-term,  $f_2(\nu, \nu_{ja})$ , in general is assumed to be identical to  $f(\nu, \nu_{ja})$ , the band function of the unpolarized absorption. The form of the A-term is given by the derivative of  $f(\nu, \nu_{ja})$ , i.e.  $f_1 = df/d\nu$ .

When dealing with transitions which do not show vibrational structure the situation is more complicated. However, for an electric dipole allowed transition it can be argued<sup>8)9)</sup> that again equations (1) and (2) are valid for the electronic band, the matrix elements in  $A$  and  $B$  now involving only electronic states and  $f(\nu, \nu_{ja})$  representing the shape function of the overall absorption band. We remark however, that this may not always be true (cf Chapter I). In particular one can expect the assumption that the shape of the B-term is similar to that of the absorption to be only an approximation if two close vibronic manifolds are coupled by the magnetic field, as in the triarylcarbenium ions. We will nevertheless use the approximation here since we cannot think of any better alternative. But it implies that in the discussion of the MCD of the triarylcarbenium ions we shall not emphasize the B-terms.

With the above assumptions the  $A$  and  $B$  parameters of a transition can be extracted from the experimental spectra provided the absorption band is completely isolated from other electronic transitions (i.e. the shape function is known).<sup>8)9)</sup> However, for the triarylcarbenium ions we expect two overlapping bands and in order to determine their  $A$  and  $B$  parameters one has to decompose, one way or another, the observed absorption spectrum into the

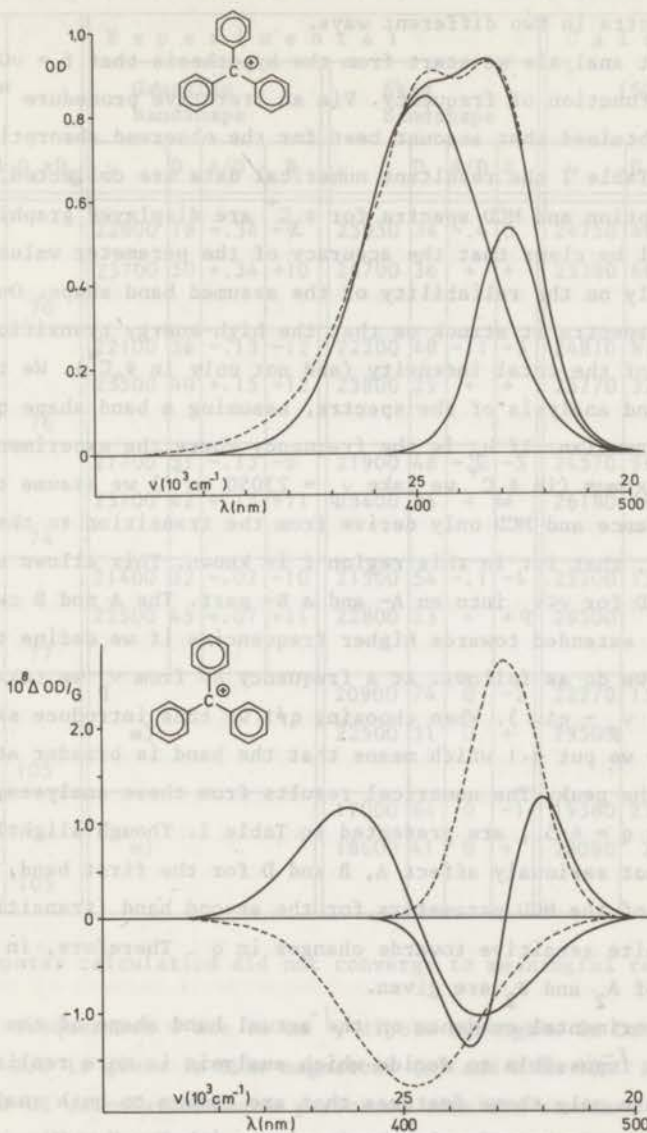


Figure 9. At the top are depicted the two Gaussians which are obtained from the analysis and their sum (full lines). The broken line is the observed absorbance. At the bottom of the figure the corresponding A-terms (full lines) and B-terms are given.

individual bands. Assuming that only two transitions are involved, we have analyzed the spectra in two different ways.

In the first analysis we start from the hypothesis that  $f = \nu G$ , where  $G$  is a Gaussian function of frequency. Via an iterative procedure <sup>\*</sup>) those two Gaussians were obtained that account best for the observed absorption and MCD spectra. In Table I the resultant numerical data are collected, while the decomposed absorption and MCD spectra for  $\phi_3C^+$  are displayed graphically in figure 9. It will be clear that the accuracy of the parameter values obtained depends critically on the reliability of the assumed band shape. On inspection of the analyzed spectra it struck us that the high-energy transition appropriates so much of the total intensity (and not only in  $\phi_3C^+$ ). We therefore performed a second analysis of the spectra, assuming a band shape quite different from Gaussian. If  $\nu_p$  is the frequency where the experimental absorbance is maximum (in  $\phi_3C^+$  we take  $\nu_p = 23050 \text{ cm}^{-1}$ ) we assume that for  $\nu \ll \nu_p$  the absorbance and MCD only derive from the transition to the lowest-energy state  $E_1$ , that is: in this region  $f$  is known. This allows a decomposition of the MCD for  $\nu \ll \nu_p$  into an A- and a B- part. The A and B curves thus found now can be extended towards higher frequencies if we define the missing part of  $f$ . This we do as follows. At a frequency  $\Delta\nu$  from  $\nu_p$  we take  $f(\nu_p + \Delta\nu) = f(\nu_p - q\Delta\nu)$ . When choosing  $q \neq 1$  we thus introduce skew band shapes. Actually we put  $q < 1$  which means that the band is broader at the high energy side of the peak. The numerical results from these analyses, performed graphically with  $q = 4/5$ , are presented in Table I. Though slightly different values of  $q$  do not seriously affect A, B and D for the first band, it appeared that the values of the MCD parameters for the second band (transition to the  $E_2$  state) are quite sensitive towards changes in  $q$ . Therefore, in Table I only the signs of  $A_2$  and  $B_2$  are given.

Lacking experimental evidence on the actual band shape of the transition to  $E_1$ , it seems impossible to decide which analysis is more realistic and we therefore will use only those features that are common to both analyses.

In the series of the triarylcarbenium ions with  $X = H, CH_3, C(CH_3)_3, Cl, OCH_3$  and  $N(CH_3)_2$  the frequency at which the transition to  $E_1$  is maximum,

<sup>\*</sup>) We are indebted to Mrs. G. Gerritsen-de Vries and Drs. A.P. Vuyk for their help in the construction of the necessary computer program.

Table I. Relevant spectroscopic parameters for the triarylcabenium ions.

X	band	$D_1+D_2$	Experimental								Calculated (SCF-CI)				
			Gaussian bandshape				Skew bandshape								
			$\nu$	D	A/D	B	$\nu$	D	A/D	B	$\nu$	D	$D_1+D_2$	A/D	B
H	$E_1$	70	22800	19	-0.34	-9	23050	34	-0.4	0	24750	46	112	+0.31	-22
	$E_2$		23700	50	+0.34	+10	24700	36	+	+	25380	66		-0.31	+22
CH <sub>3</sub>	$E_1$	76	22100	36	-0.13	-12	22200	48	-0.1	-5	24810	81	113	+0.18	-31
	$E_2$		23500	40	+0.15	+12	23800	29	+	+	25770	32		-0.19	+31
C(CH <sub>3</sub> ) <sub>3</sub>	$E_1$	74	21700	31	-0.13	-9	21900	48	-0.2	-5	24570	96	114	+0.10	-17
	$E_2$		23100	42	+0.13	+11	23400	26	+	+	26180	18		-0.10	+17
Cl	$E_1$	77	21400	32	-0.07	-10	21500	54	-0.1	-4	23200	138	142	-0.01	-2
	$E_2$		22500	45	+0.07	+11	22800	23	+	+	29500	4		0	+2
OCH <sub>3</sub>	$E_1$	105	*)				20900	74	0	-2	22270	151	155	-0.01	-2
	$E_2$		*)				22500	31	0	+	29500	4		0	+2
N(CH <sub>3</sub> ) <sub>2</sub>	$E_1$	105	*)				17000	64	0	-1	19380	235	257	-0.02	-3
	$E_2$		*)				18600	41	0	+	28090	22		+0.02	+3

\*) Computer calculation did not converge to meaningful result.

Units: frequencies  $\nu$  are in  $\text{cm}^{-1}$ , dipole strengths in Debye<sup>2</sup> ( $D^2$ ),

A/D is given in Bohr magnetons ( $\beta$ ) and B in  $10^{-3} \beta D^2 \text{ cm}$ .

The SCF-CI calculations were performed with the standard program in our department. The parameters were those described by Van der Lugt<sup>10</sup>). The methyl and t-butyl group were taken into account merely as an inductive perturbation (core integrals -8.6 and -8.1 eV respectively). All triarylcabenium ions were given twist angles of  $30^\circ$  and all C-C bonds were taken equal (1.39Å).

In the table are not included the z-polarized transitions to the  $A_2$ -state (dipole strength  $\ll D^2$ ). The B-terms as calculated arise from the magnetic coupling between  $E_1$  and  $E_2$ .

decreases. The total dipole strength for the cations (i.e.  $D_1 + D_2$ ) is constant ( $\sim 75 D^2$ ) when  $X = H, CH_3, C(CH_3)_3$  and  $Cl$ , while this quantity has a value of  $105 D^2$  for  $X = OCH_3$  or  $N(CH_3)_2$ . The ratio  $D_1/D_2$  which is  $\leq 1$  for the trityl cation, increases upon substitution. Regarding the MCD parameters one finds that  $A_1/D_1$  and  $B_1$  are negative while the corresponding quantities for the second transition have opposite signs. (At this point we note that the negative value of  $A_1/D_1$  is quite remarkable since mostly positive A/D values are observed in electric dipole allowed transitions in high symmetric aromatic systems (see §7)). The absolute magnitude of  $A_1/D_1$ , which has a maximum for the unsubstituted ion, decreases in the series  $X = \text{methyl, } t\text{-butyl, } Cl$  and vanishes for  $X = \text{methoxy or dimethylamino}$ .

#### 4. Calculations

In an attempt to account for the observed effects in the various ions MO calculations of the PPP type were performed, including CI between all singly excited states. The results are tabulated in Table I. It appears that in a qualitative sense the calculations reproduce the observed phenomena: there is a nice agreement between the trends of the calculated and observed values of the frequency  $\nu_1$ ; the calculated total dipole strength is constant for  $X = H, CH_3$  and  $C(CH_3)_3$  and larger for the other substituents. The ratio  $D_1/D_2$  increases as a function of the substituent  $X$ . As for the MCD data: for all compounds  $B_1$  is negative and  $B_2$  positive, whereas the value of A/D decreases upon substitution. However, in as far as the A/D values do not approach zero, they have the wrong sign.

Now one could imagine that in a particular PPP-calculation the sequence of two nearby excited states is obtained incorrectly because of accidental errors due to the various approximations in the PPP-scheme. However, such an error persisting in the complete series seems an unsatisfactory result, which deserves closer investigation. In the following we shall describe some relevant features of the two lowest excited E-states of the triaryl-carbenium ions in terms of Hückel m.o.'s. It will appear that this enables one to better understand the signs and magnitudes of the observed magnetic moments.

#### Wave functions

As is well known, in benzene the highest occupied m.o.'s are twofold

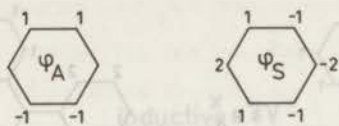


Figure 10. Coefficients of the atomic orbitals in the two highest occupied m.o.'s,

$\phi_A$  and  $\phi_S$ , in benzene. Note that  $\phi_A$  and  $\phi_S$  are not normalized.

degenerate and the associated wave functions, which are completely determined by symmetry, have the form<sup>11)</sup>

$$\phi_{\pm} = \frac{1}{\sqrt{6}} \sum_{j=0}^5 e^{\pm \frac{2\pi i}{6} j} \phi_j \quad (3)$$

An alternative set of wave functions can be formed out of  $\phi_+$  and  $\phi_-$  by taking the real and imaginary parts  $\phi_S$  and  $\phi_A$  (cf. figure 10).

In the trityl cation the nonbonding molecular orbital has  $a_2$  symmetry in  $D_3$  whereas the highest bonding level is five-fold degenerate in the Hückel approximation and is described by a wave function of  $a_1$  symmetry and two orbital pairs with e symmetry. The  $a_1$ -orbital and the e-type wave functions, when expressed in the  $\phi_A$ ,  $\phi_S$  of the peripheral rings may be written as follows

$$a_1 = \frac{1}{\sqrt{12}} (\phi_A^I + \phi_A^{II} + \phi_A^{III})$$

$$e_A \begin{cases} e_A^x = \frac{1}{\sqrt{8}} (\phi_A^{II} - \phi_A^{III}) \\ e_A^y = \frac{-1}{\sqrt{24}} (2\phi_A^I - \phi_A^{II} - \phi_A^{III}) \end{cases} \quad (4)$$

$$e_S \begin{cases} e_S^y = \frac{1}{\sqrt{24}} (\phi_S^{II} - \phi_S^{III}) \\ e_S^x = \frac{-1}{\sqrt{72}} (2\phi_S^I - \phi_S^{II} - \phi_S^{III}) \end{cases}$$

In (4) the superscript attached to  $\phi_A$  and  $\phi_S$  denotes one of the phenyl rings in  $\phi_3C^+$  (see for the numbering of the rings figure 1). The shape of the

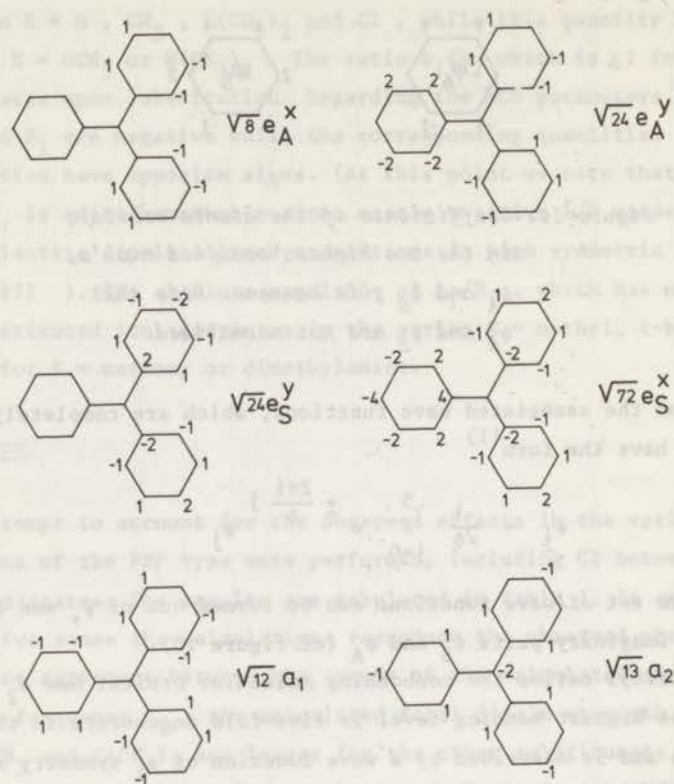


Figure 11. Coefficients of the atomic orbitals in the highest bonding and nonbonding molecular orbitals of  $\phi_3C^+$ . The orbitals  $e_A^x$ ,  $e_A^y$ ,  $e_S^x$ ,  $e_S^y$  and  $a_1$  are all of equal energy ( $\alpha-B$ ), the  $a_2$ -orbital has an energy  $\alpha$ .

nonbonding orbital and the highest occupied orbitals is illustrated in figure 11.

Of course the complex wave functions (3) can also be used in the construction of the two highest bonding e-levels in  $\phi_3C^+$  and since here both e-levels are mutually degenerate, it is immaterial whether the orbitals based on (3) or those described by (4) are chosen as a basis.

This is no longer true in the substituted trityl cations. If at the carbon atoms 5, 11 and 17 the Coulomb integral is changed from  $\alpha$  to  $\alpha + \Delta\alpha$ , the orbitals (4) remain unaffected but it is found from first order perturbation theory that their energies change by an amount  $(d_5^2 + d_{11}^2 + d_{17}^2)\Delta\alpha$ ,



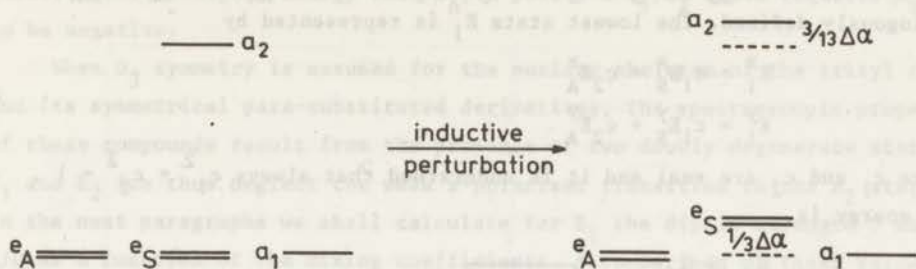


Figure 12. Orbital diagram of  $\phi_3C^+$  before and after an inductive perturbation ( $\Delta\alpha > 0$ ).

where  $d_i$  denotes the coefficient of atomic orbital  $i$  in the m.o. concerned. The resulting orbital energy picture is given in figure 12. Later on we shall see that this particular perturbation can account for some of the observed spectral properties of some substituted trityl cations. Anticipating this perturbation, we shall use the wave functions (4) as a basis.

### Configuration interaction

In a first approximation the excited states can be obtained from an orbital picture by promoting an electron from an occupied to an unoccupied orbital. In  $\phi_3C^+$  therefore the lowest excited singlet state will be five-fold degenerate ( $A_2 + E_A + E_S$ ) as a result of the one electron jumps  $a_1 \rightarrow a_2$ ;  $e_A \rightarrow a_2$  and  $e_S \rightarrow a_2$ . Taking a substituent into account by a simple inductive perturbation of the para-carbon atoms, this five-fold degeneracy is partly removed in the substituted triphenylcarbenium ions since now the promotions  $e_S \rightarrow a_2$  and  $e_A \rightarrow a_2$  are at different energies (see figure 13). Inclusion of configuration interaction will now mix  $E_A$  and  $E_S$  states, giving rise to two new double degenerate states  $E_1$  and  $E_2$ , where  $E_1$  always denotes the state which is lowest in energy.

If one describes all E-states by the real basis vectors  $E^x$  and  $E^y$  (which are symmetric and antisymmetric with respect to the two-fold rotation axis  $C_2^x$ ), configuration interaction amounts to solving

$$\begin{vmatrix} H_{SS} - E & H_{SA} \\ H_{AS} & H_{AA} - E \end{vmatrix} = 0 \quad (5)$$

In this equation  $H_{SS} = (E_S^x | H | E_S^x) = (E_S^y | H | E_S^y)$  whereas  $H_{AA}$  and  $H_{AS}$  ( $=H_{SA}$ ) are analogously defined. The lowest state  $E_1$  is represented by

$$\begin{aligned} E_1^x &= c_1 E_S^x + c_2 E_A^x \\ E_1^y &= c_1 E_S^y + c_2 E_A^y \end{aligned} \quad (6)$$

where  $c_1$  and  $c_2$  are real and it is understood that always  $c_1^2 + c_2^2 = 1$ .

Its energy is

$$\frac{H_{SS} + H_{AA}}{2} - \sqrt{\Delta E^2 + H_{SA}^2}$$

where  $\Delta E = \frac{1}{2}(H_{AA} - H_{SS})$ . The ratio of the mixing coefficients for the state of lowest energy is given by

$$c_1/c_2 = \frac{-H_{SA}}{-\Delta E + \sqrt{\Delta E^2 + H_{SA}^2}} \quad (7)$$

From the last equation one concludes that the sign of  $c_1/c_2$  is independent of  $\Delta E$ , being completely determined by the sign of  $H_{SA}$ . Whether thus  $E_S$  is of

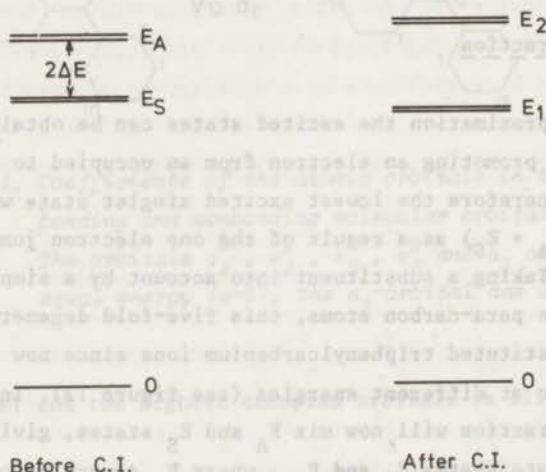


Figure 13. Ground state 0 and lowest excited states of a symmetrically para-substituted triphenylmethyl cation before and after configuration interaction. In the unsubstituted trityl cation  $\Delta E$  is zero.

lower, equal or higher energy than  $E_A$ , a positive  $c_1/c_2$  ratio requires  $H_{SA}$  to be negative.

When  $D_3$  symmetry is assumed for the nuclear skeleton of the trityl cation and its symmetrical para-substituted derivatives, the spectroscopic properties of these compounds result from the presence of two doubly degenerate states  $E_1$  and  $E_2$  (we thus neglect the weak z-polarized transition to the  $A_2$  state). In the next paragraphs we shall calculate for  $E_1$  the dipole strength  $D$  and  $A/D$  as a function of the mixing coefficients. A comparison of these values with the relevant experimental data then enables us to make some statements on the values of  $c_1$  and  $c_2$  for  $\phi_3C^+$  and its derivatives. In particular it follows that in order to account for the sign of the MCD in the transition at lowest energy, the ratio of  $c_1$  to  $c_2$  has to be positive. It thus appears that the off-diagonal matrix element of the Hamiltonian  $H_{SA}$  has to be negative. In §6 we shall consider  $H_{SA}$  in more detail.

### Dipole strengths

The x component of the electric transition moment is

$$(0|x|E_1^x) = \sqrt{2} \left\{ c_1 (e_S^x|x|a_2) + c_2 (e_A^x|x|a_2) \right\} = \sqrt{2} (c_1 s + c_2 a)$$

where the one electron transition moments  $(e_S^x|x|a_2)$  and  $(e_A^x|x|a_2)$  are abbreviated by  $s$  and  $a$ . Since the y component of the transition moment is equally large, the dipole strength of the transition to  $E_1$  equals

$$D_1 = 4 (c_1 s + c_2 a)^2 = \frac{4a^2}{1+c^2} \left( c \frac{s}{a} + 1 \right)^2 \quad (8)$$

where  $c = c_1/c_2$ .

Similarly  $D_2 = 4(-c_2 s + c_1 a)^2$  and one notes that the sum of the dipole strengths of both transitions is constant, as it should be of course. In figure 14  $D_1$  is plotted as a function of  $c$ . It appears that if  $c=0$   $D_1 = 4a^2$  and consequently  $D_2 = 4s^2$ . For  $c=\pm\infty$ , which is the case if  $E_1$  has no  $E_A$ -character,  $D_1 = 4s^2$ . At the point  $c=-a/s$  the longest wavelength transition is forbidden, while at  $c=s/a$  the transition to the  $E_2$  state carries no intensity.  $D$  being a quadratic function of  $c$ , a knowledge of  $D_1$  would provide one with two possible values of  $c_1/c_2$ .

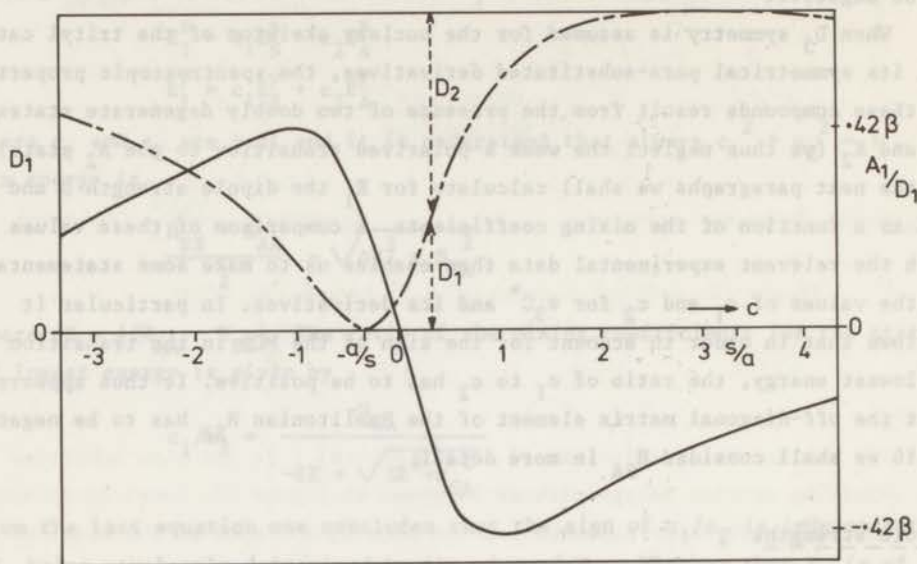


Figure 14.  $D_1$  (-----) and  $A_1/D_1$  (————) as a function of  $c$ . Note that from this figure  $D_2$  can be read as well, since  $D_1 + D_2$  is constant. In constructing the  $D_1$ -curve we have used the values  $a=1.72 D$  and  $s=5.76 D$ .

### Magnetic moments

For non-linear molecules in degenerate states the angular momentum about an axis of symmetry ( $z$ ) is  $\langle \Psi | L_z | \Psi \rangle \hbar$  where  $\langle \Psi | L_z | \Psi \rangle$  is in general non-integral and may be positive or negative.<sup>12)</sup> The presence of angular momentum in excited states can be detected in a Zeeman-experiment: with angular momentum a magnetic dipole moment  $\mu_z$  is associated and therefore also an energy effect in an external magnetic field  $H_z$ . Measurement of the Zeeman shift therefore directly yields the value of  $\langle \Psi | L_z | \Psi \rangle$ . The existence of orbital angular momentum also gives rise to a particular MCD effect: in a two-fold degenerate excited state the S-shaped A-term results from the fact that one component of the Zeeman couplet is exclusively accessible by left-, the other one by right-circularly polarized light. Conversely, the presence of an A-term in the MCD spectrum does not prove the existence of angular momentum and thus

of degeneracy, since it can be shown that two states which have an energy separation  $\delta E$  and which are coupled by the magnetic field also give rise to an S-shaped MCD, which cannot be distinguished from an ideal A-curve if  $\delta E$  is smaller than the half band width  $\Gamma$  of the transition. This may explain that in MCD language one loosely speaks of magnetic moments, even if possibly no exact degeneracy is present (cf Chapter I).

The matrix elements of  $\mu$  which are relevant for the MCD of the triaryl-carbenium ions involve the wave functions  $E_A^x$ ,  $E_A^y$ ,  $E_S^x$ , and  $E_S^y$ . From calculations it is found that  $i(e_A^x | \mu^z | e_S^y) = i(e_S^x | \mu^z | e_A^y) = +.85$  whereas the matrix elements  $i(e_A^x | \mu^z | e_A^y)$  and  $i(e_S^x | \mu^z | e_S^y)$  are of negligible magnitude. Consequently one finds for the value of A/D in the transition to the  $E_1$  state

$$A_1/D_1 = -\frac{i}{2} (E_1^x | \mu^z | E_1^y) = -\frac{i}{2} c_1 c_2 (e_S^x | \mu^z | e_A^y) = -\frac{1}{2} c_1 c_2 \cdot 0.85 \quad (9)$$

whereas  $A_2/D_2 = -A_1/D_1$ . The variation of  $A_1/D_1$  as a function of  $c$  is graphically displayed in figure 14. If  $E_1$  is identical to  $E_S$  ( $c=\pm\infty$ ) or to  $E_A$  ( $c=0$ ) it appears that  $A_1/D_1$  is zero. When on the other hand  $E_1$  is represented by  $(E_S^x \pm E_A^x)$  and  $(E_S^y \pm E_A^y)$  a large magnetic moment results. One notes that a particular value of A/D uniquely determines  $c_1/c_2$ .

##### 5. Comparison of theory and experiment

In  $\phi_3C^+$  the observed value of  $A_1/D_1$  is  $\sim .48$ . Firstly this shows that  $c$  must be positive and secondly that its value is lying near the point  $c=1$  (cf figure 14). The latter is, of course, just what we expect: if the accidentally degenerate states  $E_A$  and  $E_S$  are split because of a non-zero matrix element  $H_{AS}$  the absolute value of  $c$  is 1. The value  $c=+1$  should imply that  $D_1/D_2 = 3.5$ , whereas from experiment we expect a smaller ratio ( $\leq 1$ ) for  $\phi_3C^+$ . Perhaps therefore  $c$  has a somewhat lower value ( $D_1/D_2 \approx 1$  if  $c=+0.6$ ), but it is also possible that the magnitudes of the transition moments  $a$  and  $s$  are only qualitatively correct.

In our description the symmetrical para-substituted trityl cations derive from the parent compound by a simple inductive perturbation. As a result their spectroscopic properties can be described in terms of the orbitals of  $\phi_3C^+$ . When this is realistic, the sum of the dipole strengths of both degenerate transitions  $D_1+D_2$  should have the same value as for  $\phi_3C^+$ . From Table I it appears that this is indeed true to a good approximation for the compounds where  $X = CH_3$ ,  $C(CH_3)_3$  and  $Cl$  but not for those with  $X = OCH_3$  and

$N(CH_3)_2$ . Other than inductive effects apparently may not be neglected in the latter two compounds, whose A/D values will be shortly discussed in §7.

In an orbital picture an inductive perturbation  $\Delta\alpha$  at the para-carbon atoms results in a bathochromic shift of the transition to  $E_1$  if  $\Delta\alpha$  is positive (see figure 12). This explains the decrease in  $\nu_1$  in the series  $X = H, CH_3, C(CH_3)_3$ . In the case that  $X = Cl$ , where one expects  $\Delta\alpha$  to be negative, a hypsochromic shift should occur. That this is not observed is presumably due to the presence of e.g. small mesomeric interactions.

When in the orbital diagram an energy splitting  $\Delta E$  is present (see figure 13) configuration interaction will yield values of  $c$  which are not equal to 1 (cf. equation (7)). It can be seen from (7) that  $c_1/c_2$  grows if, with constant  $H_{AS}$ ,  $\Delta E$  (which is positive) increases. This is exactly what happens if we insert the observed  $A_1/D_1$  and  $D_1/D_2$  data for the triaryl-carbenium ions with  $X = CH_3, C(CH_3)_3$  and  $Cl$  in figure 14. The A/D values for these compounds all have the same sign as for  $\phi_3C^+$ , but they are considerably smaller in absolute magnitude. Together with the observation that here the ratio  $D_1/D_2$  is increased as compared with  $\phi_3C^+$ , this means that on substitution one proceeds towards the right on the  $c$ -axis in figure 14, i.e.  $E_1$  more and more approaches  $E_S$ . What specific  $c$ -values are reached is difficult to say: on the one hand the magnitude of  $A_1/D_1$  suggests that we should have rather large values of  $c$ ,  $c > s/a$  say. That  $c$  should be larger than  $s/a$  is also supported by the observed negative sign of  $B_1$ , since it is easy to show that  $B_1$  is negative for positive  $c$  except for the region  $1 \leq c \leq s/a$  (but we remark that it is uncertain whether one may use electronic B-terms to describe the magnetic coupling of two severely overlapping bands). On the other hand in our model  $c$  being larger than  $s/a$  would require the transition to  $E_2$  to be nearly forbidden. Apparently we are here confronted with the qualitative nature of our description. Irrespective of the precise value of  $c$  however, its sign is known beyond doubt and it will be shown that this will allow some interesting conclusions to be drawn.

#### 6. The sign of $(E_S | H | E_A)$

In §4 it was derived that regardless of the relative position of  $E_A$  and  $E_S$ , a positive  $c_1/c_2$  ratio should result from a negative value of  $(E_S | H | E_A)$ . We will now consider this matrix element in more detail.

Remembering that  $E_S$  and  $E_A$  represent the one-electron jumps  $e_S \rightarrow a_2$  and

$e_A \rightarrow a_2$  one obtains<sup>13)</sup>

$$(E_S | H | E_A) = (E_S^y | H | E_A^y) = -(e_S^y | H^{SCF} | e_A^y) + 2(a_2 e_S^y | | e_A^y a_2) - (a_2 a_2 | | e_S^y e_A^y) \quad (10)$$

where  $(ij || kl)$  stands for  $(i(1)j(1) | \frac{1}{r_{12}} | k(2)l(2))$ .

Substituting for  $e_S^y$  and  $e_A^y$  the expansions (4), each of the terms in (10) breaks down into six terms. These terms can be easily transformed into one another by explicitly using the fact that in the molecule three twofold axes of symmetry are present. The result is

$$(E_S | H | E_A) = -\frac{1}{4}(\phi_S^{II} | H^{SCF} | \phi_A^I) + \frac{1}{2}(a_2 \phi_S^{II} | | \phi_A^I a_2) - \frac{1}{4}(a_2 a_2 | | \phi_S^{II} \phi_A^I) \quad (11)$$

The first term of (11) is reduced as follows

$$(\phi_S^{II} | H^{SCF} | \phi_A^I) = \sum_{\substack{\mu(\text{ring II}) \\ \nu(\text{ring I})}} c_\mu^{S II} c_\nu^{A I} (H_{\mu\nu}^{core} - \frac{1}{2} P_{\mu\nu} \gamma_{\mu\nu}) \quad (12)$$

where  $c_\mu^{S II}$  is the coefficient of the atomic orbital centered on atom  $\mu$  in the m.o.  $\phi_S^{II}$ .  $P_{\mu\nu}$  is the bond order between the atoms  $\mu$  and  $\nu$  (which are on different rings) and  $\gamma_{\mu\nu}$  is the repulsion integral  $(\mu\mu | \nu\nu)$ .

With the zero differential overlap approximation the second term of (11) can be transformed to

$$(a_2 \phi_S^{II} | | \phi_A^I a_2) = \sum_{\substack{\mu(II) \\ \nu(I)}} c_\mu^{S II} c_\nu^{A I} c_\mu^{a_2} c_\nu^{a_2} \gamma_{\mu\nu} = - \sum_{\substack{\mu(II) \\ \nu(I)}} c_\mu^{S II} c_\nu^{A I} P_{\mu\nu} \gamma_{\mu\nu} \quad (13)$$

Here the last step arises because in an odd alternating cation the bond orders can be expressed in terms of the coefficients of the non-bonding m.o. only<sup>14)</sup>:

$P_{\mu\nu} = -c_\mu^{a_2} c_\nu^{a_2}$ . Finally the last term of (11) vanishes, since in the approximation of zero differential overlap the density  $\phi_S^{II} \phi_A^I$  vanishes.

So we arrive at

$$(E_S | H | E_A) = - \sum_{\substack{\mu(II) \\ \nu(I)}} c_\mu^{S II} c_\nu^{A I} \left( \frac{1}{4} H_{\mu\nu}^{core} + \frac{3}{8} P_{\mu\nu} \gamma_{\mu\nu} \right) \quad (14)$$

In this expression the second term equals  $\frac{3}{8}$  times the repulsion between the

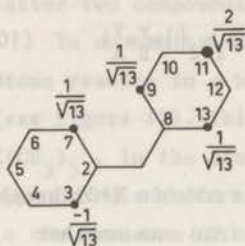


Figure 15.

Graphical representation of the Coulomb repulsion between the charge densities  $c_v^{A I} c_v^{a2}$  (confined to ring I) and  $c_\mu^{S II} c_\mu^{a2}$  (on ring II). The numbering of the atoms is given inside the rings, for the numbering of the rings see figure 1.

charge densities  $c_v^{A I} c_v^{a2}$  and  $c_\mu^{S II} c_\mu^{a2}$ , which are confined respectively to ring I and II of the propeller. This repulsion is graphically displayed in figure 15, where it is understood that the interaction is a Coulomb repulsion between the charge distributions on ring I and those on ring II. Since the distances C3-C9 and C7-C13 are equal, there remain only a repulsion between the charges on C7 with those on C9 and C11 and an attraction between the charge densities on C3 with those on C11 and C13. It is evident from the figure that the repulsive interaction will dominate, leading to a positive contribution to  $(E_S | H | E_A)$ .

The first term of (14) represents the bonding between different rings. Following the standard procedure in MO theory of taking only into account bonding between atoms which are directly linked<sup>13)</sup>, we might neglect this term. As a consequence  $(E_S | H | E_A)$ , being completely determined by the repulsion term in (14), would be positive, which is at variance with the sign of the observed magnetic moment in the lowest excited state. Therefore we will not neglect the one-electron term in (14). Obviously the largest share in this term is taken by  $H_{7,9}^{core}$ , which enters (14) with a coefficient  $-\frac{1}{4}$ . Since all phenyl rings in  $\phi_3C^+$  make an angle of  $30^\circ$  with the central plane, the overlap between the a.o.'s on C7 and C9 is negative and  $H_{7,9}^{core}$  is positive. Whence one concludes that the ultimate sign of  $(E_S | H | E_A)$  is determined by the competition of a (negative) bonding energy and a (positive) electron repulsion energy. Since an estimate of the magnitude of both terms yield values of  $-0.07\text{eV}$  and  $+0.06\text{eV}$ , it appears that the one-electron and two-electron terms counterbalance quite effectively. The interaction energies being so small, it might be that with SCF instead of Hückel starting orbitals this result is perhaps not valid anymore. We believe however, that this is not likely. In the triphenylmethyl radical the charge density on all atoms is zero<sup>14)</sup>. The triphenylmethyl cation



in its  $E_S$  or  $E_A$  state can be thought to result from  $\phi_3C^+$  by the removal of one electron from the  $e_S$  or  $e_A$  orbital. As in these orbitals the coefficient on Cl is zero for symmetry reasons,  $\phi_3C^+$  has a charge density zero on Cl in its  $E_S$  or  $E_A$  state. This means that to a very good approximation the  $e_S$  and  $e_A$  orbitals can be constructed from the benzene<sup>+</sup>-orbitals, which in turn are symmetry-determined. Consequently one would consider  $e_S$  and  $e_A$  to be very adequate orbitals for  $\phi_3C^+$ . The non-bonding orbital however, its coefficient at Cl not being determined by symmetry, might have coefficients different from those in figure 11.

This means that the first term in (14) will retain its form, being negative for a 30° propeller. However, the repulsion term in  $(E_S|H|E_A)$  which contains the nonbonding m.o., might change somewhat. If the absolute magnitude of the coefficient at Cl in the  $a_2$ -orbital is larger than  $2/\sqrt{13}$  - and SCF calculations bear out this to be the case - all charges in figure 15 will be somewhat smaller, resulting in a smaller Coulomb interaction. But the interaction stays repulsive. In conclusion we therefore judge it necessary and significant to include in  $(E_S|H|E_A)$  the bonding between the rings to obtain a negative value for the matrix element as is imperative to conciliate the signs of the calculated and observed magnetic moments in the lowest excited states of the triarylcarbenium ions.

## 7. Discussion

From the experimental MCD spectra of the cations  $(p-X-\phi)_3C^+$  where  $X = H, CH_3, C(CH_3)_3$  and Cl it is found that the value of  $A_1/D_1$  is maximum for the trityl cation and decreases as a function of the substituent X. With a simple model, which makes use of the Hückel orbitals of  $\phi_3C^+$ , the signs of the magnetic moments can be understood if care is taken not to neglect the bonding between different rings. The magnitudes of the magnetic moments are governed by (9) and vary in the series because  $c_1/c_2$  changes as a function of  $\Delta E$ .

It may be useful at this point to consider the magnetic moments in the  $Ar_3C^+$  series from a slightly different point of view. If the complex wave functions (3) are used to describe the highest bonding e-level in  $\phi_3C^+$  one obtains

$$\begin{cases}
 \psi^{++} = \frac{1}{3\sqrt{2}} \sum_J \sum_{1J} e^{+\frac{2\pi i}{3} J} e^{+\frac{2\pi i}{6} 1J} \phi_{1J} \\
 \psi^{--} = (\psi^{++})^* \\
 \psi^{+-} = \frac{1}{3\sqrt{2}} \sum_J \sum_{1J} e^{+\frac{2\pi i}{3} J} e^{-\frac{2\pi i}{6} 1J} \phi_{1J} \\
 \psi^{-+} = (\psi^{+-})^*
 \end{cases} \quad (15)$$

As can be easily verified, this set is related to (4) by

$$\begin{aligned}
 \psi^{++} &= (\psi^{--})^* = \frac{1}{2} \{ (e_S^x - e_A^x) + i(e_S^y - e_A^y) \} \\
 \psi^{+-} &= (\psi^{-+})^* = \frac{1}{2} \{ (e_S^x + e_A^x) + i(e_S^y + e_A^y) \}
 \end{aligned} \quad (16)$$

In the orbitals (15) one may recognize two relevant aspects. Firstly there are the complex coefficients  $\exp(\pm\frac{2\pi i}{3} J)$  which derive from the  $C_3$  symmetry of the propeller and secondly the coefficients  $\exp(\pm\frac{2\pi i}{6} 1J)$  which arise from the local  $C_6$  symmetry of the propeller blades. Although both coefficients can give rise to angular momentum, it is not hard to see that the magnetic moment due to  $\exp(\pm\frac{2\pi i}{6} 1J)$  will by far outweigh that due to  $\exp(\pm\frac{2\pi i}{3} J)$ , since of course the magnitude of the angular momentum depends heavily on the extent to which the orbital motion of the electrons around an axis is actually possible. The magnetic moment in an  $E_S$  state, deriving from the orbitals  $\frac{1}{\sqrt{2}}(e_S^x \pm ie_S^y)$  originates from the circular motion of the electrons around the  $C_3$ -axis and is therefore very small. If however, the excited state is of the type  $E_S-E_A$ , a large magnetic moment arises from the in-phase circular motion of the electrons around the local  $C_6$ -axes. Although the threefold axis of symmetry in the triarylcarbenium ions is indispensable for the occurrence of A-terms in the MCD (without it no degenerate states were possible), the presence of the complex benzene-like orbitals in the molecular wave function actually determines the magnitude of the A-term. Reasoning along these lines the A-terms of the substituted trityl cations may be viewed upon as follows. The highest occupied m.o.'s of the  $Ar_3C^+$  system result from a combination, like in (4), of the highest occupied m.o.'s of the  $ArH$  molecule. The latter are exactly degenerate if  $ArH$  is benzene, but are split in their real components

if ArH is toluene, t-butylbenzene or chlorobenzene. In these cases magnetic moment is present only to the extent that configuration interaction in the  $\text{Ar}_3\text{C}^+$  ion restores partly the complex character of the benzene orbitals. This explains the decrease in  $A_1/D_1$  going from the trityl cation to  $(\text{p-X-}\phi)_3\text{C}^+$  with  $\text{X} = \text{CH}_3$ ,  $\text{C}(\text{CH}_3)_3$  or  $\text{Cl}$ .

In dimethylaniline or anisole the highest occupied  $\pi$ -electron m.o.'s not only are split but in addition they have presumably lost to a fair extent their  $\phi_S$  and  $\phi_A$  character (mesomeric effect). This leads to a vanishing value of  $A_1/D_1$  for the trianisylcarbenium ion and crystal violet. We hasten to add that, of course, zero A/D values can also result from the absence of trigonal symmetry. We mention this as a possibility for crystal violet, since X-ray diffraction studies on solid  $(\text{p-NH}_2\text{-}\phi)_3\text{C}^+\text{ClO}_4^-$  indicate<sup>15)</sup> that here the cation is an unsymmetrical propeller with twist angles of  $29^\circ$ ,  $34^\circ$  and  $34^\circ$  (but the trianisylcarbenium ion in the solid state has  $D_3$  symmetry<sup>16)</sup>).

In the triphenylcarbenium ion  $E_1$  to a good approximation is described by the wave functions  $\Psi^{+-}$  and  $\Psi^{-+}$ ,  $E_2$  by  $\Psi^{++}$  and  $\Psi^{--}$ . As the magnitude of the magnetic moment is determined by the complex coefficients  $\exp(\pm \frac{2\pi i}{6} 1_j)$ ,  $\Psi^{+-}$  and  $\Psi^{--}$  denote the low-energy Zeeman components of  $E_1$  and  $E_2$ , respectively. However, this does not yet fix the signs of A/D since the coefficient  $\exp(\pm \frac{2\pi i}{3} J)$  determines whether the lowest Zeeman component is accessible by right or by left circularly polarized light. This situation is quite contrary to that with aromatic systems that approach cylindrical symmetry (e.g. triphenylene<sup>17)</sup>, coronene<sup>17)</sup> and porphyrins<sup>18)</sup>) where, because of the presence of one complex coefficient in the wave function of a degenerate excited state, the lowest Zeeman component always transforms as the operator for right circularly polarized light, resulting in positive A/D values. In the  $E_1$  state of  $\phi_3\text{C}^+$  both complex coefficients are in antiphase, leading to a negative A/D value.

## References

1. G.N.Lewis and M.Calvin, 1939, Chem.Rev. 25, 273  
G.N.Lewis, T.T.Magel and D.Lipkin, 1942, J.Amer.Chem.Soc. 64, 1774
2. M.S.Newman and N.C.Deno, 1951, J.Amer.Chem.Soc. 73, 3644
3. D.W.A.Sharp and N.Sheppard, 1957, J.Chem.Soc. 674
4. R.E.Weston, Jr., A.Tsukamoto and N.N.Lichtin, 1966, Spectrochim.Acta 22, 433
5. A.H.Gomes de Mesquita, C.H.MacGillavry and K.Eriks, 1965, Acta Cryst. 18, 437
6. I.I.Schuster, A.K.Colter and R.J.Kurland, 1968, J.Amer.Chem.Soc. 90, 4679  
R.Dehl, W.R.Vaughan and R.S.Berry, 1959, J.Org.Chem. 24, 1616  
J.Chem.Phys. 34, 1460  
R.J.Kurland, I.I.Schuster and A.K.Colter, 1965, J.Amer.Chem.Soc. 87, 2279  
A.K.Colter, I.I.Schuster and R.J.Kurland, 1965, J.Amer.Chem.Soc. 87, 2278  
J.W.Rakshys, Jr., S.V.McKinley and H.H.Freedman, 1970, J.Amer.Chem.Soc. 92, 3518  
1971, J.Amer.Chem.Soc. 93, 6522
7. M.S.de Groot, I.A.M.Hesselmann and J.H.van der Waals, 1966, Mol.Phys. 10, 241
8. A.D.Buckingham and P.J.Stephens, 1966, Ann.Rev.Phys.Chem. 17, 399
9. P.N. Schatz and A.J.McCaffery, 1969, Quarterly Reviews 23, 552
10. W.Th.A.M.van der Lugt, 1968, Thesis Leiden
11. M.Goeppert-Mayer and A.L.Sklar, 1938, J.Chem.Phys. 6, 645
12. G.Herzberg, Electronic Spectra and Electronic Structure of Polyatomic Molecules (D.van Nostrand Co., Inc., Princeton, N.J., 1966) p.12
13. R.G.Parr, Quantum Theory of Molecular Electronic Structure (W.A.Benjamin, Inc., New York, 1963)
14. A.Brickstock and J.A.Pople, 1954, Trans.Farad.Soc. 50, 901
15. K.Erics. Cited by H.H.Freedman in G.A.Olah and P.von R.Schleyer, Carbonium Ions IV (Wiley Interscience, New York, 1973) p.1560
16. P.Anderson and B.Klewe, 1965, Acta Chem.Scand. 19, 791
17. P.J.Stephens, P.N.Schatz, A.B.Ritchie and A.J.McCaffery, 1968, J.Chem.Phys. 48, 132
18. V.E.Shashoua, 1965, J.Amer.Chem.Soc. 87, 4044  
P.J.Stephens, W.Suetaka and P.N.Schatz, 1966, J.Chem.Phys. 44, 4592  
E.A.Dratz, Ph.D.Thesis University of California, Berkeley, 1966

### CHAPTER III

#### MAGNETIC CIRCULAR DICHROISM OF AZULENE

##### 1. Introduction

The absorption spectrum of azulene in an alkane solvent (see figure 1) in the visible and UV region consists of four transitions. The weak  $O \rightarrow A$  band ( $\nu_{\max} 15700$ ;  $\epsilon_{\max} 326$ ) is known to be y polarized (for the definition of the molecular axes see figure 2) and the  $O \rightarrow B$  transition ( $\nu_{\max} 29200$ ;  $\epsilon_{\max} 4700$ ) is x polarized as found from polarized absorption measurements on a solid solution of azulene in a naphthalene crystal<sup>1)</sup>. The very strong band ( $\epsilon_{\max} 53200$ ) at  $36400 \text{ cm}^{-1}$  is long axis polarized. It is the fourth singlet-singlet transition since absorption polarization measurements<sup>2)</sup> reveal that the shoulder at  $33800 \text{ cm}^{-1}$  ( $\epsilon_{\max} 4050$ ) is a separate y polarized band ( $O \rightarrow C$ ).

From an inspection of the MCD spectrum of azulene (figure 1) it appears that, while the MCD in the  $O \rightarrow A$  and  $O \rightarrow C$  bands behaves normally (in the sense that MCD and absorbance have similar band shapes), the MCD in the  $O \rightarrow B$  band does not. As will be shown in the second part of this chapter, the very peculiar shape of the magnetic circular dichroism in the  $O \rightarrow B$  band is brought about by vibronic coupling via totally symmetric vibrations.

Although azulene is a non-alternating hydrocarbon and therefore lacks the so-called pairing properties, Pariser<sup>3)</sup> succeeded in predicting qualitatively the azulene absorption spectrum, including in his calculation configuration interaction between singly excited configurations, based on Hückel MO's.

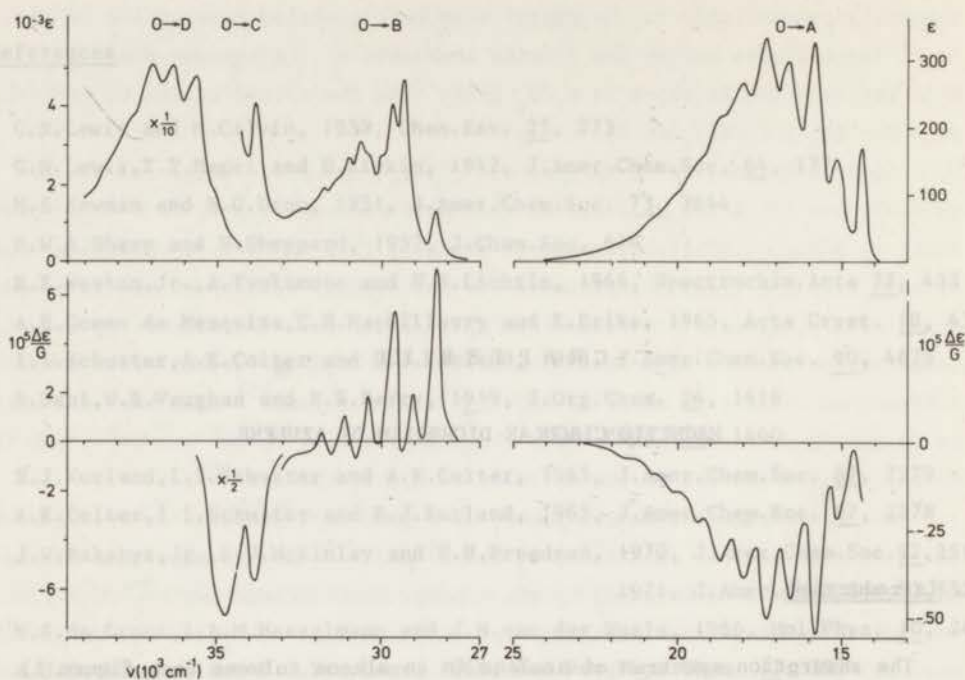


Figure 1. Unpolarized absorption (top half) and magnetic circular dichroism per Gauss (lower half) of azulene in *n*-heptane at room temperature.

We will show that MO theory can also account qualitatively for the MCD in at least the  $O \rightarrow A$  and  $O \rightarrow C$  bands. Despite this favourable result we pursue matters further and also calculate the MCD in the  $O \rightarrow A$  and  $O \rightarrow C$  transitions using the experimental values of transition energies and electric dipole matrix elements (but, of course, calculated values for magnetic dipole transition moments) in the molecular orbital calculations. This is taken to indicate that the relevant magnetic dipole matrix elements are calculated correctly in MO theory. The latter result is important in the discussion of the MCD in the  $O \rightarrow B$  band, in which we need reliable values of magnetic dipole transition moments.

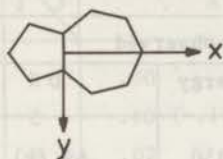


Figure 2.  
Reference frame for azulene.

## 2. MO calculations

Using the experimentally determined geometry<sup>4)</sup> of azulene a SCF - MO calculation of the PPP type was performed followed by configuration interaction between all singly excited states. Matrix elements of the electric dipole operator  $\vec{F}$ , the magnetic dipole operator  $\vec{\mu}$  and electric dipole velocity operator  $\vec{v}$  between the ground state and excited states and between singly excited states were calculated using either  $2p_z$  - atomic orbitals or Löwdin orthogonalized atomic orbitals. Some of the results of these calculations are tabulated in Table I - IV.

The transition energies and dipole strengths from our calculations are in essential agreement with those found by Pariser<sup>3)</sup>, Bloor<sup>5)</sup> and other authors<sup>6)7)8)</sup>. As can be seen from an inspection of Table I they also compare favourably with experiment since it will appear later that the observed dipole strength of the  $0 \rightarrow C$  transition is a minimum value while that of the  $0 \rightarrow B$  band contains a large amount of vibronically induced intensity (meaning that the experimental value of  $x_{OB}^2$  will be lower than 3.20).

The calculated matrix elements in Table II - IV are obtained from Löwdin ao's. When in the calculation a different value results from the use of Slater ao's, this value is put in parentheses.

Table I Calculated and observed transition energies  $[\text{cm}^{-1}]$ , dipole strengths  $[\text{Debye}^2]$  and polarization directions.

Transition	calculated		observed	
	energy	D	energy	D
0 $\rightarrow$ A	17580	2.96 (y)	14350	.69 (y)
0 $\rightarrow$ B	27700	2.37 (x)	28370	3.20 (x)
0 $\rightarrow$ C	35550	11.29 (y)	33800	2.07 (y)
0 $\rightarrow$ D	39550	104.45 (x)	35650	42.51 (x)

Experimental frequencies are those for the various (0,0) transitions.

Table II Cartesian components of  $\vec{r}_{IJ}$  [Debye]

I \ J	O	A	B	C	D
O	2.64 (x)				
A	1.74 (y)	-2.06 (x)			
B	1.54 (x)	.64 (y)	-2.83 (x)		
C	3.36 (y)	-2.34 (x)	1.21 (y)	-2.21 (x)	
D	10.13 (x)	1.46 (y)	-.41 (x)	-1.05 (y)	-3.36 (x)

Table III Matrix elements  $\mu_{IJ}^z$  [i.Bohr magneton]

I \ J	O	B	D
A	-.39 (-.36)	-2.06 (-1.92)	.11 (.26)
C	-.11 (-.06)	1.18 (1.14)	-.48 (-.24)



Table IV Cartesian components of  $\nabla_{IJ}$   $[e A^{-1}]$

I \ J	A	B	C
B	.00 (y)	0	
C	-.10 (-.11) (x)	.04 (y)	0
D	.02 (y)	-.03 (-.04) (x)	.03 (.04) (y)

3. The MCD in the  $0 \rightarrow A$  and  $0 \rightarrow C$  transitions

3a. The  $0 \rightarrow A$  transition

The general expression for the MCD in electric dipole allowed transitions in isotropic solutions was discussed in chapter I. When considering the singlet-singlet transitions of azulene, there are no degenerate states which could be split by a magnetic field and it is sufficient to consider the MCD B-terms only. A further consequence of the absence of degeneracy is that all electronic and vibrational wave functions may be chosen real. The MCD in a y polarized transition  $a \rightarrow j$  of azulene is in the  $\pi$ -electron approximation given by

$$B(a \rightarrow j) = -\text{Im} \left[ \sum_{k \neq a, j} \left\{ \frac{\mu_{ka}^z}{E_{ka}} x_{jk} + \frac{\mu_{jk}^z}{E_{kj}} x_{ka} \right\} + \frac{\mu_{ja}^z}{E_{ja}} (x_{jj} - x_{aa}) \right] y_{aj} \quad (1)$$

Dealing with spectra which do not show rotational structure, the indices in (1) refer to vibronic states.

If the relevant transitions in a given spectrum show poor vibrational fine structure only, it is usual to use (1) as it stands on the understanding that the indices a, k and j refer to electronic states. Strictly speaking, this is only true if the vibrational manifolds in the groundstate and all excited states are identical and vibronic coupling is absent. Then  $B(a \rightarrow j)$  and  $D(a \rightarrow j)$  have the same band forms. Having in azulene an extensive  $0 \rightarrow A$  band with a clear fine structure we can study the dependence of B/D in this transition as a function of frequency, without adopting the abovementioned assumption of identical vibrational wave functions in all states.

In the Born-Oppenheimer approximation, neglecting for the moment the dependence of electronic matrix elements on nuclear coordinates and assuming that only the zero point vibrational level of the groundstate is populated, we may describe the vibronic states by a product of an electronic wave function, defined for a fixed nuclear geometry and a vibrational wave function. Studying the transition from the vibronic groundstate to different vibrational levels of the A state, we make the substitution

$$\begin{aligned} a &\rightarrow O_o \\ j &\rightarrow A_a \\ k &\rightarrow K_k \end{aligned} \quad (2)$$

From now on we shall use in this chapter capital letters to denote electronic wave functions, evaluated at the groundstate equilibrium geometry of the molecule, and lower case letters to denote the vibrational wave functions of these states.

The dipole strength in the individual transition we consider is then given by

$$D(O_o \rightarrow A_a) = y_{OA}^2 (o|a)(a|o) \quad (3)$$

Using the sum rule we find  $D(O \rightarrow A) = \sum_a D(O_o \rightarrow A_a) = y_{OA}^2$  (3a)

Incorporating (2) in equation (1) and reducing the sum over vibronic states to one over electronic states and one over vibrational states (making use of the fact that vibrational wave functions belonging to the same electronic state form an orthonormal set) we get

$$B(O_o \rightarrow A_a) = -\text{Im} \left[ \sum_{K \neq O, A} \sum_k \left\{ \frac{\mu_{KO}^z}{E_{Kk} - E_{Oo}} x_{AK} (a|k)(k|o) + \frac{\mu_{AK}^z}{E_{Kk} - E_{Aa}} x_{KO} (a|k)(k|o) \right\} + \frac{\mu_{AO}^z}{E_{Aa} - E_{Oo}} (x_{AA} - x_{OO})(a|o) \right] y_{OA} (o|a)$$

Rewriting an energy difference between vibronic states as a sum of an electronic and a vibrational energy difference ( $E_{Ii} - E_{Jj} = E_I - E_J + \epsilon_i - \epsilon_j = E_{IJ} + \epsilon_{ij}$ ) we obtain

$$B(O_o \rightarrow A_a) = -\text{Im} \left[ \sum_{K \neq O, A} \sum_k \left\{ \frac{\mu_{KO}^z}{E_{KO} + \epsilon_{ko}} x_{AK} (a|k)(k|o) + \frac{\mu_{AK}^z}{E_{KA} + \epsilon_{ka}} x_{KO} (a|k)(k|o) \right\} + \frac{\mu_{AO}^z}{E_{AO} + \epsilon_{ao}} (x_{AA} - x_{OO})(a|o) \right] y_{OA} (o|a) \quad (4)$$

The evaluation of  $B(O_0 \rightarrow A_a)$  requires knowledge of electronic matrix elements and energies, and of vibrational integrals and energies. Reasonable estimates of the electronic quantities may be made, e.g. from semi-empirical quantum-chemical calculations, but the vibrational overlap-integrals and energies are much more difficult to obtain theoretically. One therefore mostly neglects all  $\epsilon$ 's when calculating the total electronic MCD. In §3b we also will make use of this approximation, which we shall discuss further in §3c.

### 3b. Numerical calculations

The total MCD in the visible absorption band of azulene is obtained by summing  $B(O_0 \rightarrow A_a)$  over all vibrational fine structure  $a$ .

$$\sum_a B(O_0 \rightarrow A_a) = B(O \rightarrow A) \quad (5)$$

When neglecting all  $\epsilon$ 's, we can perform the summation over  $a$  in equation (4) to obtain

$$B(O \rightarrow A) = -\text{Im} \left[ \sum_{K \neq O, A} \left\{ \frac{\mu_{KO}^z}{E_{KO}} x_{AK} + \frac{\mu_{AK}^z}{E_{KA}} x_{KO} \right\} + \frac{\mu_{AO}^z}{E_{AO}} (x_{AA} - x_{OO}) \right] y_{OA} \quad (6)$$

With the help of the calculated electric and magnetic transition dipole matrix elements and energies (Table I - III) we now can find the contributions of all terms in (6) to  $B(O \rightarrow A)$ . Because the only appreciable contributions prove to be those from the last term and from the second term with  $K = B$  or  $D$ , we may write

$$B(O \rightarrow A) \approx -\text{Im} \left[ \frac{\mu_{AB}^z}{E_{BA}} x_{BO} + \frac{\mu_{AD}^z}{E_{DA}} x_{DO} + \frac{\mu_{AO}^z}{E_{AO}} (x_{AA} - x_{OO}) \right] y_{OA} \quad (7)$$

Using this expression, Table V is constructed. From this table one finds  $B(O \rightarrow A) = + .636 \cdot 10^{-3} \beta D^2$  cm. If we had included all terms from (6), taking into account the lowest 10 singlet states,  $B(O \rightarrow A)$  would have taken the value  $+ .602 \cdot 10^{-3} \beta D^2$  cm. This rather small difference only in part results from cancelling contributions, the absolute magnitude of the individual terms which are omitted in constructing Table V being smaller than  $.05 \cdot 10^{-3}$ . From the table we conclude that the calculated B term has the right sign, but is over-estimated. To a marked extent this is to be ascribed to the fact that the absolute magnitudes of the electric dipole transition moments and electric dipole moments, that follow from the calculations, are too large. If we use

Table V Contributions of the terms in (7) to B(O→A)

	first term	second term	last term	total
MO theory (Löwdin ao's)	+ .536	-.082	+ .182	+ .636
MO theory (Slater ao's)	+ .507	-.207	+ .166	+ .466
$\vec{r}_{IJ}$ and $E_{IJ}$ from experiment, $\mu^z_{IJ}$ from MO theory (Löwdin ao's)	+ .207	-.024	+ .023	+ .21
observed				

Units:  $10^{-3} \beta D^2 \text{ cm}$

The second row is obtained using experimental (o,o) transition energies and experimental electric dipole transition moments, the signs of which are assumed to be the same as that calculated. The value +.207 results from the use of the total dipole strength of the B band. However, because this band is subject to strong vibronic coupling, the actual experimental value of  $x_{OB}$  should be about half as low, which reduces the value for the total calculated B(O→A) from +.21 to +.10 .

for these the experimental values (cf. third row in Table V and the footnote attached to that table), the value of B surprisingly well agrees with the experimental one, being predominantly determined by the magnetic coupling of the states A and B.

### 3c. Further discussion of equation (4)

The quantum-chemical calculations bear out that the second term of (4) is dominating the MCD. Since it is reasonable to assume that this result does not rest on the neglect of vibrational energy differences in (4), we now can discuss some aspects of this neglect in more detail.

The second term of (4), which we repeat here for convenience, reads

$$-\text{Im} \sum_{K \neq 0, A} \mu^z_{AK} x_{KO} y_{OA} \left[ \frac{(a|k)(k|o)}{E_{KA} + \epsilon_{ka}} \right] (o|a) \quad (8)$$

While in the last term of (4) the necessary vibrational matrix elements and energy differences could be extracted from experiment, this is not possible in (8). In fact, we might find the absolute magnitudes for the Franck-Condon factors  $(o|a)$  and  $(k|o)$ , but the quantities  $(a|k)$  and  $\epsilon_{ka}$ , being related to transitions between excited vibronic states, are not within direct experimental reach. Therefore we must look for other ways to evaluate the expression between square brackets in (8).

When the electronic transitions to A and K have a large separation compared to their band widths we have to a good approximation

$$\sum_k \frac{(a|k)(k|o)}{E_{KA} + \epsilon_{ka}} (o|a) = \frac{(a|o)(o|a)}{E_{KA}} \quad (9)$$

and MCD and absorption will have the same band forms as indeed is mostly assumed. We remark however that, strictly speaking, the equality expressed in (9) only holds exactly when the sets of vibrational wave functions  $\{a\}$  and  $\{k\}$  are identical, since we then have

$$(a|k) = \delta_{ak} \quad (10)$$

$$\text{and } \epsilon_{ka} = 0 \text{ if } k=a$$

Note that the equations (10) imply the absorptions  $O \rightarrow A$  and  $O \rightarrow K$  to have identical shapes, which from experiment is known not to be true in general. Conversely, a constant B/D value in an electronic absorption band does not necessarily mean that (9) is valid: when writing down the equality

$$\sum_k \frac{(a|k)(k|o)}{E_{KA} + \epsilon_{ka}} (o|a) = \frac{(a|o)(o|a)}{E_{KA} + \epsilon(a)} \quad (11)$$

With  $\epsilon$  as an unknown quantity, the constancy of B/D merely signifies that  $\epsilon$  is not a function of  $a$ . That is

$$\sum_k \frac{(a|k)(k|o)}{E_{KA} + \epsilon_{ka}} (o|a) = \frac{(a|o)(o|a)}{E_{KA} + \text{constant}} \quad (12)$$

It is tempting to conclude from the rather constant experimental B/D value (compare Table VI) in the long A band of azulene, in which the MCD is introduced to a large extent by coupling with the near state B, that

Table VI B/D values in the first absorption band of azulene.

band	$\lambda$ (nm)	$\nu$ ( $\text{cm}^{-1}$ )	$10^4$ B/D ( $\beta$ cm )
1	697	14347	1.57
2	659	15175	1.57
3	630	15873	1.82
4	602	16610	1.65
5	577	17331	1.65
6	555	18018	1.65
7	538	18587	1.70
8	520	19230	1.58
9	498	20080	1.52
10	481	20790	1.62

The B and D values for the individual vibrational bands were obtained by dividing the total B (  $.100 \cdot 10^{-3} \beta D^2$  cm ) and D (  $.685 D^2$  ) over the vibrational bands with weighting factors  $p_i / \nu_i$  ( $p_i$  is the height and  $\nu_i$  the frequency of the peak).

equation (12) holds to a good approximation in this case. We must be careful at this point however, as a large fraction of the total intensity in the B band is brought about by vibronic coupling via totally symmetric vibrations (see §4), implying that also the magnetic dichroism of vibrational sublevels of the A band is no longer completely described by (4).

The last term of (4), although not contributing appreciably to the MCD of the O→A transition (cf. §3b) in itself is interesting since it describes the contribution to the MCD of the change of static electric dipole moment in a vibronic transition. From (4) it follows that the frequency dependence of this contribution is governed by

$$\frac{(o|a)(a|o)}{E_{AO} + \epsilon_{ao}} \quad (13)$$

The denominator of this function being the energy of the transition Oo→Aa

and the enumerator the Franck-Condon factor which determines what part of the total dipole strength is present in the vibrational band considered (see equations 3 and 3a), one can find the function (13) from the experimental absorption spectrum. We note the particular frequency dependence of the last term in (4). Combined with the expression for the dipole strength (equation 3) we obtain when limiting ourselves to the last term in (4)

$$\frac{B(O_0 \rightarrow A_a)}{D(O_0 \rightarrow A_a)} = \frac{\mu_{AO}^z}{E_{Aa} - E_{O_0}} \frac{x_{AA}^{-x_{OO}}}{y_{OA}} \quad (14)$$

It follows that this ratio is proportional to  $\lambda$ , the wavelength of absorption. Whenever the last term of (4) should dominate the MCD, the experimental B/D ratio must be proportional to  $\lambda$ , being a maximum for the (o,o) band and decreasing when proceeding towards shorter wavelengths. Especially in the broad O $\rightarrow$ A transition of azulene this frequency dependence should be very pronounced. From the experimental B/D values for this transition (cf. Table VI) we cannot detect a lowering of B/D going to shorter wavelengths and we conclude that the change of electric dipole moment does not contribute decisively to the MCD (which is in complete accord with the results from the quantum-mechanical calculations).

### 3d. The O $\rightarrow$ C transition

From fluorescence polarization experiments the shoulder in the absorption spectrum at 33800 cm<sup>-1</sup> is known to be short axis polarized<sup>2)</sup>. As its neighbouring bands are both x polarized, it is a separate electronic transition. Such a transition indeed is predicted in MO theory.

When restricting ourselves to the five lowest singlet states and using the same approximations as we did in the calculation of the magnetic circular dichroism of the O $\rightarrow$ A transition, the MCD of the (o, $\bar{o}$ ) band of the second y polarized transition in azulene is given by

$$B(O_0 \rightarrow C\bar{0}) \approx -\text{Im} \left[ \frac{\mu_{CB}^z}{E_{BC}} x_{BO} + \frac{\mu_{CD}^z}{E_{DC}} x_{DO} + \frac{\mu_{CO}^z}{E_{CO}} (x_{CC}^{-x_{OO}}) \right] y_{CO} (o|\bar{o})(\bar{o}|o) \quad (15)$$

and the dipole strength in the same vibrational band is

$$D(O_0 \rightarrow C\bar{0}) = y_{CO}^2 (o|\bar{o})(\bar{o}|o) \quad (16)$$

In Table VII the contributions of the three terms of (15) to the value of  $B(O_0 \rightarrow C\bar{0}) / D(O_0 \rightarrow C\bar{0})$  are tabulated. The largest share in the MCD of the O→C transition is taken by the magnetic coupling with the close and very intense D band (second term of equation 15). Coupling with B is less important; although the magnetic dipole transition moment in this case is larger, it cannot by far compensate for the much smaller  $x_{BO} / E_{BC}$  ratio.

Table VII Contributions of the terms of (15) to  $B(O_0 \rightarrow C\bar{0}) / D(O_0 \rightarrow C\bar{0})$

	first term	second term	last term	total
MO theory (Löwdin ao's)	+0.069	+0.367	+0.005	+0.441
MO theory (Slater ao's)	+0.067	+0.179	+0.003	+0.248
$\vec{r}_{IJ}$ and $E_{IJ}$ from experiment, $\mu_{IJ}^z$ from MO theory (Löwdin ao's)	+0.12	+1.12	----	+1.24
observed				+0.31

Units:  $10^{-3} \beta$  cm.

Since the absolute value for  $y_{CO}$  is a lower bound (see text) the actual value of B/D will be smaller than 1.24. The observed B/D value will be higher if in the absorption spectrum at  $33800 \text{ cm}^{-1}$  there is also O→D intensity present.

From a comparison of the two last rows of Table VII we conclude that  $\mu_{DC}^z$  is calculated with the correct sign, its absolute magnitude being too large rather than too small. This conclusion, most probably, is not violated when we take into account the relatively large uncertainty in the energy denominator in the second term of (15) which describes the MCD in the  $(o, \bar{o})$  band of the O→C transition due to magnetic coupling with the Dd manifold.

The magnetic coupling of the Cc and Dd manifolds is also of consequence for the MCD in the O→D band. If the latter transition acquires its ellipticity predominantly from the coupling with the state C, one expects  $B(O \rightarrow D) \approx -B(O \rightarrow C)$ .



Since however  $D(O \rightarrow D)$  is larger than  $D(O \rightarrow C)$  by an order of magnitude, it may be understood that the MCD of the  $O \rightarrow D$  band is too small to detect. On inspection of figure 1, it follows that the shoulder at  $35000 \text{ cm}^{-1}$  on the broad D band is in fact to a large extent brought about by the  $O \rightarrow C$  transition. This could place the origin of the  $O \rightarrow D$  band near  $35650 \text{ cm}^{-1}$ . Moreover it shows that the  $O \rightarrow C$  transition is partly overwhelmed by the much stronger  $O \rightarrow D$  band. Assuming the  $(o, \bar{o})$  band of  $O \rightarrow C$  is pure, the experimental dipole strength of the  $O \rightarrow C$  transition is larger than  $2.07 D^2$ .

### 3e. Origin dependence

In calculating B terms of low symmetry compounds one encounters the problem of origin dependence<sup>9)10)</sup>. This problem arises because in the numerical calculation of  $B(a \rightarrow j)$  one limits the sum in (1) to a restricted basis set  $k$ . As a result the MCD in  $y$  polarized bands in azulene, which has  $C_{2v}$  symmetry, depends on the choice of origin, and we now investigate how seriously this could influence our results for the  $O \rightarrow A$  and  $O \rightarrow C$  transition.

When our calculation would yield a correct result with an origin lying at some point X at the x-axis (see figure 1), the origin dependent part of  $\mu_{ij}^z$  in (1) equals  $XV_{ij}^y$ . It is reasonable to assume that in azulene this origin lies somewhere in between the centers of the five and seven membered rings, that is  $|X| < 2 \text{ \AA}$ . It then can easily be seen from a comparison of the  $V_{ij}^y$  (see Table IV) with the corresponding  $\mu_{ij}^z$ , which determine the MCD in the  $O \rightarrow A$  and  $O \rightarrow C$  transitions (see Table III), that for azulene the origin dependent parts may contribute to a very minor extent to the relevant magnetic dipole transition moments.\*) As in addition it can be shown that no new terms, other than those already included, enter the expressions for the MCD of the  $O \rightarrow A$  and  $O \rightarrow C$  bands, we conclude that the magnetic circular dichroism of azulene in the visible and ultraviolet region of the spectrum is practically origin independent. This favourable result emerges because states which are coupled strongly by the magnetic field and thus form the basis for the MCD, are only weakly coupled by the electric dipole velocity operator.

\*) Although the electric dipole moments  $x_{jj}$  and  $a_{aa}$  are origin dependent, their difference is not.

#### 4. The O + B band of azulene

##### 4a. Introduction

The O+B transition of azulene has, when measured as a solid solution of azulene in a naphthalene crystal at low temperatures, an extraordinary rich vibrational fine structure<sup>1)11)</sup>. In fact, the number of lines is so numerous that the spectrum could only tentatively be assigned<sup>1)</sup>. The spectrum, which changes if naphthalene as a host is substituted by durene, biphenyl or cyclododecane<sup>12)</sup>, is predominantly x polarized, although some perpendicularly polarized intensity is present too.

In an important paper<sup>13)</sup> Hunt and Ross, who studied the gas phase spectrum, proposed that the B state of azulene strongly couples with the D state by means of totally symmetric vibrations. They estimated that the greater part of the intensity in the O+B band originates from the nearby and intense O+D transition.

On inspection of the observed spectra in solution (figure 3) one notes the peculiar behaviour of the MCD in the O+B band, the shape of which is quite different from that of the unpolarized absorption, and we thought it would be interesting to see whether vibronic coupling effects can account for the observed phenomena. In doing this our discussion will be centered around the following points.

First we show that vibronic coupling involving nontotally symmetric vibrations cannot explain the characteristic band shape of the MCD in the O+B band.

Secondly, we analyze the ordinary absorption and the MCD spectrum allowing for vibronic interaction between the states B and D via totally symmetric modes. This analysis not only establishes the precise amount of borrowed intensity in the O+B band system, it also provides a quantitative answer about the different mechanisms that are responsible for the intensity throughout the entire band system.

Lastly, we shall discuss some consequences of the results obtained, particularly how they compare with the thorough study of the O+B band which was made recently by Lacey et al<sup>12)</sup>.

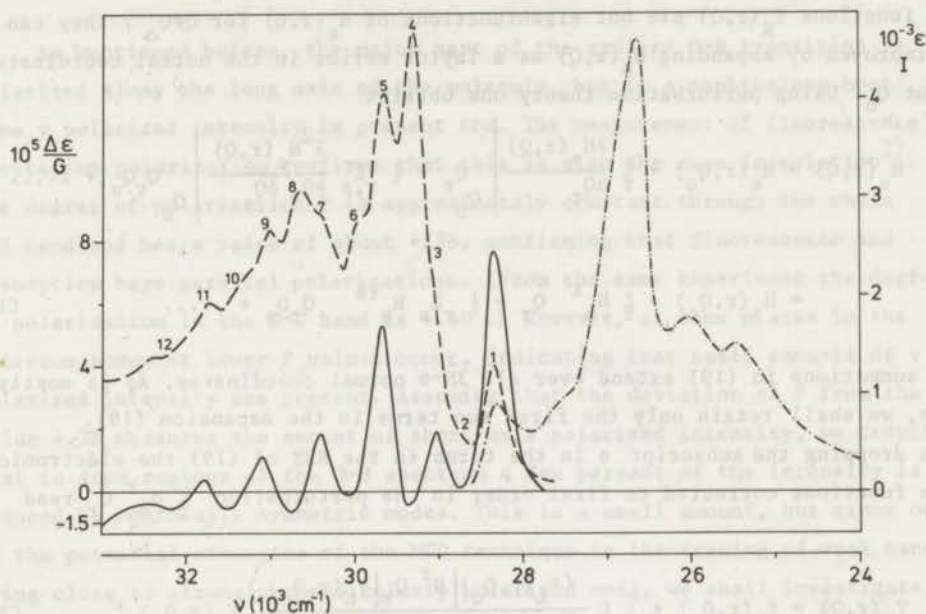


Figure 3.  $O \rightarrow B$  band of azulene in *n*-heptane at room temperature. Absorption (---), fluorescence (-.-.-) and MCD (—). The fluorescence spectrum is not corrected for the efficiency of the detection system.

#### 4b. Vibronic coupling

The complete Hamiltonian for a molecular system is a function of the coordinates of all electrons and nuclei (denoted by  $r$  resp.  $Q$ ).

$$H_{\text{total}} = T_e + V(r, Q) + T_n = H_e(r, Q) + T_n \quad (17)$$

When we solve the Schrödinger equation

$$H_e(r, Q_0) \psi_K(r, Q_0) = E_K(Q_0) \psi_K(r, Q_0) \quad (18)$$

with  $H_e$  defined at the nuclear equilibrium configuration  $Q_0$  in the ground state, the functions  $\psi_K(r, Q)$  are not eigenfunctions of  $H_e(r, Q)$  for  $Q \neq Q_0$ . They can be improved by expanding  $H_e(r, Q)$  as a Taylor series in the normal coordinates about  $Q_0$ . Using perturbation theory one obtains

$$\begin{aligned}
 H_e(r, Q) &= H_e(r, Q_0) + \sum_r \frac{\partial H_e(r, Q)}{\partial Q_r} \bigg|_{Q_0} Q_r + \frac{1}{2} \sum_{r,s} \frac{\partial^2 H_e(r, Q)}{\partial Q_r \partial Q_s} \bigg|_{Q_0} Q_r Q_s + \dots \\
 &= H_e(r, Q_0) + \sum_r H_e^r Q_r + \frac{1}{2} \sum_{r,s} H_e^{rs} Q_r Q_s + \dots
 \end{aligned}
 \tag{19}$$

The summations in (19) extend over all  $3N-6$  normal coordinates. As is mostly done, we shall retain only the first two terms in the expansion (19).

When dropping the subscript  $e$  in the terms in the RHS of (19) the electronic wave functions corrected to first order in the perturbation  $\sum_r H_e^r Q_r$  read

$$\psi_K(r, Q) = \psi_K(r, Q_0) + \sum_L \sum_r \frac{(\psi_L(r, Q_0) | H^r Q_r | \psi_K(r, Q_0))}{E_K(Q_0) - E_L(Q_0)} \psi_L(r, Q_0)
 \tag{20}$$

or, with an obvious change of notation

$$(\bar{K} | = (K | + \sum_L \sum_r \frac{H^{rLK}}{E_{KL}} (L | Q_r
 \tag{21}$$

This is the conventional treatment of vibronic coupling<sup>14)15)16)</sup>, based on the classical paper by Herzberg and Teller<sup>17)</sup>. In the above one has neglected the action of  $T_n$ , the nuclear kinetic energy (cf. equation 17), on the wave functions  $\psi_K$ . Recently it has been pointed out that corrections due to the kinetic energy of the nuclei cannot always be neglected<sup>18)</sup>. Especially when in a transition moment  $(K | \vec{r} | K')$  the expansions of  $K$  and  $K'$  yield contributions to the electric dipole matrix elements of roughly the same absolute magnitude but different sign, contributions due to  $T_n$  can become non-negligible. The O+B transition in azulene, borrowing intensity via  $a_1$  vibrations, most probably couples predominantly with the near O+D band, which is very strong. Therefore the so-called non-Born-Oppenheimer terms<sup>18c)</sup> presumably will be small and in the forthcoming we will neglect them.

#### 4c. The role of nontotally symmetric vibrations

As mentioned before, the major part of the azulene O→B transition is polarized along the long axis of the molecule, but in a naphthalene host some y polarized intensity is present too. The measurement of fluorescence excitation polarization confirms that this is also the case in solution<sup>2)</sup>. The degree of polarization P is approximately constant through the whole O→B band and has a value of about +.38, confirming that fluorescence and absorption have parallel polarizations. (From the same experiment the degree of polarization in the O→D band is +.40.) However, at some places in the spectrum somewhat lower P values occur, indicating that small amounts of y polarized intensity are present. Assuming that the deviation of P from the value +.38 measures the amount of short-axis polarized intensity, we deduce that in some regions of the O→B spectrum a few percent of the intensity is induced by nontotally symmetric modes. This is a small amount, but since one of the potential strengths of the MCD technique is the tracing of weak bands lying close to strong perpendicularly polarized ones, we shall investigate whether the characteristic MCD in the O→B band possibly results from the magnetic coupling between x and y polarized vibrational bands within the O→B spectrum.

The term in (1) which might give rise to large MCD effects is

$$\text{Im} \frac{\mu_{jk}^z}{E_{kj}} x_{aj} y_{ka} \quad (22)$$

Here k is a vibronic state of  $A_1$  symmetry and j is a nontotally symmetric vibronic state. When both states belong to the Bb manifold they may lie close together, and we must examine if they can give rise to large MCD effects because of the small denominator in (22).

Considering the matrix element of the magnetic dipole operator in (22) in the Born-Oppenheimer approximation we get

$$\mu_{jk}^z = (\bar{B} | b | \mu^z | \bar{B} | b') = (b | \mu_{\bar{B}\bar{B}}^z(Q) | b')$$

As  $\mu^z$  is an electronic operator,  $\mu_{\bar{B}\bar{B}}^z$  vanishes identically because the electronic state B, being non-degenerate, cannot carry any magnetic moment. Consequently the MCD in transitions to nontotally symmetric vibrational levels will be second or higher order in the vibronic perturbation, just as is the

dipole strength. Therefore we shall neglect the role of nontotally symmetric modes in the discussion of the peculiar shape of the MCD in the O→B band.

#### 4d. Vibronic coupling via totally symmetric modes

Having established that the O→B transition in azulene borrows intensity via  $a_1$  vibrations, we now assume that it couples predominantly with the nearby and very intense O→D band. Then the electric dipole strength in a transition from the vibronic ground state to a vibronic level Bb can be written as

$$D(O_0 \rightarrow B_b) = x_{OB}^2 \alpha_b^2 + x_{OD}^2 \beta_{rb} \beta_{r'b} + 2x_{OB} x_{OD} \alpha_b \beta_{rb} \quad (23)$$

where we have used the abbreviations

$$\begin{aligned} (o|b) &= \alpha_b \\ \sum_r \frac{H_{DB}^r}{E_{BD}} (o|Q_r|b) &= \beta_{rb} \end{aligned} \quad (24)$$

The various terms in (23) measure respectively the Franck-Condon intensity, the borrowed intensity and the intensity due to interference terms. Since

$$\sum_b \alpha_b^2 = 1 \quad (25)$$

and, because of the definition of equilibrium geometry in the ground state,

$$\sum_b \beta_{rb} \alpha_b = (o|Q_r|o) = 0 \quad (26)$$

it follows that although interference terms do contribute to the energy absorption in individual subbands, they do not affect the intensity integrated over all vibrational structure.

If we describe the MCD of the second transition in azulene in terms of the lowest five electronic states, as we did before for the A and C bands, we have, when allowing for the vibronic coupling between the B and D manifolds,

$$\begin{aligned} B(O_0 \rightarrow B_b) &= \text{Im} \left[ \sum_a \frac{\mu_{BA}^z (b|a) + \mu_{DA}^z \sum_r \frac{H_{DB}^r}{E_{BD}} (b|Q_r|a)}{E_{Aa} - E_{Bb}} y_{AO} (a|o) + \right. \\ &+ \left. \sum_c \frac{\mu_{BC}^z (b|c) + \mu_{DC}^z \sum_r \frac{H_{DB}^r}{E_{BD}} (b|Q_r|c)}{E_{Cc} - E_{Bb}} y_{CO} (c|o) \right] \cdot \left[ x_{OB} (o|b) + x_{OD} \sum_r \frac{H_{DB}^r}{E_{BD}} (o|Q_r|b) \right] \end{aligned}$$

In carrying out the summation over  $a$  in the first term one may replace the energy denominators  $E_{Aa} - E_{Bb}$  by an average value  $E_{AB} + \epsilon$  (compare §3c). In principle  $\epsilon$  is a function of  $b$ , but since it seems improbable that the strong fluctuations in the MCD are brought about by variations in the energy denominators, we take  $\epsilon = 0$  for convenience. Then we obtain with the help of (24)

$$B(O_0 \rightarrow B_b) = \text{Im} \left[ \frac{y_{AO}}{E_{AB}} \{ \mu_{BA}^z \alpha_b + \mu_{DA}^z \beta_{rb} \} + \frac{y_{CO}}{E_{CB}} \{ \mu_{BC}^z \alpha_b + \mu_{DC}^z \beta_{rb} \} \right] (x_{OB}^{\alpha_b} + x_{OD}^{\beta_{rb}}) \quad (27)$$

At this point the experimental values of  $B(O_0 \rightarrow B_b)$  and  $D(O_0 \rightarrow B_b)$  might be confronted with their theoretical counterparts. Taking the observed values of the quantities  $D(O_0 \rightarrow B_b)$  and  $B(O_0 \rightarrow B_b)$  and the quantum mechanical estimates of the electronic matrix elements and energy differences we could solve the system of equations (23) and (27) and find  $\alpha_b$  and  $\beta_{rb}$  for each vibrational band.

In this way however, one could expect considerable systematic errors in the result, which we have tried to eliminate in the following way. It is known from experience that transition energies and oscillator strengths from MO calculations, although qualitatively correct, in general are not in very good quantitative agreement with the experimental values. Dipole strengths e.g. are mostly overestimated in MO theory. Therefore we introduce two reduction factors  $P$  and  $Q$  assumed to be constant throughout the band, by writing

$$\begin{aligned} D^{\text{exp}}(O_0 \rightarrow B_b) &= P D(O_0 \rightarrow B_b) \\ B^{\text{exp}}(O_0 \rightarrow B_b) &= Q B(O_0 \rightarrow B_b) \end{aligned} \quad (28)$$

where  $P$  and  $Q$  are positive numbers independent of  $b$ . The suffix  $\text{exp}$  denotes experimental values.

Perhaps it is useful to express explicitly what we are hoping to gain from the introduction of  $P$  and  $Q$ . We want to perform an analysis of the azulene  $O \rightarrow B$  band to find the relative contributions of the various terms on the RHS of (23) to the different bands. The factors  $P$  and  $Q$  are introduced to eliminate as far as possible systematic errors which arise in the theoretical estimates of the various electronic matrix elements and other effects (internal field corrections, to mention one) which we may hope to be constant throughout the band.

In Table VIII we present the results of the solution of the  $\alpha_b, \beta_{rb}$ ,

Table VIII Analysis of the O+B band.

Peak	$\nu$	distance from (o,o)	Experimental		Calc.vibr. matrix-el.		Calc.Intensity			Calc.MCD		
			$D_b$	$B_b$	$\alpha_b$	$\beta_{rb}$	FC	borr	inter-ference	FC	borr	inter-ference
1	28370	0	.134	-9.15	.884	-.057	.408	.075	-.349	-15.7	.11	6.44
2	28740	370	.051	0	.012	.045	.000	.047	.004	.00	.07	-.07
3	29030	660	.030	-1.62	.333	-.014	.058	.005	-.032	-2.22	.01	.60
4	29370	1000	.523	.35	.021	.148	.000	.501	.022	-.01	.76	-.40
5	29690	1320	.447	-5.00	.294	.095	.045	.208	.194	-1.74	.32	-3.58
6	30070	1700	.305	0	.029	.111	.000	.282	.022	-.02	.43	-.41
7	30440	2070	.304	-1.24	.107	.099	.006	.225	.073	-.23	.34	-1.35
8	30720	2350	.320	.31	.011	.116	.000	.311	.009	.00	.47	-.16
9	31100	2730	.281	-.78	.079	.099	.003	.224	.054	-.12	.34	-1.00
10	31500	3130	.229	.33	.001	.100	.000	.228	.001	.00	.35	-.02
11	31800	3430	.196	-.06	.028	.088	.000	.179	.017	-.02	.27	-.32
12	32200	3830	.165	.52	.023	-.088	.000	.179	-.014	-.01	.27	.26

P = .220  
Q = .152  
83% of the total intensity and 16% of the total MCD is borrowed.

Units: frequencies in  $\text{cm}^{-1}$ , intensities in  $D^2$ , MCD in  $10^{-5} \text{BD}^2 \text{cm}$   
See for the numbering of the peaks figure 3. The frequencies are taken from the extrema in the MCD spectrum. The experimental  $B_b$  values were obtained from the area of the MCD of the individual vibrational peaks.

The dipole strength of the (o,o) transition was determined by measuring the area of this band.

The shoulders in the absorption spectrum which are due to band 2 and 3, are more pronounced in the spectrum at  $77^\circ \text{K}$ . The dipole strengths of band 2 and band 3 were estimated by resolving graphically the low temperature spectrum in this region into Gaussian components. For the other bands (lying at  $\nu_b$  and having a height  $p_b$ ) the dipole strength was found by distributing their total integrated intensity with weighting factors  $p_b / \nu_b$ .



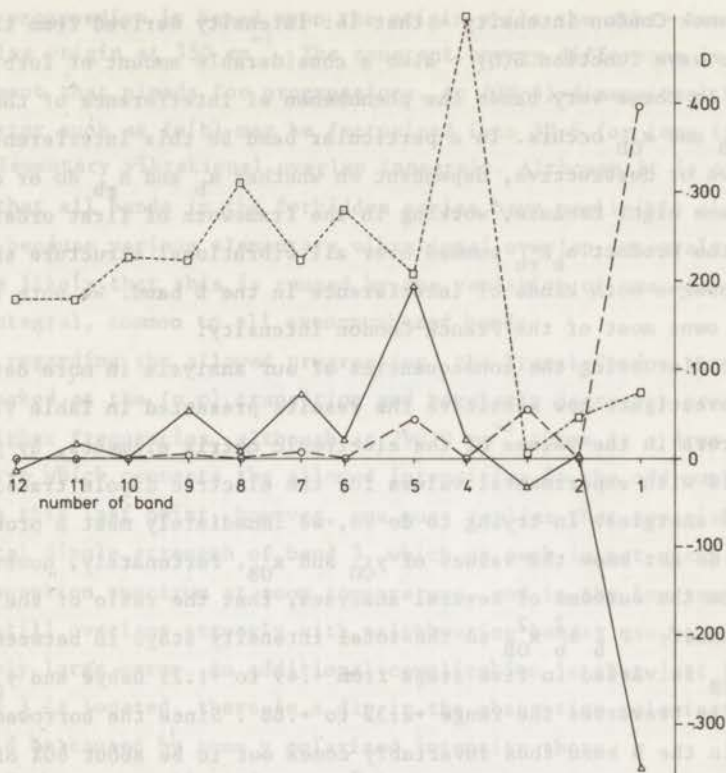


Figure 4. Calculated composition of the total intensity in the O+B band.

( - - - - ) : Franck-Condon intensity

( ..... ) : borrowed intensity

( ——— ) : intensity due to interference terms.

P and Q from the system of coupled equations (23), (25), (26), (27) and (28) when calculated values for all electronic matrix elements and energies are used. The contributions to the total absorption of Franck-Condon intensity, borrowed intensity and intensity due to interference terms are in addition graphically displayed in figure 4.

From a comparison of figure 3 and figure 4 it appears that the complicated absorption spectrum of the O+B band decomposes into two series.

The even-numbered bands derive their intensity almost exclusively from the D-character in the electronic wave function which describes the B-state.

These bands we name the forbidden series. In addition there are the vibrational bands which are odd-numbered, which carry relatively large MCD and have

besides Franck-Condon intensity - that is: intensity derived from the  $B(Q_0)$  part in the wave function  $B(Q)$  - also a considerable amount of forbidden intensity. In these very bands the phenomenon of interference of the transition moments  $x_{OB}$  and  $x_{OD}$  occurs. In a particular band Bb this interference is constructive or destructive, dependent on whether  $\alpha_b$  and  $\beta_{rb}$  do or do not have the same sign. Because, working in the framework of first order vibronic coupling, the product  $\alpha_b \beta_{rb}$  summed over all vibrational structure should give zero, we observe both kinds of interference in the B band. We note that band 1 (o,o band) owns most of the Franck-Condon intensity.

Before discussing the consequences of our analysis in more detail we first investigate how sensitive the results presented in Table VIII are towards errors in the values of the electronic matrix elements, by performing the analysis with experimental values for the electric dipole transition moments and energies. In trying to do so, we immediately meet a problem because we do not know the values of  $y_{CO}$  and  $x_{OB}$ . Fortunately, however, it appears from the outcome of several analyses, that the ratio of the Franck-Condon intensity  $P \sum_b \alpha_b^2 x_{OB}^2$  to the total intensity stays in between .19 and .15 when  $x_{OB}$  is varied in five steps from +.49 to +1.29 Debye and  $y_{CO}$  independently traverses the range +2.32 to +.88. Since the borrowed intensity in the B band thus invariably comes out to be about 80% of the total absorption, the experimental value of  $x_{OB}^2$  is taken as  $.20 \times (3.20)$  i.e.

$x_{OB} = .8$  Debye. At first sight it is surprising that the introduced values for  $x_{OB}$  and  $y_{CO}$  scarcely influence the calculated Franck-Condon intensity, but in fact it is not: errors in the input values of the electronic matrix elements are to a large extent absorbed in P and Q. That is why the latter may vary strongly from one analysis to another. Just to give an idea of the variations that result: when the analysis is performed using experimental values for the electronic transition moments and energies one finds  $P = .805$  and  $Q = .575$ , but  $\alpha_1 = .885$ ,  $\alpha_2 = .011$ ,  $\beta_1 = -.046$  and  $\beta_2 = .037$ . Therefore the results which are presented in Table VIII may be considered as representative for the O+B absorption system.

As could already have been expected from the very characteristic shape of the MCD spectrum, we find two types of bands in the O+B spectrum. The odd-numbered bands, which do have both allowed and forbidden character are equidistant in the frequency scale, their distance being ca  $650 \text{ cm}^{-1}$ . The other series also consists of equally spaced vibrational bands with distance  $650 \text{ cm}^{-1}$ , band 2 being at  $350 \text{ cm}^{-1}$  from the (o,o) band. Accordingly one expects that the two series of bands are in fact two progressions in a  $650 \text{ cm}^{-1}$  frequency.

The first progression is based upon the origin while the other one is built upon a false origin at  $350 \text{ cm}^{-1}$ . The constant energy difference is not the only argument that pleads for progressions. An  $(3N-6)$ -dimensional Franck-Condon factor such as  $(o|b)$  may be factorized into  $3N-6$  (or less if mode mixing occurs) elementary vibrational overlap integrals. Although it is of course possible that all bands in the forbidden series have negligible allowed character because various elementary vibrational overlap integrals are zero, it is more likely that this is caused by the vanishing of one elementary overlap integral, common to all even-numbered bands.

When regarding the allowed progression, the Franck-Condon contour is sharply peaked at the  $(o,o)$  transition and regularly decreases proceeding towards higher frequencies, although at  $29030 \text{ cm}^{-1}$  there is a drop in the smooth curve which connects the allowed intensities in the odd-numbered bands. Concerning this last point, however, one must realize that especially the experimental dipole strength of band 3, which as such is not visible at all in the absorption spectrum at room temperature, and in the low temperature spectrum still overlaps strongly with neighbouring bands, can be subject to a relatively large error. An additional complication is that just in the region where band 3 is located, there is a dip in the absorption polarization curve<sup>2)</sup>, which could be caused by some  $y$  polarized intensity there.

One of the most salient features of the Franck-Condon spectrum is the large concentration of allowed electronic intensity in the  $(o,o)$  band. This indicates that the minima of the potential energy hypersurfaces in the ground state and the B state are situated at nearly the same point in normal coordinate space. In azulene therefore there clearly is no large change in equilibrium geometry going from the ground state to the second excited singlet state. This result has a direct bearing on the recent work of Small *et al.*<sup>19)</sup> in which possible explanations are discussed why azulene fluoresces from its second, and not its first, excited state. Indeed, it places their discussion on the anomalous fluorescence properties on a much firmer basis.

In our analysis we have determined how much intensity in each vibrational band results from first order coupling with the state D. We were able to do this because those portions in the wave function for the second excited singlet state deriving from the electronic states B and D contribute very differently to absorption and MCD. On the basis of the theory developed here, however, one cannot draw any pertinent conclusions about the question which specific vibrations are effective in the vibronic coupling process. The nice regularity in the analyzed  $O \rightarrow B$  band does suggest that one could be dealing

with only two progressions which do carry the dominant portion of the intensity and MCD, but at this stage we cannot estimate if more frequencies are involved in the spectrum and how important their contributions are. The complexity of the crystal spectra and the gas phase spectrum in fact suggests that contributions of vibrations other than those with frequencies of  $350\text{ cm}^{-1}$  are not of negligible consequence.

What we want to do finally, however, is see how our findings compare with the detailed study of Lacey et al<sup>12)</sup> on the azulene O→B transition.

#### 4e. Lacey's interpretation of the azulene O→B spectrum<sup>12)</sup>.

As mentioned, the O→B band of azulene in a host at low temperatures is unusually rich in lines. Sidman and McClure<sup>1)</sup> who studied the spectrum at  $20^{\circ}\text{K}$  with naphthalene as a host, found that the transition was predominantly long-axis polarized, but the spectrum was so complex that they could only assign part of the vibrational fine structure. Lacey et al remeasured the transition and found on replacing the naphthalene host by biphenyl, durene or cyclododecane some characteristic frequencies were shifted. Another peculiarity these authors noted in connection with the second transition of azulene is the complete lack of mirror-symmetry between absorption and fluorescence (cf. figure 3). While in the fluorescence there is only one prominent peak at ca  $1580\text{ cm}^{-1}$  from the origin, in absorption there are two: one at  $1000\text{ cm}^{-1}$  and the other at  $1300\text{ cm}^{-1}$  (band 4 and 5 respectively; see figure 4).

Stating that normally in aromatic molecules, even when a change in equilibrium configuration occurs, vibrational frequencies in ground and fluorescent state do not change that much, Lacey et al propose that in the azulene O→B absorption a prominent vibrational level (with a vibrational wave function in, say the normal coordinate  $Q_1$ ) at  $1580\text{ cm}^{-1}$  would have been present if there were no vibronic interaction with state D. However, because strong first order coupling between the  $1580\text{ cm}^{-1}$  level with state D via  $Q_1$  occurs, the level is depressed to about  $1200\text{ cm}^{-1}$  above the zero-point vibrational B state. In addition to this level there is another one, described by a vibrational wave function involving another normal coordinate  $Q_2$ , which couples only weakly to D and therefore does not shift much in frequency. The two vibronic levels, each being coupled to state D by a different ground state normal vibration, now interact because they do not form a basis in which the total Hamiltonian (first two terms of (19)) is diagonal. So, according to

Lacey, the two levels repel each other yielding eigenstates at 1300 and 1000  $\text{cm}^{-1}$  above the zero-point vibrational level of B; the corresponding wave functions mix and give rise to a flow of intensity from the strong 1300  $\text{cm}^{-1}$  band to the weak 1000  $\text{cm}^{-1}$  band. This mixing can be described as a rotation of normal coordinates in the fluorescent state and is known as the Duschinsky effect<sup>20)21)</sup>. After the Duschinsky coupling, the total wave function representing the upper state of the transition which is situated at 1000  $\text{cm}^{-1}$  from the O+B origin reads

$$c_1 \left| B + \sum_{i=1}^2 \frac{H_{DB}^i}{E_{BD}} Q_i \cdot D \right\rangle \left| 1_1 0_2 \right\rangle + c_2 \left| B + \sum_{i=1}^2 \frac{H_{DB}^i}{E_{BD}} Q_i \cdot D \right\rangle \left| 0_1 1_2 \right\rangle \quad (29)$$

The other state is described by

$$-c_2 \left| B + \sum_{i=1}^2 \frac{H_{DB}^i}{E_{BD}} Q_i \cdot D \right\rangle \left| 1_1 0_2 \right\rangle + c_1 \left| B + \sum_{i=1}^2 \frac{H_{DB}^i}{E_{BD}} Q_i \cdot D \right\rangle \left| 0_1 1_2 \right\rangle \quad (30)$$

The coefficients  $c_1$  and  $c_2$  are chosen in such a way that (29) and (30) diagonalize the total Hamiltonian.

From our analysis of the azulene O+B band it follows that indeed the Duschinsky effect may here be important: in both progressions a considerable amount of borrowed intensity is present and because it is quite unevenly (see figure 4) distributed over the two progressions, it is likely that more than one vibration is active in generating it.

Although we do agree with Lacey about the importance of the Duschinsky effect in azulene, we do not agree with the detailed vibronic mechanism which they proposed to explain the vibrational structure in the absorption spectrum. In line with calculations made by Hunt and Ross<sup>13)</sup>, Lacey et al put the fraction of the total intensity in the O+B band that derives from coupling with D equal to 2/3 but in setting up the model that must account for the particular band shapes of fluorescence and absorption, they neglect the contribution of the Franck-Condon intensity. We find that the ratio of forbidden and total intensity is even higher, namely 4/5. How seriously however the Franck-Condon transition moment influences the O+B band form is clear if one compares the actual absorption (figure 3) with that part of it which results if one assumes the Franck-Condon intensity to vanish (borrowed intensity curve in figure 4).

We further remark that the detailed mechanism used by Lacey et al to explain the observation that the fluorescence is peaked at 1580  $\text{cm}^{-1}$  and the

absorption at  $1300\text{ cm}^{-1}$  and  $1000\text{ cm}^{-1}$  from the origin, would imply that in this particular case the values of  $c_1$  and  $c_2$  in (29) and (30) are such that the Franck-Condon transition moment in the  $1000\text{ cm}^{-1}$  band becomes equal to zero. Further we think it probable that the  $1000\text{ cm}^{-1}$  and  $1300\text{ cm}^{-1}$  frequencies are not fundamentals but overtones.

Another possible mechanism which can account for different band forms of absorption and fluorescence was described by Craig and Small<sup>22)</sup>. If totally symmetric vibrations are active in the Herzberg-Teller coupling of the fluorescent state with another state there is the possibility of transition moment interference. Craig and Small showed on the basis of model calculations that when in absorption the 0-1 vibrational transition shows e.g. constructive interference, in emission the 1-0 vibrational band is governed by destructive interference between the Franck-Condon and borrowed transition moments, and vice versa. The authors applied their theory to the  $3400\text{ \AA}$  transition of phenanthrene and in passing they made the remark that it could be applicable to the azulene O+B transition as well. Indeed our results show that transition moment interference is a quite important effect in the second transition of azulene. On the basis of the presently available data however, we judge it premature to try to give any pertinent explanation for the different band forms in absorption and emission. First one should find the distribution of allowed and forbidden intensity over the vibrational modes in the fluorescence, which could be achieved by a MCPL measurement.

To conclude, we emphasize the potential utility of the MCD technique to trace intensity induced by totally symmetric vibrations. Based upon the fact that an electronic wave function contributes differently in the generation of electric and magnetic dipole transition moments, the applicability of the method seems to be general. One can expect it to be especially useful in the determination of the variation of the electronic transition moment with interatomic distance in diatomic molecules<sup>23)</sup>.

## References

- 1 J.W. Sidman and D.S. McClure, 1956, J. Chem. Phys. 24, 757
- 2 H. Zimmermann and N. Joop, 1960, Z. Elektrochem., Ber. Bunsengesellschaft Physik. Chem. 64, 1219
- 3 R. Pariser, 1956, J. Chem. Phys. 25, 1112
- 4 O. Bastiansen and J.L. Derissen, 1966, Acta Chim. Scand. 20, 1319
- 5 J.E. Bloor, 1965, Can. J. Chem. 43, 3026
- 6 J. Koutecky, P. Hochman and J. Michl, 1964, J. Chem. Phys. 40, 3439
- 7 K. Nishimoto and L.S. Forster, 1965, Theoret. Chim. Acta 3, 407
- 8 N.L. Allinger, J.C. Tai and T.W. Stuart, 1967, Theoret. Chim. Acta, 8, 101
- 9 L. Seamans and A. Moscovitz, 1972, J. Chem. Phys. 56, 1099
- 10 D.J. Caldwell and H. Eyring, 1971, The Theory of Optical Activity (Wiley-Interscience, New York)
- 11 A.R. Lacey, R.G. Body, G. Frank and I.G. Ross, 1967, J. Chem. Phys. 47, 2199
- 12 A.R. Lacey, E.F. McCoy and I.G. Ross, 1973, Chem. Phys. Letters, 21, 233
- 13 G.H. Hunt and I.G. Ross, 1962, J. Mol. Spectry 9, 50
- 14 J.A. Pople and J.W. Sidman, 1957, J. Chem. Phys. 27, 1270
- 15 J.N. Murrell and J.A. Pople, 1956, Proc. Phys. Soc. (London) A69, 245
- 16 A.C. Albrecht, 1960, J. Chem. Phys. 33, 156
- 17 G. Herzberg and E. Teller, 1933, Z. Physik. Chem. B21, 410
- 18a P. Geldof, R. Rettschnik and G. Hoijtink, 1971, Chem. Phys. Letters, 10, 549  
b G. Orlandi and W. Siebrand, 1972, *ibid.* 15, 465  
c W. Siebrand and G. Orlandi, 1973, J. Chem. Phys. 58, 4513
- 19 G.J. Small and S. Kusserow, 1974, J. Chem. Phys. 60, 1558
- 20 F. Duschinsky, 1937, Acta Physicochim. URSS 1, 551
- 21 G.J. Small, 1971, J. Chem. Phys. 54, 3300
- 22 D.P. Craig and G.J. Small, 1969, J. Chem. Phys. 50, 3827
- 23 P.A. Fraser, 1954, Can. J. Phys. 32, 515

## CHAPTER IV

### MCD OF THE TRANSITION TO THE ${}^3_{n\pi^*}$ -STATE IN THIOKETONES \*)

#### 1. Introduction

Most thioketones exhibit a weak  ${}^1(n+\pi^*)$  transition in the visible part of the spectrum<sup>1)2)</sup>. At the long wavelength side of this band there is often a shoulder perceptible, which is believed to be caused by a singlet-triplet transition<sup>3)4)</sup>. In two thioketones, thiocamphor and thiocyclopentanone, we have measured the magnetic circular dichroism of this transition. In addition to the MCD we have observed in thiocamphor the circular dichroism of the shoulder at  $\sim 18$  kK, as well as the circular polarization of the luminescence (CPL). The results of these measurements prove that the transition indeed must be considered a S-T transition.

The organization of this chapter is as follows. First we discuss the measurements of the optical activity in absorption and emission and their consequences (§2). In §3 we develop the theoretical framework to understand quantitatively the MCD of singlet-triplet transitions in isotropic solutions. Then we are ready to confront the observed MCD spectra with the theory.

\*) Presented in part at the Euechem Conference on Optical Activity, Caen, May 1973.



## 2. Optical activity

In an electronic transition  $a \rightarrow j$  the circular dichroism is governed by the rotational strength  $R_{aj}$  and the unpolarized absorption by the dipole strength  $D_{aj}$ . The degree of circular anisotropy obtained from the experimental spectra is measured by the dissymmetry factor  $g$ .

$$g = \frac{4R_{aj}}{D_{aj}} = \frac{\int \frac{\Delta OD}{\nu} d\nu}{\int \frac{OD}{\nu} d\nu}$$

where OD denotes the absorbance and  $\Delta OD$  the differential absorbance of the sample. In the expression for  $g$  the integrations are over the entire electronic absorption band.

In the reverse transition the rotational strength  $R_{ja}$  and dipole strength  $D_{ja}$  are observable as CPL and unpolarized luminescence, respectively. The dissymmetry factor in emission,  $g_{lum}$ , equals

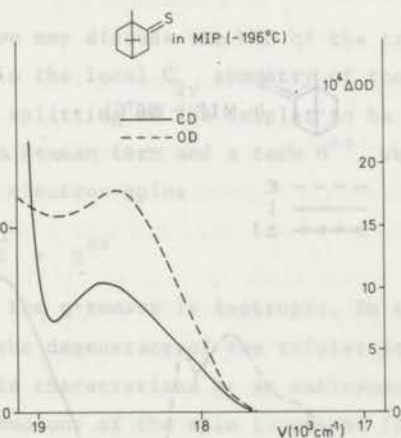


Figure 1. Circular dichroism —, (measured as differential absorbance) and absorption (measured as absorbance) of thiocomphor in methylcyclohexane/isopentane at  $-196^\circ\text{C}$ .

$$g_{lum} = \frac{4R_{ja}}{D_{ja}} = \frac{\int \frac{\Delta I}{v^3} dv}{\int \frac{I}{v^3} dv}$$

It can be shown (cf. Chapter V) that - provided the equilibrium geometries in the states a and j are equal -  $R_{aj}=R_{ja}$ ,  $D_{aj}=D_{ja}$  and thus  $g=g_{lum}$ . The latter fact, generally, offers the possibility to identify a transition in emission with one in absorption.

From the observed CD and absorption spectra of thiocamphor (see figure 1) we find that the band at  $\sim 18$  kK has a g-value of between  $+3 \cdot 10^{-3}$  and  $+5 \cdot 10^{-3}$  (the rather large uncertainty arises because we can only estimate the dipole strength of the transition, owing to the overlap with the  $^1(n+\pi^*)$ -band). In the emission (cf. figure 2) the dissymmetry factor equals  $+(4 \pm 1) \cdot 10^{-3}$ . Since because of its long life-time ( $.14 \cdot 10^{-3}$  sec) the emission may be assigned to phosphorescence<sup>3)</sup>, we conclude from the similarity of the g-values that in thiocamphor the shoulder at  $\sim 18$  kK is due to a singlet-triplet transition (where we have assumed that at  $77^\circ\text{K}$  in emission all triplet sub-levels are equally populated).

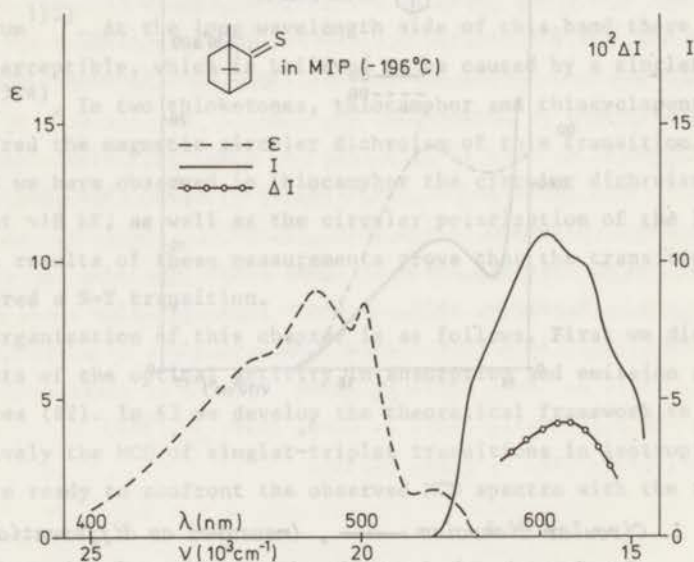


Figure 2. Unpolarized absorption ( $\epsilon$ ), emission ( $I$ ) and circular polarization ( $\Delta I$ ) of thiocamphor in methylcyclohexane/isopentane at  $-196^\circ\text{C}$ .

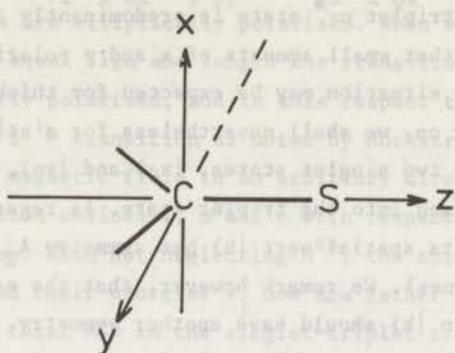


Figure 3. Reference frame for the thiocarbonyl chromophore.

### 3. MCD in singlet-triplet transitions

We shall assume that we may discuss the MCD of the transition to the  $^3n\pi^*$  state of our ketones in the local  $C_{2v}$  symmetry of the chromophore (see figure 3). We consider the splitting of the triplet to be governed by a hamiltonian consisting of a Zeeman term and a term  $H^{ss}$ , which describes the dipolar interaction of the electron spins

$$H = g\beta\vec{H} \cdot \vec{S} + H^{ss} \quad (1)$$

where we have assumed that the  $g$ -tensor is isotropic. In the absence of a magnetic field,  $H^{ss}$  lifts the degeneracy of the triplet state yielding three sub-states, each of which is characterized by an antisymmetrized product of a spatial wave function  $|k\rangle$  and one of the spin functions (2)

$$|T_x\rangle, |T_y\rangle, |T_z\rangle \quad (2)$$

For a two-electron system these spin functions are related to the familiar two-electron spin functions  $|\tau_1\rangle$ ,  $|\tau_0\rangle$  and  $|\tau_{-1}\rangle$  by

$$|\tau_1\rangle = \frac{\tau_x + i\tau_y}{\sqrt{2}}, \quad |\tau_0\rangle = |\tau_2\rangle, \quad |\tau_{-1}\rangle = \frac{\tau_x - i\tau_y}{\sqrt{2}} \quad (3)$$

The singlet-triplet transition probability arises from spin-orbit coupling

of singlet and triplet states. From experiment it is known that in formaldehyde the transition to the triplet  $n\pi^*$  state is predominantly z-polarized<sup>5)</sup>, and from calculations<sup>6)7)</sup> that small amounts of x and y polarized intensity are present too. A similar situation may be expected for thioketones. Anticipating a generalization later on, we shall nevertheless for a start describe the MCD which arises when only two singlet states,  $|x\sigma\rangle$  and  $|y\sigma\rangle$ , which transform as x and y in  $C_{2v}$ , are mixed into the triplet state. As regards this triplet state we shall assume that its spatial part  $|k\rangle$  has symmetry  $A_2$  in  $C_{2v}$  (as is the case with our thioketones). We remark however, that the essence of our argument is not invalidated when  $|k\rangle$  should have another symmetry.

Since  $|k\rangle$  has symmetry  $A_2$  and the spin functions  $T_u$  transform like the corresponding rotations  $R_u$  ( $u=x,y,z$ ), the spin-orbit coupling connects the singlet state  $|x\sigma\rangle$  to  $|kT_x\rangle$  and  $|y\sigma\rangle$  to  $|kT_y\rangle$ . From first order perturbation theory the wave functions for the triplet sub-levels then are

$$\begin{pmatrix} |kT_x\rangle + \lambda_x |x\sigma\rangle \\ |kT_y\rangle + \lambda_y |y\sigma\rangle \\ |kT_z\rangle \end{pmatrix} \quad (4)$$

The (imaginary) coefficient  $\lambda_u$  is given by

$$\lambda_u = \frac{(u\sigma | H^{SO} | kT_u)}{E(kT_u) - E(u\sigma)} \quad (5)$$

where u is x or y and  $H^{SO}$  the part of the Hamiltonian pertaining to spin-orbit coupling. The relevant matrix element of the electric dipole operator  $\vec{m}$  for the transition from the ground state  $|\sigma\rangle$  to the triplet states  $|kT_x\rangle$  and  $|kT_y\rangle$  is now non-vanishing

$$\begin{aligned} (\sigma | \vec{m} | kT_x + \lambda_x x\sigma) &= \lambda_x (\sigma | \vec{m} | x) = \lambda_x \vec{m}_{ox} \\ (\sigma | \vec{m} | kT_y + \lambda_y y\sigma) &= \lambda_y (\sigma | \vec{m} | y) = \lambda_y \vec{m}_{oy} \end{aligned} \quad (6)$$

In discussing the MCD which arises from this situation we shall proceed as follows. Firstly we consider the MCD when the magnetic field is in the molecular z-direction and so large that we may neglect  $H^{SS}$  in (1). Secondly we study the case where  $\vec{H}$  is in an arbitrary direction and the dipolar coupling not neglected. Then we shall calculate the MCD for a solution of randomly oriented molecules.

(1) When applying a magnetic field  $H_z$  and taking  $H^{SS}$  equal to zero the triplet sub-levels are, in order of decreasing energy, given by  $\tau_1, \tau_0$  and  $\tau_{-1}$ . From (3) and (6) it follows that the transition moments to the upper and

lower Zeeman levels are  $\frac{-1}{\sqrt{2}}(\lambda_{x\ o_x}^{\vec{m}} + i\lambda_{y\ o_y}^{\vec{m}})$  and  $\frac{1}{\sqrt{2}}(\lambda_{x\ o_x}^{\vec{m}} - i\lambda_{y\ o_y}^{\vec{m}})$ , which implies that both transitions are elliptically polarized. When we assume that  $\lambda_{x\ o_x}^{\vec{m}}$  and  $\lambda_{y\ o_y}^{\vec{m}}$  have equal sign and length the transition to  $\tau_1$  is left-, that to  $\tau_{-1}$  right-circularly polarized, and in this respect the S-T transition is quite similar to an  $^1S \rightarrow ^1P$  transition as noted by Hochstrasser<sup>8)</sup>.

We now take the magnetic field in an arbitrary direction (Z) which is defined by its direction cosines l, m and n with respect to the x, y and z axes in the molecular frame. When not neglecting  $H^{ss}$ , the spin functions  $\theta_j$  of the triplet sub-states and their energies  $v_j$  now are rather complicated functions of l, m and n<sup>9)</sup>. The total MCD in the singlet-triplet transition is, as a function of frequency,

$$\Delta\epsilon(\nu) = -2\alpha\nu \sum_{j=1}^3 f_j(\nu - \nu_o - \nu_j) \text{Im}(\langle o | \vec{m} \cdot \hat{X} | \theta_j \rangle) (\theta_j | \vec{m} \cdot \hat{Y} | o) \quad (7)$$

where it is assumed that the light propagates parallel to the magnetic field.  $\hat{X}$  and  $\hat{Y}$  are unit vectors in the X and Y directions of a right-handed reference frame (X, Y, Z) and  $\alpha$  is

$$\alpha = \frac{8\pi^3 N}{10^3 hc \log_e 10}$$

In (7)  $|\theta_j\rangle$  stands for the complete wave function of the sub-level j, including singlet contamination due to spin-orbit coupling, whereas  $|o\rangle$  denotes the wave function for the ground state. The function  $f_j(\nu - \nu_o - \nu_j)$  is a normalized shape factor, ad hoc introduced to describe the band form of the transition  $o \rightarrow \theta_j$ . The function is peaked at the frequency  $\nu_o + \nu_j$ , where  $\nu_o$  is the mean of the energies of the three triplet levels. We shall assume that the functional form of  $f_j$  is independent of j, which seems a reasonable approximation, especially at high magnetic fields. Furthermore we consider  $\nu_j$  to be very small as compared to the half-width of f. When expanding  $f(\nu - \nu_o - \nu_j)$  as a series around  $\nu - \nu_o$  and retaining in the expansion only the first two terms, we obtain

$$\Delta\epsilon(\nu) = -2\alpha\nu \sum_{j=1}^3 \left[ f(\nu - \nu_o) - \nu_j \frac{\partial f(\nu - \nu_o)}{\partial \nu} \right] \text{Im}(\langle o | \vec{m} \cdot \hat{X} | \theta_j \rangle) (\theta_j | \vec{m} \cdot \hat{Y} | o) \quad (8)$$

Using the principle of spectroscopic stability<sup>10)</sup> the contribution to  $\Delta\epsilon$  of the first term between square brackets in (8) can be rewritten as

$$\sum_{u=x,y,z} f(\nu - \nu_o) \text{Im}(\langle o | \vec{m} \cdot \hat{X} | T_u \rangle) (T_u | \vec{m} \cdot \hat{Y} | o) \quad (9)$$

Since the singlet contamination in  $T_u$  is purely imaginary, all terms in (9) vanish. Similarly in the second term of (8), which may be transformed to

$$2\alpha\nu \frac{\partial f(\nu-\nu_0)}{\partial \nu} \text{Im} \sum_j (o|\vec{m}\cdot\hat{X}(g\beta H_Z S_Z + H^{SS})|\theta_j)(\theta_j|\vec{m}\cdot\hat{Y}|o) \quad (10)$$

the part pertaining to  $H^{SS}$  is zero. So in our approximation the MCD is not influenced by the dipolar part of (1) and equals

$$\Delta\varepsilon(\nu) = 2\alpha\nu \frac{\partial f(\nu-\nu_0)}{\partial \nu} g\beta H_Z \text{Im} \sum_r (o|\vec{m}\cdot\hat{X}|\Xi_r)(\Xi_r|\vec{m}\cdot\hat{Y}|o) \quad (11)$$

where we have transformed to the basis  $\Xi_r$  ( $r=1, 0, -1$ ) in which the Zeeman term  $g\beta H_Z S_Z$  is diagonal with eigenvalues  $g\beta H_Z r$ . This basis is connected to  $(\tau_1, \tau_0, \tau_{-1})$  by

$$\Xi_r = \sum_s c_{rs} \tau_s \quad (12)$$

The matrix  $C$  is explicitly given elsewhere<sup>11</sup>. Since in the summation in (11)  $r=0$  does not contribute and the contributions to  $\Delta\varepsilon$  of  $r=1$  and  $r=-1$  are equal, we find from (11) and (12)

$$\Delta\varepsilon(\nu) = 2\alpha\nu \frac{\partial f(\nu-\nu_0)}{\partial \nu} g\beta H_Z \text{Im} (o|\vec{m}\cdot\hat{X}|\sum_s c_{1s} \tau_s)(\sum_s c_{1s} \tau_s|\vec{m}\cdot\hat{Y}|o) \quad (13)$$

Appreciating the singlet-character associated with the spin functions, we obtain

$$\Delta\varepsilon(\nu) = 2\alpha\nu \frac{\partial f(\nu-\nu_0)}{\partial \nu} g\beta H_Z \left[ -\frac{n}{2} \{ (\lambda_{x\text{ox}}^{\vec{m}} \cdot \hat{X}) (\lambda_{y\text{oy}}^{\vec{m}} \cdot \hat{Y}) - (\lambda_{x\text{ox}}^{\vec{m}} \cdot \hat{Y}) (\lambda_{y\text{oy}}^{\vec{m}} \cdot \hat{X}) \} \right] \quad (14)$$

Averaging over all orientations of the molecule with respect to  $H_Z$  we finally have

$$\begin{aligned} \Delta\varepsilon(\nu) &= -\frac{2}{3}\alpha\nu \frac{\partial f(\nu-\nu_0)}{\partial \nu} g\beta H_Z (\lambda_{x\text{ox}}^{\vec{m}} \cdot \hat{i}) (\lambda_{y\text{oy}}^{\vec{m}} \cdot \hat{j}) \\ &= -\frac{2}{3} \alpha H_Z \nu \frac{\partial f(\nu-\nu_0)}{\partial \nu} A \end{aligned} \quad (15)$$

Where  $\hat{i}$  and  $\hat{j}$  are unit vectors in the  $x$  and  $y$  directions.

The total unpolarized absorption, which of course is not affected by the field, equals

$$\varepsilon(\nu) = \frac{\alpha}{3} \nu f(\nu-\nu_0) \left\{ |\lambda_{x\text{ox}}^{\vec{m}}|^2 + |\lambda_{y\text{oy}}^{\vec{m}}|^2 \right\} = \frac{\alpha}{3} \nu f(\nu-\nu_0) D \quad (16)$$

From a comparison of the MCD parameter  $A$  from (15) and the dipole strength  $D$

we get

$$\frac{A}{D} = \frac{g\beta(\lambda_{x'ox} \vec{m}_{ox} \cdot \hat{i})(\lambda_{y'oy}^* \vec{m}_{oy} \cdot \hat{j})}{|\lambda_{x'ox} \vec{m}_{ox}|^2 + |\lambda_{y'oy}^* \vec{m}_{oy}|^2} \quad (17)$$

We can illustrate the implications of (17) for the speculative case when  $\hat{i} \cdot \lambda_{x'ox} \vec{m}_{ox} = \hat{j} \cdot \lambda_{y'oy}^* \vec{m}_{oy}$ . Then we have

$$\frac{A}{D} = \frac{g\beta}{2} = -\frac{\mu}{2} \quad (18)$$

where  $\mu$  is the magnetic moment of the highest Zeeman state. Since an identical relationship is found for a transition between a singlet ground state and an orbitally degenerate E-state<sup>12)</sup> we conclude that for this very specific situation also in isotropic solution the MCD in a S+T transition behaves like a singlet-singlet A-term. In general, however, there are main differences. The principal use of A/D-values for singlet-singlet transitions is the determination of orbital angular momentum. With singlet-triplet transitions, assuming the spin-orbit coupling to be small, spin is a good quantum number and the spin magnetic moment is known a priori. What here can be found from A/D are the sign and the magnitude of the ratio  $\lambda_{x'ox} \vec{m}_{ox} \cdot \hat{i} / \lambda_{y'oy}^* \vec{m}_{oy} \cdot \hat{j}$  (cf. (17)).

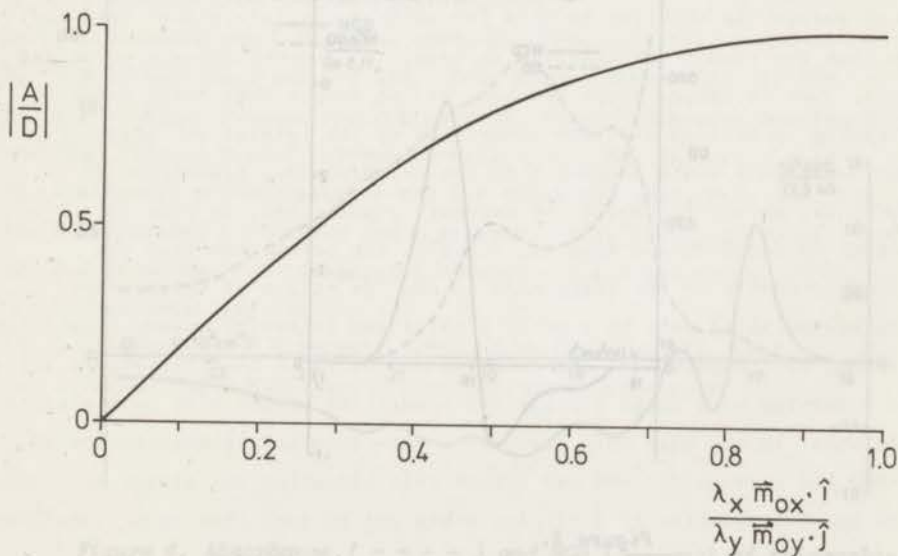


Figure 4.

From figure 4 it appears that A/D decreases rather slowly with a decrease of this ratio. Therefore the MCD technique seems particularly suited to trace small spin-orbit couplings next to large ones.

In two respects the situation is more complex than we have assumed so far. Firstly we have confined ourselves to the MCD which originates in the coupling of triplet sub-levels by  $\vec{H} \cdot \vec{S}$ . In addition to this, however, the Zeeman Hamiltonian  $\vec{H} \cdot \vec{L}$ , which in a  $C_{2v}$  molecule gives rise to B-terms in the MCD, may contribute to the MCD in the S-T band. But this B-type MCD can be separated from the A-term because of its different shape function ( $f(v-v_0)$ ).

Secondly we have assumed that the singlet-triplet transition contains only two perpendicular polarizations (x and y). In general, however, one has also to allow for the presence of z-polarized intensity. This yields two extra terms in the expression for  $\Delta\epsilon$  in (15), obtainable by adding to the  $(\lambda_{x\ o x}^{\vec{m}} \cdot \hat{i})(\lambda_{y\ o y}^{\vec{m}} \cdot \hat{j})$  part of (15) the terms  $(\lambda_{y\ o y}^{\vec{m}} \cdot \hat{j})(\lambda_{z\ o z}^{\vec{m}} \cdot \hat{k})$  and  $(\lambda_{z\ o z}^{\vec{m}} \cdot \hat{k})(\lambda_{x\ o x}^{\vec{m}} \cdot \hat{i})$ .

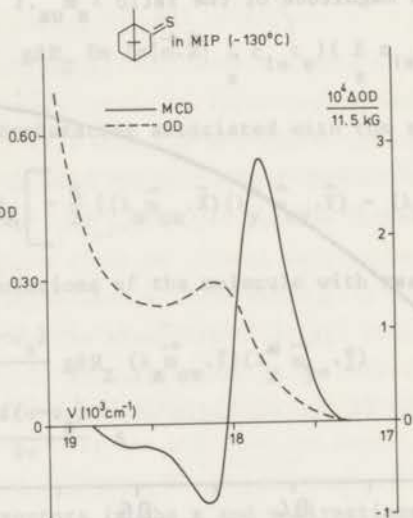


Figure 5.



#### 4. Discussion

In figure 5 we show the absorption and MCD spectrum in the 18 kK region of thiocamphor at  $-130^{\circ}\text{C}$ . Apart from a rather large hypsochromic shift upon lowering the temperature (cf. the position of the band in figure 1) the spectra at room temperature are similar. The MCD signal is linearly dependent on the strength of the magnetic field in the range 2-17 kG, as expected. Although the MCD contains a pronounced A-term contribution, there is also B-type MCD present. The value of A/D, graphically determined, is  $\sim -0.20\beta$ . For thiocyclopentanone (cf. figure 6) we find  $A/D \approx -0.15\beta$ .

Also with biacetyl we have observed a peculiar MCD in a shoulder at the foot of the  $^1(n+\pi^*)$  transition (figure 7). If the band at 20 kK would be a S $\rightarrow$ T transition (the lowest triplet level of biacetyl is reported at  $19700\text{ cm}^{-1}$ )<sup>13)</sup>, it is tempting to conclude from the nearly complete lack of A-type MCD that only one of the triplet sub-levels is active. But we recall that a vanishing A-term also can result from interfering contributions of three spin-levels. With biacetyl this presumably is the case<sup>14)</sup>. In interpreting the MCD some

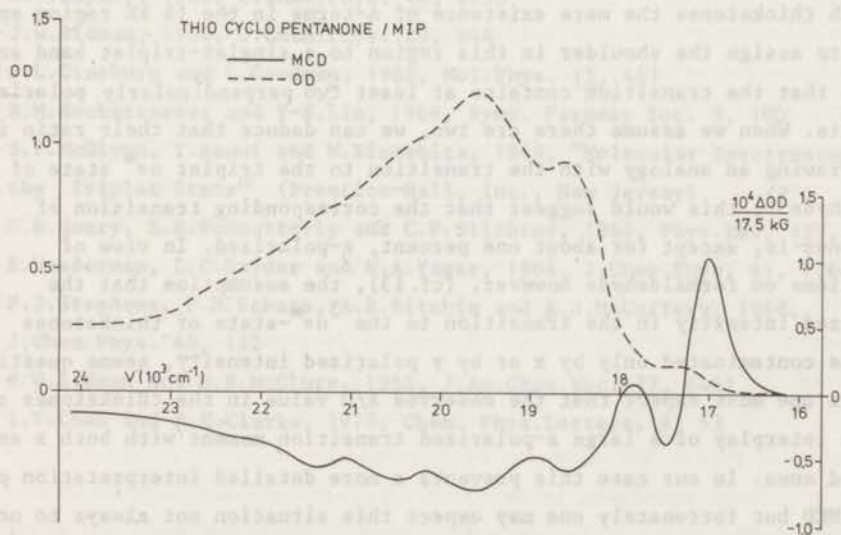


Figure 6. Absorbance ( - - - ) and MCD ( — ) of thiocyclopentanone in the  $^1(n+\pi^*)$  transition and (to the right) of the  $^3(n+\pi^*)$  band.

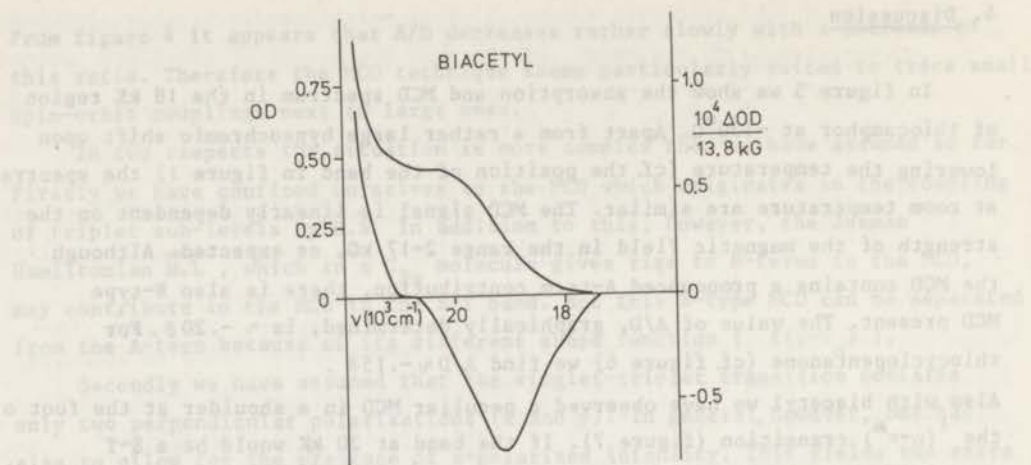


Figure 7. Absorbance (upper curve) and MCD of biacetyl (pure liquid).

care must be taken, however, since to observe the MCD we had to perform the measurements using the pure liquid.

With thioketones the mere existence of A-terms in the 18 kK region enables us both to assign the shoulder in this region to a singlet-triplet band and to conclude that the transition contains at least two perpendicularly polarized components. When we assume there are two, we can deduce that their ratio is  $\sim 1:10$ . Drawing an analogy with the transition to the triplet  $n\pi^*$  state of formaldehyde<sup>5)</sup>, this would suggest that the corresponding transition of thioketones is, except for about one percent, z-polarized. In view of calculations on formaldehyde however, (cf. §3), the assumption that the z-polarized intensity in the transition to the  $^3n\pi^*$ -state of thioketones should be contaminated only by x or by y polarized intensity, seems questionable. Therefore one must expect that the observed A/D value in the thioketones arises from the interplay of a large z-polarized transition moment with both x and y polarized ones. In our case this prevents a more detailed interpretation of the S-T MCD but fortunately one may expect this situation not always to occur, since the spatial symmetry of a triplet state can be such that only transitions to two triplet-levels  $T_u$  carry intensity.

## 5. Conclusion

CD, CPL and MCD measurements provide convincing evidence that in thioketones the weak absorption band at the onset of the  $^1(n \rightarrow \pi^*)$  transition is a singlet-triplet transition. The utility of the MCD-technique for the study of small spin-orbit couplings next to large ones in singlet-triplet transitions is demonstrated.

## References

1. K.J.Rosengren, 1962, Acta Chem.Scand. 16, 2284
2. M.J.Janssen, 1960, Rec.Trav.Chim. 79, 464
3. C.A.Emeis and L.J.Oosterhoff, 1971, J.Chem.Phys. 54, 4809
4. D.S.L.Blackwell, C.C.Liao, R.O.Loutfy, P. de Mayo and S.Paszyc, 1972, Mol.Photochem. 4, 171
5. W.T.Raynes, 1966, J.Chem.Phys. 44, 2755
6. J.W.Sidman, 1958, J.Chem.Phys. 29, 644
7. J.L.Ginsburg and L.Goodman, 1968, Mol.Phys. 15, 441
8. R.M.Hochstrasser and T-S.Lin, 1969, Symp. Faraday Soc. 3, 100
9. S.P.McGlynn, T.Azumi and M.Kinoshita, 1969, "Molecular Spectroscopy of the Triplet State" (Prentice-Hall, Inc., New Jersey)
10. C.H.Henry, S.E.Schnatterly and C.P.Slichter, 1965, Phys.Rev. 137, A583
11. E.Wasserman, L.C.Snyder and W.A.Yager, 1964, J.Chem.Phys. 41, 1764
12. P.J.Stephens, P.N.Schatz, A.B.Ritchie and A.J.McCaffery, 1968, J.Chem.Phys. 48, 132
13. J.W.Sidman and D.S.McClure, 1955, J.Am.Chem.Soc. 77, 6461
14. I.Y.Chan and R.H.Clarke, 1973, Chem. Phys.Letters, 9, 53

## CHAPTER V

### THE OPTICAL ACTIVITY OF LOW-SYMMETRY KETONES

#### 1. Introduction

Chiral systems (i.e. pieces of matter lacking rotation reflection axes) exhibit optical activity. Such systems can exist in two different geometrical forms which relate as an object and its mirror image. If the chiral entity is a molecule, the two enantiomeric forms have been termed (+) and (-) or d and l (according to the sense of rotation of plane polarized light they give rise to) and, more recently, R and S (according to their molecular structure).

Compare now the interactions between a particular molecule in its R configuration with right or left circularly polarized light, respectively. Unless both interactions are zero, they will be different: the molecule at hand is optically active and may in its transitions exhibit Cotton effects. The differential absorption of left and right circularly polarized light leads to circular dichroism (CD) while the different dispersions of both kinds of light give rise to optical rotation dispersion (ORD).

Both phenomena have been known since long. In 1811 Arago found that crystalline quartz rotates the plane of linearly polarized light and in 1847 the circular dichroism of amethyst quartz was measured by Haidinger. Shortly after the detection of the optical activity of chiral crystals it was discovered that isotropic solutions of certain molecules also may exhibit a differential refraction and absorption of left and right circular light. Exactly a century ago, Van 't Hoff concluded that the very fact that some

molecules are capable to rotate the plane of polarized light, and thus are not superimposable on their mirror images, has to be of consequence for molecular structure: the tetrahedral structure around a saturated carbon atom had been proven. Since then the detection of chirality with polarized light has been of great use in problems of structural chemistry. In the early days the measurement of optical activity for technical reasons mostly was restricted to the determination of the rotation at the sodium D line. Later on, when spectropolarimeters became commercially available, routine measurements of the dispersion of the optical rotation in the visible and near ultraviolet region of the spectrum became possible. Nowadays optical activity is usually recorded as circular dichroism, which in general is - as to sensitivity and ease of interpretation - superior to ORD. While in a CD measurement the optical activity as a function of frequency is recorded for all transitions separately (if in the absorption spectrum the bands do not overlap) the ORD, not being confined to absorption regions only, is brought about by the sum of the contributions of all individual bands. Consequently, if the optical activity is registered as a rotation, one has to disentangle the partial rotations of the separate electronic transitions from the total dispersion curve. This, incidentally, can be done exactly by transforming the entire ORD spectrum into a CD spectrum by means of the Kramers-Kronig relations. In practice this procedure is not feasible however, because with the available apparatus one can scan only a limited region of the spectrum. This latter fact causes the CD to be superior to the ORD in general, but it may work out just the other way round on some special occasions. Namely, if one wants information on the optical activity of a transition in an inaccessible spectral region, one can get this occasionally from an ORD experiment, but certainly not from a CD measurement. Furthermore if the detection of the optical activity in absorption bands turns out to be impossible owing to the smallness of the effect, one always can increase the concentration or pathlength and measure the ORD outside the absorption region.

After having touched on the ways optical activity data are gathered, we would like to dwell for a while on the question how the optical activity of a molecule can provide information on molecular chirality. Since Condon it is known that the optical activity of an electronic transition is governed by its rotational strength, which in turn is defined by the scalar product of the quantummechanical electric and magnetic dipole transition moments. The molecular wave functions, incorporated in the integrands of the spectral transition moments, depend heavily on the nuclear coordinates and thus a connection

between optical activity and chirality is laid. At least in principle, for the actual road leading from experimental CD to chirality is sometimes long and slippery owing to the well-known difficulties encountered in finding satisfactory wave functions.

Therefore it is not surprising that chemists have tried to find other, easier routes and often with considerable success. We refer here to the many well-known sector rules which correlate in an empirical way the contributions to the optical activity of the separate atoms and their relative positions in a molecule. One of the most famous sector rules is the octant rule for chiral ketones, which has proven to be extremely fertile in the exploration of e.g. the field of conformational analysis. Notwithstanding the generally greater accuracy and applicability of e.g. diffraction methods and NMR techniques in the elucidation of molecular structures, it is in particular these sector rules which permit one to consider the optical activity as an indispensable tool in structural chemistry, especially when one wants to study flexible or larger molecules. This being the more so since recently it turned out to be possible to measure the optical activity of excited species<sup>1)</sup> (Circular Polarization of Luminescence). Just as the circular dichroism provides information on the chirality of the molecule in its ground state, the CPL incorporates the essential features of the structure in the excited state. This information, emitted by the fluorescent or phosphorescent molecule by means of unequal amounts of right and left circularly polarized radiation, in general cannot be detected that easily by other techniques. One perhaps still better can appreciate the potential value of the CPL technique when realizing that a confrontation of CD and CPL provides the change of the rotatory strength brought about by the change in conformation upon excitation. In a way this is the leading thought in our discussions later on.

Until now we have not discussed the spectroscopic facets of optical activity, which often are sufficiently interesting to justify a study in the field. In optical activity a large dissymmetry factor - which relates to the ratio of CD and unpolarized absorption - is often indicative of a magnetically allowed transition, this being so because the CD depends linearly on the electric (and magnetic) dipole transition moment while the ordinary absorption is governed by the squared electric dipole transition moment. Thus it is often possible to assign transitions (e.g. the  $n \rightarrow \pi^*$  transition in ketones or thio-ketones or bands in transitionmetal complexes) as magnetically allowed ones if they do show a large dissymmetry factor. Another case arises if a transition in emission can be identified as phosphorescence (e.g. by means of its life time)

and has a dissymmetry factor which is equal to that of a weak absorption band at roughly the same frequency. The latter band can then be assigned as the reverse transition, i.e. a S→T transition (cf. Chapter IV). Mostly fluorescence occurs from one (the lowest) excited singlet state, while in absorption it may not be certain whether the longest wavelength transition is pure or overlaps with another nearby band. Measurement of the optical activities in absorption and emission can settle this question.

As to be shown in this chapter the electronic rotational strength, obtainable from the experimental CD by integrating over all its vibrational fine structure, is a quantity which pertains to the equilibrium geometry of the molecule in its vibronic ground state. When this ground state is not chiral a zero electronic rotational strength should be observed. Perhaps this situation is approached with a solution of (1R) - 2'-O<sup>18</sup>- $\alpha$ -fenchocampheronequinone<sup>2)</sup> whose optical activity is due to the presence of molecules which have an O<sup>18</sup> incorporated in their cis- $\alpha$ -diketone moiety. The fact that the integrated CD in the visible absorption band approaches zero is in accordance with the expectation that the structures of molecules with an O<sup>18</sup> resp. O<sup>16</sup> in them, will not be very different. However, while the integrated ellipticity is small, the ellipticity itself is not, reaching appreciable positive (and negative) values at various wavelengths. Apparently we here meet a case where the molecular vibrations monopolize the generation of optical activity. But also in other cases, e.g. ketones of the types studied in this chapter, vibrations do try to appropriate appreciable parts of the ellipticity and it is a tempting task trying out how successful they are. Particularly, it will appear that the study of vibronic optical activity will be of help in the controversy which arose when Weigang<sup>3)</sup> suggested — contrary to the implications of the theory of Moffitt and Moscovitz<sup>4)</sup> — that the integrated CD of ketones might contain a large contribution entirely due to vibrations, i.e. deviations from equilibrium geometry. Weigang put forward his theory to explain the occurrence of CD curves, which cross zero within an absorption band (to describe such curves, Klyne and Kirk<sup>5)</sup> coined the term "bisignate"). According to Weigang, the short wavelength lobe of a bisignate CD curve is of purely vibrational origin while the long wavelength branch contains the optical activity due to static molecular structure.

We have measured the optical activity of a number of ketones, not only in absorption but also in the fluorescence. The new information that is acquired from the emission experiments shall give us the unique opportunity to verify a qualitative theory which we put forward to account for the occurrence or

absence of bisignate Cotton effects in absorption and emission, and which shows that bisignate Cotton effects can be perfectly well explained with the theory of Moffitt and Moscovitz.

### Outline of the chapter

We start with a short survey of the theories which connect the chirality of ketones with their rotational strength in the  $^1(n \rightarrow \pi^*)$  transition (§2). Then we report and discuss in §3 the CD and CPL spectra of several saturated ketones. To start with we first discuss a ketone with  $C_2$  symmetry, trans  $\beta$ -hydrindanone. Next the low-symmetry ketones are discussed, stress being laid on the occurrence of bisignate Cotton effects.

The theories, previously given by Moffitt and Moscovitz and by Weigang, on the influence of nuclear motion on rotational strength are summarized and discussed in §4.

Lastly, we present in §5 a theory on the mechanism by which the optical activity in an absorption band is generated as a function of excitation energy, which will enable us to explain qualitatively the shapes of the observed CD and CPL spectra and to learn more about the origin of bisignate Cotton effects.

### 2. Relationship between rotational strength and structure

If  $\epsilon_L$  ( $\epsilon_R$ ) is the molecular decadic extinction coefficient measured with left (right) circularly polarized light one has the familiar relations<sup>6)</sup> that for a given absorption band connect its dipole strength  $D$  and rotational strength  $R$  with its absorbance and circular dichroism:

$$D = 92.0 \cdot 10^{-40} \int_{\text{band}} \frac{\epsilon_L + \epsilon_R}{2} \frac{d\nu}{\nu} = 92.0 \cdot 10^{-40} \int_{\text{band}} \frac{\epsilon}{\nu} d\nu \quad (1)$$

$$R = 23.0 \cdot 10^{-40} \int_{\text{band}} (\epsilon_L - \epsilon_R) \frac{d\nu}{\nu} = 23.0 \cdot 10^{-40} \int_{\text{band}} \frac{\Delta\epsilon}{\nu} d\nu \quad (2)$$

where  $D$  and  $R$  are expressed in cgs units.

As already indicated, an experimental dissymmetry factor can be defined as

$$g(\nu) = \frac{\Delta\epsilon(\nu)}{\epsilon(\nu)} \quad (3)$$

The dissymmetry factor for the entire band is given by



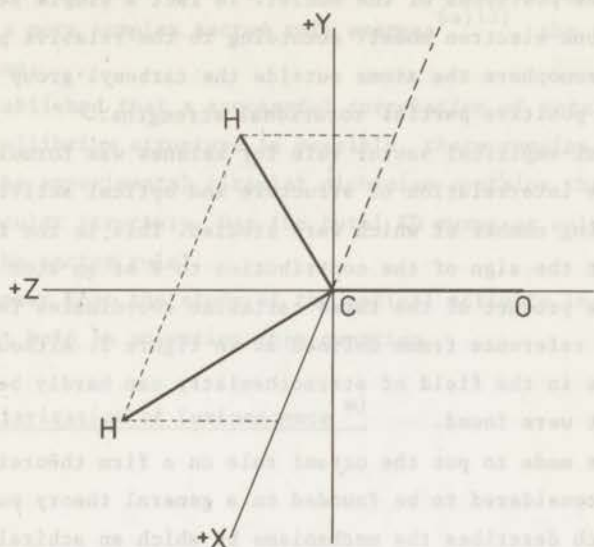


Figure 1. Reference frame for formaldehyde (and ketones).

$$g = \frac{4R}{D} = \frac{\int_{\text{band}} \frac{\Delta \epsilon}{\nu} d\nu}{\int_{\text{band}} \frac{\epsilon}{\nu} d\nu} \quad (4)$$

and it follows that if absorption and CD have similar band shapes, the two g-factors are identical.

Equation (2) prescribing how the quantum mechanical quantity R can be obtained from experiment, we are now left with the question how to infer from it the structural information we want.

The  $n \rightarrow \pi^*$  transition in the carbonyl group is magnetic dipole allowed along the z-axis (cf. figure 1), and in order to render it optically active, it should become electric dipole allowed too. Assuming chiral ketones to consist of a planar (achiral) carbonyl chromophore, whose wave functions are mixed by the static electric field of the extrachromophoric nuclei, Kauzmann, Walter and Eyring were able to show that in this way the  $n \rightarrow \pi^*$  transition acquires optical activity. But the almost quantitative agreement between calculated and experimental rotational strength they obtained for 3-methylcyclopentanone<sup>7)</sup> appeared later on to be fortuitous.<sup>8)</sup> It is clear that this so-called one-electron model lays a very direct connection between rotatory strength and structure, for the perturbing potential originates in charge densities which

are centered at the positions of the nuclei. In fact a simple sector rule emerges from the one-electron model: according to the relative positions with respect to the chromophore the atoms outside the carbonyl group contribute negative, zero or positive partial rotational strengths.

In 1961 a semi-empirical sector rule for ketones was formulated<sup>9)</sup>, to account for the interrelation of structure and optical activity of ketones, a rapidly increasing number of which were studied. This is the famous octant rule, stating that the sign of the contribution to R of an atom is determined by the sign of the product of the three cartesian coordinates for that atom in a right-handed reference frame defined as in figure 2. Although the success of the octant rule in the field of stereochemistry can hardly be overestimated, deviations from it were found.

Attempts were made to put the octant rule on a firm theoretical basis, and these can be considered to be founded on a general theory put forward by Tinoco<sup>10)</sup>, which describes the mechanisms by which an achiral chromophore acquires optical activity from its chiral environment. In ketones the electrostatic interaction between the electric quadrupole charge density of the  $n \rightarrow \pi^*$  transition and the chirally disposed transition dipoles in the C-C and C-H groups appears to be crucial in the process of generating optical activity. The magnitude of the coupling may be calculated using either theoretical values for the C-C and C-H transition charge densities or, what amounts to the same, experimental polarizabilities of the bonds<sup>6a)</sup>. When one represents a bond by an isotropic polarizability, situated at its midpoint, a simple octant behaviour

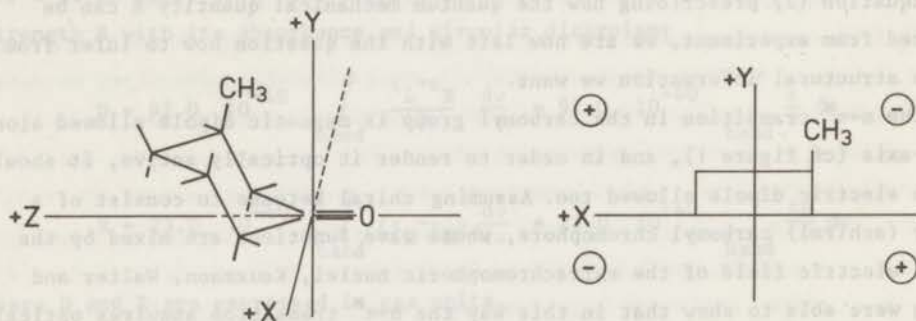


Figure 2. Left: reference frame for the octant rule  
Right: octant rule if the z-coordinates of all relevant atoms are positive.

is found<sup>11)</sup>; if however one takes into account the anisotropy of the polarizability a more complex sector rule emerges<sup>6a)12)</sup>, the direction of the bond counting too.

Having established that a successful correlation of rotatory strength with ground state equilibrium structure is possible, there remains the question which part of the experimental circular dichroism contains the information on the static molecular structure. Has the total CD curve or only part of it to be faced with the sector rule?

It will appear that the study of the optical activity in the fluorescence will be of great help in answering this question.

### 3. Circular Polarization of Luminescence \*)

#### 3a. General

In many respects the measurement of the circular polarization of the luminescence is the emission analogue of a circular dichroism experiment. When a sufficiently high concentration of molecules in their fluorescent state can be created, e.g. by irradiation with unpolarized light, the amount of photons of the two circular polarization states in the spontaneous emission will be different — provided the fluorescent species are chiral. So one defines<sup>1)</sup>

$$\Delta I(\nu) = I_L(\nu) - I_R(\nu) \quad (5)$$

where  $I_L$  ( $I_R$ ) is the intensity of the part of the emission which is left (right) circularly polarized (in relative quanta per unit of frequency interval). The mean intensity of the fluorescence is given by

$$I(\nu) = \frac{I_L(\nu) + I_R(\nu)}{2} \quad (6)$$

while the dissymmetry factor takes the form

$$g_{lum}(\nu) = \frac{\Delta I(\nu)}{I(\nu)} \quad (7)$$

For a given electronic transition the relations between the experimental and

\*) We are grateful to Mrs. Dr. L. E. Closs (Chicago) for performing the CPL-measurements and for numerous discussions during her stay at our department.

theoretical quantities are <sup>6a)</sup>

$$R^{em} = \text{constant} \times \int_{\text{band}} \frac{\Delta I}{v^3} dv \quad (8)$$

$$D^{em} = 4 \text{ constant} \times \int_{\text{band}} \frac{I}{v^3} dv \quad (9)$$

Unlike in absorption we encounter in emission the situation that the values of D and R usually are not obtained separately since in the fluorescence experiment only the relative intensity distribution  $I(v)$  is measured and thus the value of the constant in (8) and (9) is not known. We must realise however that the g-value for the luminescence band

$$g_{lum} = \frac{\int_{\text{band}} \frac{\Delta I}{v^3} dv}{\int_{\text{band}} \frac{I}{v^3} dv} = \frac{4R^{em}}{D^{em}} \quad (10)$$

is available and that knowledge of  $D^{em}$ , e.g. from a determination of the radiative lifetime of the upper state, then leads to  $R^{em}$ .

In line with the foregoing, the maximum of the I-curve in the figures is always put equal to 1.0 .

For all compounds the optical density (OD), circular dichroism ( $\Delta OD$ ), fluorescence (I) and circular anisotropy of fluorescence ( $\Delta I$ ) were measured with the same sample solution. When during the measurement the composition of the solution changed - e.g. because of photoracemisation or photoreactions - the experiment was (more quickly) repeated with a fresh solution. In all compounds examined, the fluorescence proved to be a broad, structureless band, the CPL of which was determined using a 15 nm bandwidth.

### 3b. Hydrindanone

Before discussing the optical activities in absorption and emission of low symmetry ketones we first recall some results of the thorough study by Emeis on the  $C_2$  symmetry compound trans-8-hydrindanone <sup>6)6a)</sup>. (For the spectra see figure 3, for the choice of axes figure 1).

Making use of the full symmetry of the molecule in its initial and final state Emeis has shown that the large circular dichroism in the  $n \rightarrow \pi^*$  transition of hydrindanone arises from the presence of z-polarized magnetic and electric

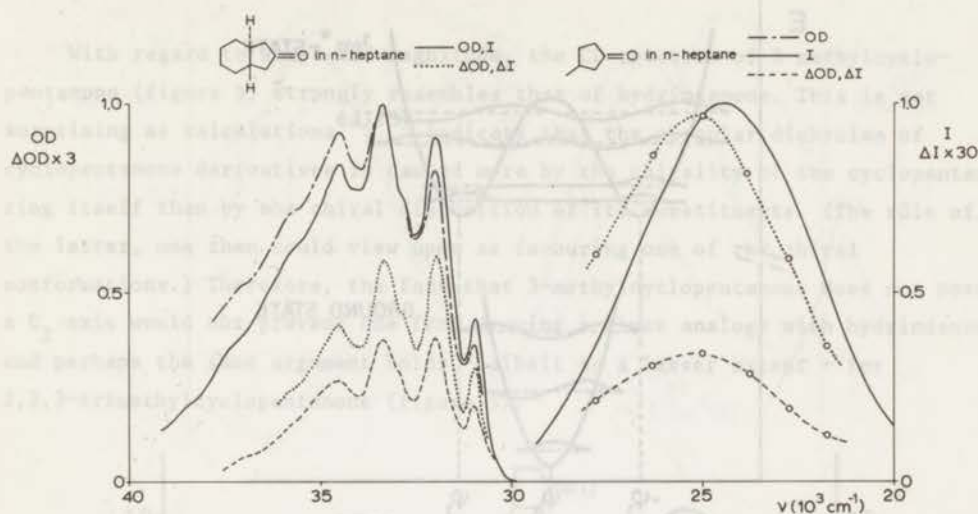


Figure 3. Hydrindanone and 3-methylcyclopentanone

Left: unpolarized absorption (OD) and circular dichroism ( $\Delta OD$ )

Right: unpolarized fluorescence (I) and CPL ( $\Delta I$ )

The fluorescence curves for both compounds coincide.

Note that the scale factors for  $\Delta OD$  and  $\Delta I$  are different.

dipole transition moments. Electric dipole moments in transitions from the vibronic ground state to non-totally symmetric vibrational levels of the  $^1n\pi^*$  state, with components in a plane perpendicular to the z-axis, do contribute to  $D^{abs}$  but not to  $R^{abs}$ . This fact, together with the circumstance that the observed spectra show considerable fine structure, enabled Emeis to decompose the experimental absorption spectrum into the allowed and forbidden (i.e. vibrationally induced) parts and, moreover, to establish a precise value for the magnetic moment in this  $n\pi^*$  transition.

The CPL spectrum of hydrindanone (which is shown in figure 3) is in essential agreement with that reported by Emeis. When the CPL is compared with the CD one observes a drastic lowering of the dissymmetry factor in the fluorescence band compared to that in the absorption band. (Note that in the figures  $\Delta OD$  and  $\Delta I$  have different scale factors.) As shown by Emeis, this points to an excited state in which the nuclear configuration around the carbon atom of the carbonyl group is pyramidal: in the  $^1n\pi^*$  state the C-O bond is no longer directed along the -z-axis but, while still being in the yz plane,

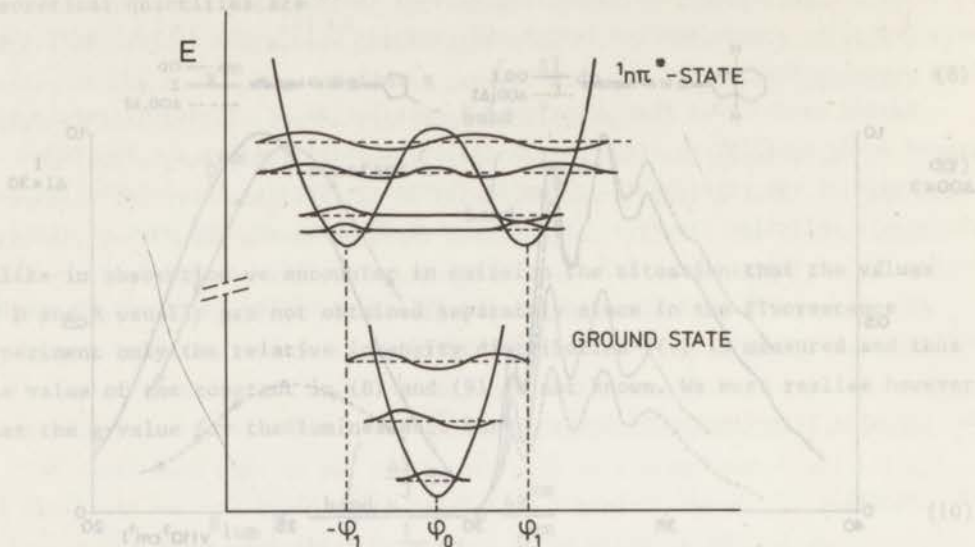


Figure 4. Hydrindanone

Electronic energy curves and vibrational wave functions and energies for the out-of-plane bending mode.

it makes an angle  $\phi_1$  or  $-\phi_1$  with it, leading to a situation which is displayed in figure 4.

Whereas in the ground state conformation the electric dipole transition moment is directed along the z-axis, in the two pyramidal configurations (which are identical) the transition is allowed in the x-direction too. Hence the dipole strength is larger in emission than in absorption. As however the value of the z-component of the electric dipole transition moment probably will not change much upon excitation, and from calculations it follows that the z-component of the magnetic dipole transition moment in emission has about the same magnitude as in absorption, the rotational strengths in absorption and fluorescence are probably not very different ( the x-polarized intensity in emission does not carry rotational strength because  $\mu_x$  is zero ). Hence Emeis could conclude that the lowering of the dissymmetry factor upon excitation is primarily due to an increase of  $D^{em}$ .

### 3c. Low symmetry ketones \*)

With regard to shape and magnitude, the CD spectrum of 3-methylcyclopentanone (figure 3) strongly resembles that of hydrindanone. This is not surprising as calculations<sup>6a)13)</sup> indicate that the circular dichroism of cyclopentanone derivatives is caused more by the chirality of the cyclopentanone ring itself than by the chiral disposition of its substituents. (The rôle of the latter, one then could view upon as favouring one of the chiral conformations.) Therefore, the fact that 3-methylcyclopentanone does not possess a  $C_2$  axis would not prevent one from drawing a close analogy with hydrindanone<sup>\*\*)</sup>, and perhaps the same argument holds - albeit to a lesser extent - for 2,2,3-trimethylcyclopentanone (figure 5).

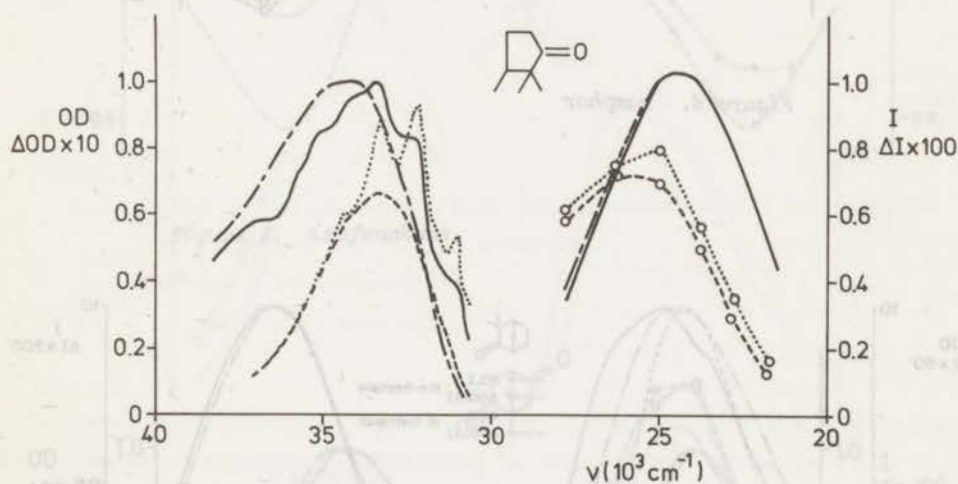


Figure 5. 2,2,3-trimethylcyclopentanone

\*) All the compounds studied were put at our disposal by Dr. W.C.M.C.Kokke (formerly at this department), except for epi-androsterone which we obtained from Dr. H.J.C.Jacobs of these laboratories.

\*\*\*) For the moment we neglect the fact that at room temperature a solution of 3-methylcyclopentanone in an alkane solvent is not conformationally pure, this being the most plausible explanation for Djerassi's observation that the magnitude of the CD of a solution of 3-methylcyclopentanone increases upon lowering the temperature.<sup>14)</sup>

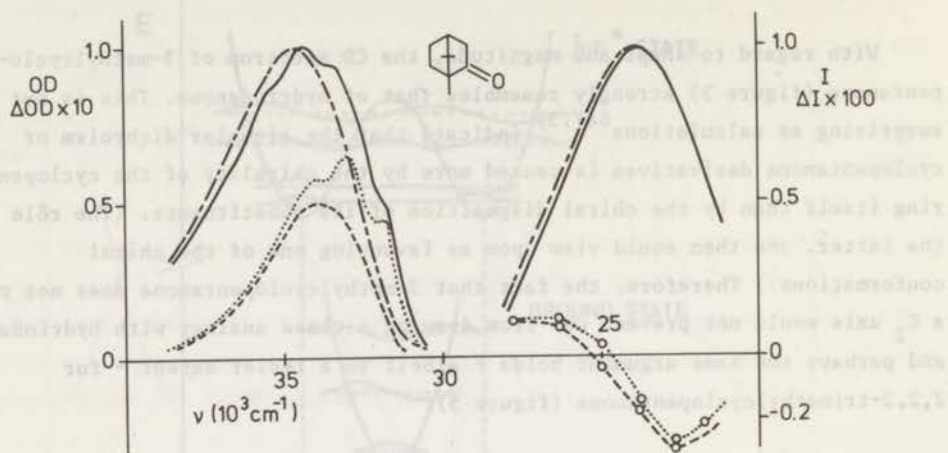


Figure 6. camphor

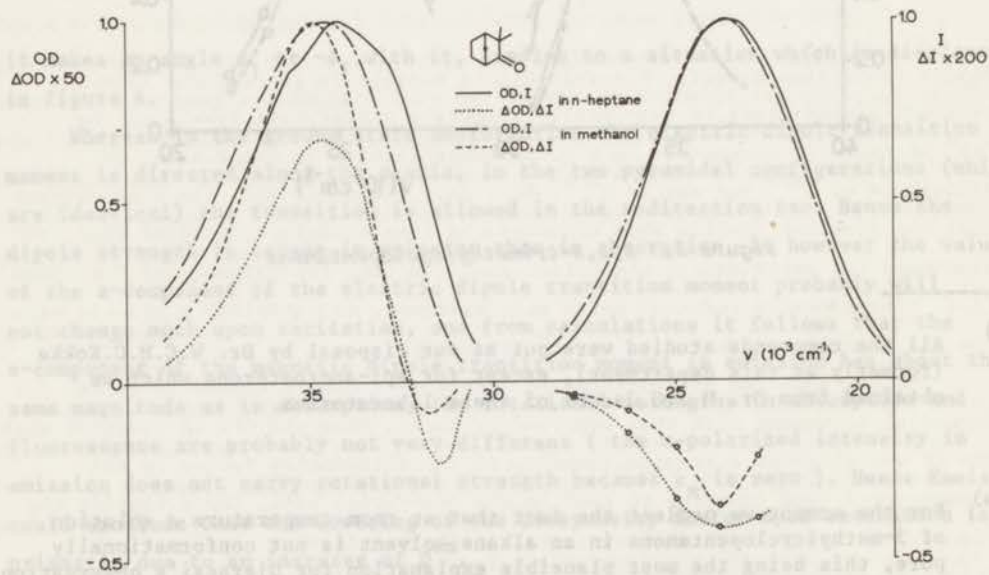


Figure 7. camphenilone



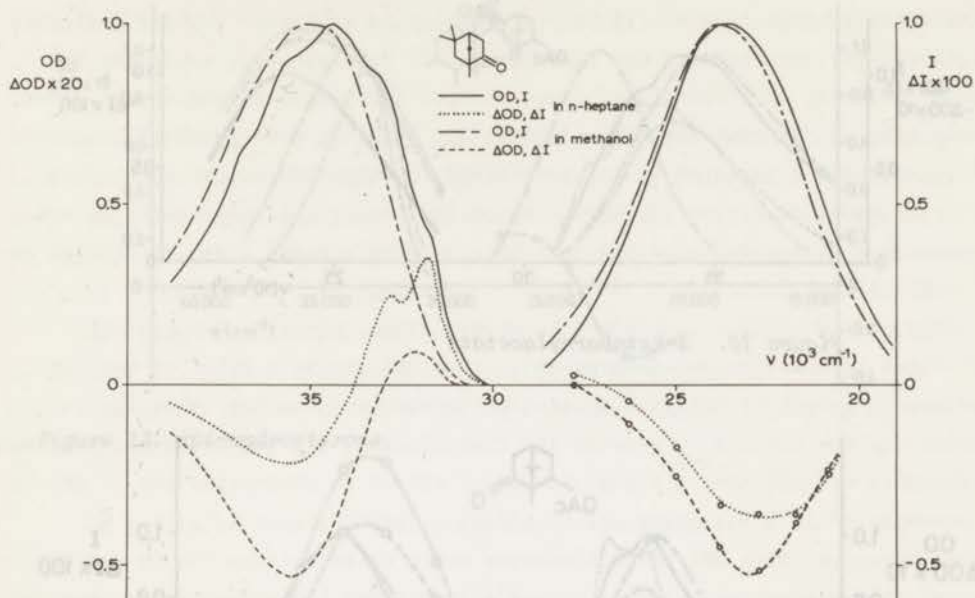


Figure 8. isofenone

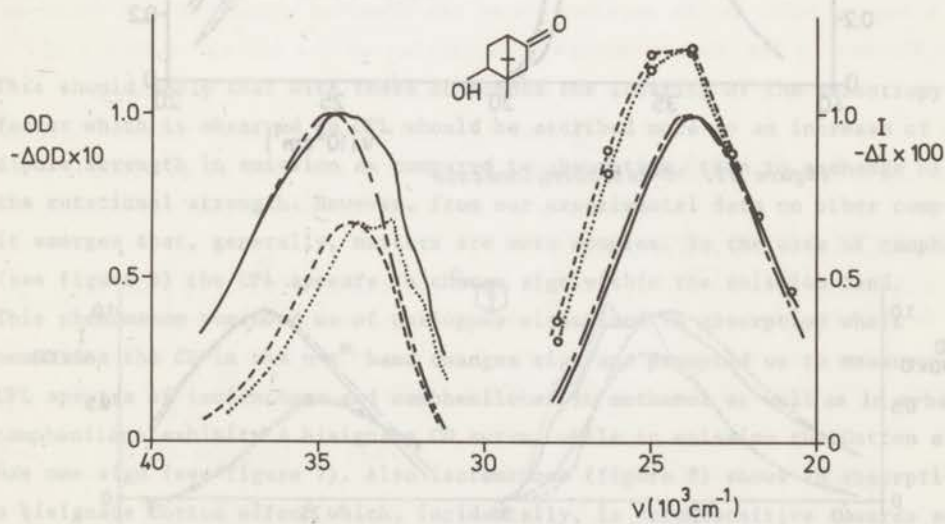


Figure 9. 5-ketoborneol

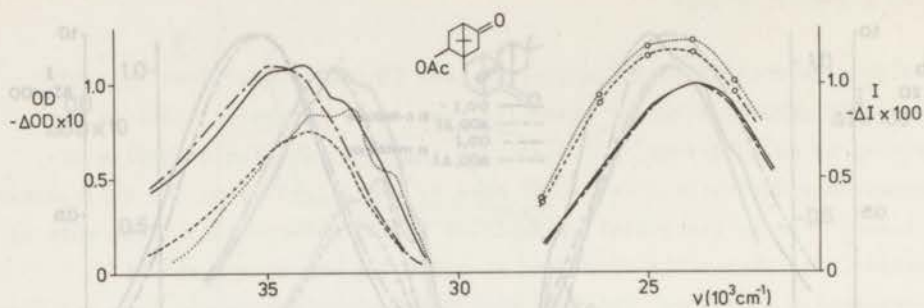


Figure 10. 5-ketobornylacetate

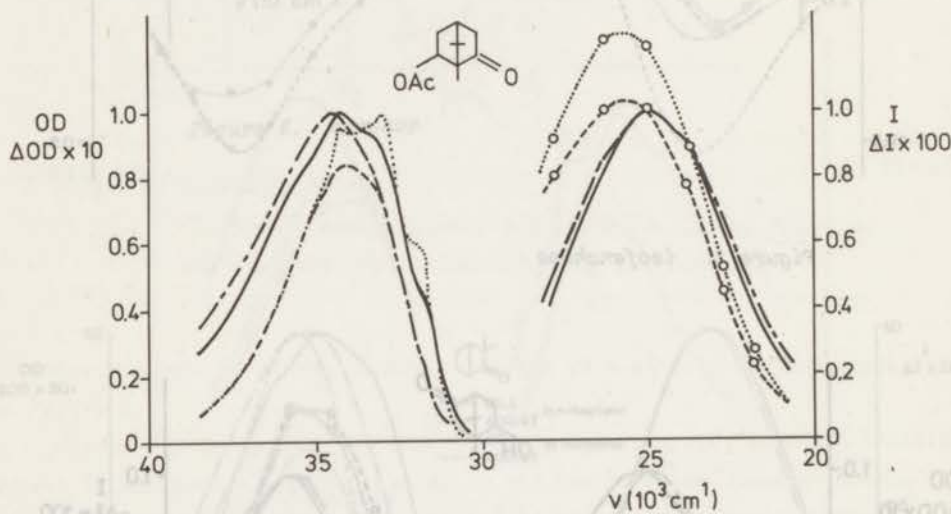


Figure 11. 6-ketobornylacetate

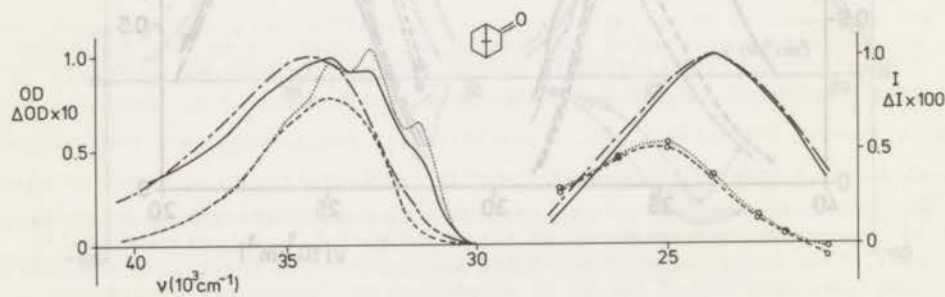


Figure 12.  $\alpha$ -fenchocampherone

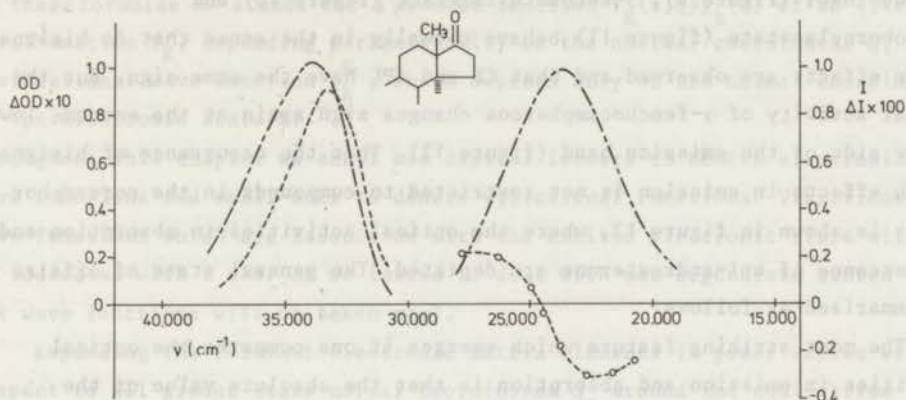


Figure 13. *epi-androsterone*

Figure 5-13.

- unpolarized absorption (OD) and fluorescence (I) in *n*-heptane
- ..... CD ( $\Delta OD$ ) and CPL ( $\Delta I$ ) in *n*-heptane
- — — OD and I in methanol
- - -  $\Delta OD$  and  $\Delta I$  in methanol

This should imply that with these compounds the lowering of the anisotropy factor which is observed in CPL should be ascribed more to an increase of the dipole strength in emission as compared to absorption, than to a change of the rotational strength. However, from our experimental data on other compounds it emerges that, generally, matters are more complex. In the case of camphor (see figure 6) the CPL appears to change sign within the emission band. This phenomenon reminded us of analogous situations in absorption where sometimes the CD in the  $n \rightarrow \pi^*$  band changes sign and prompted us to measure the CPL spectra of isofenchone and camphenilone. In methanol as well as in *n*-heptane camphenilone exhibits a bisignate CD curve, while in emission the Cotton effect has one sign (see figure 7). Also isofenchone (figure 8) shows in absorption a bisignate Cotton effect which, incidentally, is very sensitive towards solvent. In emission there is also a bisignate Cotton effect if the solvent is *n*-heptane, but not when it is methanol. Other ketones in the bicycloheptanone series,

5-ketoborneol (figure 9), 5-ketobornylacetate (figure 10) and 6-ketobornylacetate (figure 11) behave normally in the sense that no bisignate Cotton effects are observed and that CD and CPL have the same sign. But the optical activity of  $\alpha$ -fenchocampherone changes sign again at the extreme low energy side of the emission band (figure 12). That the occurrence of bisignate Cotton effects in emission is not restricted to compounds in the norcamphor series is shown in figure 13, where the optical activities in absorption and fluorescence of epi-androsterone are depicted. The general state of affairs may be summarized as follows.

The most striking feature which emerges if one compares the optical activities in emission and absorption is that the absolute value of the dissymmetry factor in emission is smaller (often much smaller) than in absorption, the ratio  $g_{lum}/g$  being far from constant for the different compounds. Furthermore we note that a bisignate Cotton effect in absorption may or may not be accompanied by a bisignate one in emission, and the same holds for a normal CD curve. With all the differences which exist between the CD and CPL spectra of the examined ketones, in one respect they all agree: in no case the sign of the CD at higher wavelengths and the sign of the CPL at shorter wavelengths (i.e. near the (0,0) band of the electronic transition) are different. In §5 we shall examine these various observations more closely. It then will appear that the bisignate Cotton effects in absorption and emission take a key position in the explanation of the observed phenomena. But first we shall discuss in the next paragraph the theories on the optical activity of ketones, previously put forward by Moffitt and Moscovitz and by Weigang.

#### 4. Optical activity of ketones in absorption

##### 4a. Theory of Moffitt and Moscovitz

In 1959 Moffitt and Moscovitz<sup>4)</sup> showed that, in the Born-Oppenheimer approximation, the rotational strength of a transition from the vibronic ground state  $O_0$  to a vibrational level  $\bar{n}$  of the excited electronic state  $N$  is given by

$$R_{O_0 \rightarrow N\bar{n}} = \text{Im} (O_0 | \vec{r} | N\bar{n}) \cdot (N\bar{n} | \vec{\mu} | O_0) \quad (11)$$

while the expression for the dipole strength reads

$$D_{O_0 \rightarrow N\bar{n}} = \left| (O_0 | \vec{r} | N\bar{n}) \right|^2 \quad (12)$$

In these formulae  $\chi_k$  stands for a product function  $\psi_K(r, Q) \chi_k^K(Q)$  of an electronic wave function  $\psi_K$ , depending parametrically on the nuclear coordinates  $Q$ , and a vibrational wave function  $\chi_k^K$ , which depends only on the normal coordinates in the electronic state  $K$ .

Throughout this chapter we shall use capital letters to denote electronic wave functions and small ones to denote vibrational functions. Vibrational wave functions which are associated with the excited electronic state will be indicated with a bar. As we intend to deal with non-degenerate states only, all wave functions will be taken real.

Expanding the relevant electronic matrix elements in power series with respect to all ground state normal coordinates  $Q_r$  around the equilibrium positions of the nuclei in the electronic ground state, defined by  $Q_r^0 = \langle o | Q_r | o \rangle = 0$  for all  $r$ , one finds

$$\vec{r}_{ON} = \vec{r}_{ON}^{(o)} + \sum_s \vec{r}_{ON}^{(1)s} Q_s + \dots \quad (13)$$

$$\vec{\mu}_{NO} = \vec{\mu}_{NO}^{(o)} + \sum_s \vec{\mu}_{NO}^{(1)s} Q_s + \dots \quad (14)$$

in these equations

$$\vec{r}_{ON}^{(o)} = \vec{r}_{ON}(Q^0) \quad (15)$$

and

$$\vec{r}_{ON}^{(1)s} = \left. \frac{\partial \vec{r}_{ON}(Q)}{\partial Q_s} \right|_{Q_s = Q_s^0} \quad (16)$$

Whereas similar expressions define  $\vec{\mu}_{NO}^{(o)}$  and  $\vec{\mu}_{NO}^{(1)s}$ .

When neglecting in (13) and (14) terms of higher than first order in  $Q$ , the expression for the rotational strength is reduced to

$$R_{Oo \rightarrow N\bar{n}} = \text{Im} \left[ \vec{r}_{ON}^{(o)} \cdot \vec{\mu}_{NO}^{(o)} (o | \bar{n}) (\bar{n} | o) + \sum_s (\vec{r}_{ON}^{(o)} \cdot \vec{\mu}_{NO}^{(1)s} + \vec{r}_{ON}^{(1)s} \cdot \vec{\mu}_{NO}^{(o)}) (o | \bar{n}) (\bar{n} | Q_s | o) \right. \\ \left. + \sum_{s,t} \vec{r}_{ON}^{(1)s} \cdot \vec{\mu}_{NO}^{(1)t} (o | Q_s | \bar{n}) (\bar{n} | Q_t | o) \right] \quad (17)$$

For the dipole strength we find

$$D_{Oo \rightarrow N\bar{n}} = \vec{r}_{ON}^{(o)} \cdot \vec{r}_{NO}^{(o)} (o | \bar{n}) (\bar{n} | o) + 2 \sum_s \vec{r}_{ON}^{(o)} \cdot \vec{r}_{NO}^{(1)s} (o | \bar{n}) (\bar{n} | Q_s | o) + \\ + \sum_{s,t} \vec{r}_{ON}^{(1)s} \cdot \vec{r}_{NO}^{(1)t} (o | Q_s | \bar{n}) (\bar{n} | Q_t | o) \quad (18)$$

Note that the expression (17) for R (and also that for D) is not complete up to second order, since terms in  $\vec{r}^{(2)} \cdot \vec{\mu}^{(0)}$  and  $\vec{r}^{(0)} \cdot \vec{\mu}^{(2)}$  are missing. This is of no consequence for the discussion here as second order terms are not important in the theory of Moffitt and Moscovitz. We yet include in (17) a second order term since we shall need it in §4b. At this stage it is useful to distinguish two limiting cases.

Case I. Small variations of  $\vec{r}_{ON}$  and  $\vec{\mu}_{NO}$  with nuclear displacements

As far as the electric dipole matrix element is concerned, it is likely that this situation holds reasonably when the transition O→N is strongly allowed, for then one can expect the variation of  $\vec{r}_{ON}$  with Q to be small compared to the relatively large value of  $\vec{r}_{ON}$  at  $Q^0$ . We remark however, that the question if in a particular strongly allowed transition the - usually small - value of  $\vec{\mu}_{NO}$  is also a slowly varying function of Q, cannot be answered a priori. Anyhow, with the abovementioned assumptions

$$R_{O \rightarrow N \bar{n}} = \text{Im} \vec{r}_{ON}^{(o)} \cdot \vec{\mu}_{NO}^{(o)} (o | \bar{n} | \bar{n} | o) \quad (19)$$

$$D_{O \rightarrow N \bar{n}} = \vec{r}_{ON}^{(o)} \cdot \vec{r}_{NO}^{(o)} (o | \bar{n} | \bar{n} | o) \quad (20)$$

Making use of the quantum mechanical sum rule, which holds under quite general circumstances, one arrives at

$$R_{O \rightarrow N} = \sum_{\bar{n}} R_{O \rightarrow N \bar{n}} = \text{Im} \vec{r}_{ON}^{(o)} \cdot \vec{\mu}_{NO}^{(o)} \quad (21)$$

$$D_{O \rightarrow N} = \sum_{\bar{n}} D_{O \rightarrow N \bar{n}} = \vec{r}_{ON}^{(o)} \cdot \vec{r}_{NO}^{(o)} \quad (22)$$

Consequently the dissymmetry factor, first introduced by Kuhn, is independent of the vibrational level of the upper state:

$$g_{O \rightarrow N \bar{n}} = \frac{4R_{O \rightarrow N \bar{n}}}{D_{O \rightarrow N \bar{n}}} = \frac{4R_{O \rightarrow N}}{D_{O \rightarrow N}} = g_{O \rightarrow N} \quad (23)$$

and we encounter the situation that absorption and circular dichroism have similar band shapes. This is not so in the other limiting case Moffitt and Moscovitz brought to the front and which is briefly discussed now.

Case II. Small variations of  $\vec{\mu}_{NO}$  with nuclear displacements

Ketones exhibit in the 3000 Å region a weak absorption band with an extinction coefficient of about 30. The fact that the extinction coefficient does not vary very much in the ketone series indicates that apparently the

transition probability to a large extent is independent of the detailed structure of the particular ketone. In the parent compound formaldehyde, which belongs to the point group  $C_{2v}$ , the  $(o, o)$  band of the  ${}^1A_1 \rightarrow {}^1A_2$  ( ${}^1n\pi^*$ ) transition is strongly magnetically allowed, justifying the neglect of  $\mu_{O, n\pi}^{(1)}$ , and for symmetry reasons electric dipole forbidden. However, a conclusion from the latter fact that in the treatment of the optical rotatory power of the 300 nm carbonyl transition  $\vec{r}_{O, n\pi}^{(o)}$  might be neglected, in general, is not warranted, because in chiral ketones, which can have at most  $C_2$  symmetry,  $\vec{r}_{O, n\pi}^{(o)}$  by no means is zero for symmetry reasons. Therefore, both the zeroth and first order terms in the expansion of the electric dipole transition moment have to be retained, yielding

$$R_{O \rightarrow N\bar{n}} = \text{Im} \left[ \vec{r}_{ON}^{(o)} \cdot \vec{\mu}_{NO}^{(o)} (o|\bar{n})(\bar{n}|o) + \sum_s \vec{r}_{ON}^{(1)s} \cdot \vec{\mu}_{NO}^{(o)} (o|\bar{n})(\bar{n}|Q_s|o) \right] \quad (24)$$

$$D_{O \rightarrow N\bar{n}} = \left| \vec{r}_{ON}^{(o)} (o|\bar{n}) + \sum_s \vec{r}_{ON}^{(1)} (o|Q_s|\bar{n}) \right|^2 \quad (25)$$

From a comparison of (24) and (25) it is clear that in general CD and absorbance will not have similar band shapes, leading to a dissymmetry factor which is a function of frequency.

Making use of the sum rule and of the fact that, because of the definition of equilibrium geometry,  $(o|Q_s|o) = 0$ , we arrive at the expressions for the total rotational strength and total dipole strength

$$R_{O \rightarrow N} = \sum_{\bar{n}} R_{O \rightarrow N\bar{n}} = \text{Im} \vec{r}_{ON}^{(o)} \cdot \vec{\mu}_{NO}^{(o)} \quad (26)$$

$$D_{O \rightarrow N} = \sum_{\bar{n}} D_{O \rightarrow N\bar{n}} = \vec{r}_{ON}^{(o)} \cdot \vec{r}_{NO}^{(o)} + \sum_{s,t} \vec{r}_{ON}^{(1)s} \cdot \vec{r}_{NO}^{(1)t} (o|Q_s Q_t|o) \quad (27)$$

And we conclude that while the dipole strength may contain contributions due to deviations from equilibrium geometry, the rotational strength does not. In other words we are faced with the comfortable situation that it is the total CD that one should try to correlate the ground state geometry with.

Although bisignate Cotton effects were not explicitly dealt with by Moffitt and Moscovitz, they are quite possible within the framework of their Case II. When the borrowed vibronic rotational strength (last term in RHS of (24)) does not vanish for all  $\bar{n}$ , it has to be positive for some values of  $\bar{n}$  and negative for others since the total CD contains no borrowed rotational strength. Whenever for some  $\bar{n}$  the second term of (24) is opposite to the first term and has a larger absolute magnitude, a CD spectrum changes sign.

Nevertheless Weigang<sup>3)</sup> extended the theory of Moffitt and Moscovitz with a Case III to explain the occurrence of bisignate Cotton effects.

#### 4b. Theory of Weigang

Whereas Moffitt and Moscovitz referred only briefly to the optical activity of absorption bands in which both the electric and the magnetic dipole transition moment is sensitive towards vibrations, Weigang<sup>3)</sup> explicitly incorporated this case (Case III) in the theory, thus using (17) as a starting point for the discussion of the optical activity of the  $n \rightarrow \pi^*$  transition in ketones. Considering a molecule in which the ground state and excited state have the same symmetry, high enough to permit a classification of the vibrational wave functions in totally symmetric and non-totally symmetric ones, Weigang correctly arrives at the result that, if  $\bar{n}$  is totally symmetric, all terms of (17) contribute to the rotational strength  $R_{00 \rightarrow N\bar{n}}$ , whereas on the other hand only the last term of (17) survives if  $\bar{n}$  is non-totally symmetric. The latter result implies that the CD in a transition to a non-totally symmetric vibrational level of the upper electronic state derives completely from deviations of the nuclei from their ground state equilibrium positions: the rotational strength is borrowed. And although there is associated with a transition to totally symmetric vibrational levels both allowed (first term of (17)) and borrowed rotational strength (last three terms of (17)), the magnitude of the former perhaps exceeds that of the latter. If this is true, the optical activities in transitions to totally symmetric resp. non-totally symmetric vibrational levels arise from quite different sources and it is conceivable that they can be opposite.

Suggesting that experimental CD spectra indeed indicate that the  $n \rightarrow \pi^*$  transition of ketones consists of two progressions with opposite CD — one progression based on the electronic origin and the other on a non-totally symmetric mode (whose frequency is in the range 600 to 900  $\text{cm}^{-1}$ ) — Weigang is able to explain the bisignate CD curves of ketones. Concerning the experimental evidence presented by Weigang we remark that, although some of the bisignate CD spectra indeed seem to consist of two series of bands with opposite signs, others are less suited to illustrate the theory. Firstly because in some cases the positions of the vibrational bands simply do not fit in the scheme, in others because the vibrational fine structure, particularly in the progression at short wavelengths, is not well enough resolved. And lastly, because sometimes the possibility cannot be excluded that Cotton effects of mixed sign



derive from conformational equilibria.

Furthermore, Weigang's theory leans heavily on the assumption that the symmetries of the ground state and the excited state are such, that one can make a distinction between totally symmetric vibrations and non-totally symmetric ones. Strictly speaking, this is only possible if the chiral ketone has  $C_2$  symmetry, but as far as we know no bisignate CD curves have been observed with such ketones. It is questionable however, to what extent the division of vibrational wave functions of low symmetry ketones into totally symmetric and non-totally symmetric ones is still meaningful since it appears from a normal coordinate analysis on camphor<sup>15)</sup> for instance, that vibrations of the carbonyl group are strongly mixed with those of the skeleton.

Apart from its implications for the optical activity of ketones in general, Weigang's theory has important practical consequences, not in the least for the organic chemist. For, realising that in the case of a bisignate CD curve, the CD lobe at shorter wavelengths originates exclusively from deviations from the equilibrium geometry, he has to disregard this lobe if he wants to correlate the CD with static structure. This procedure indeed has been used<sup>16)</sup>.

For completeness we mention that there have been offered more explanations for bisignate CD curves. In a theory put forward by Caldwell<sup>17)</sup>, the rotational strength is expanded up to second order in the normal coordinates. Making no use of local symmetry but instead using analytical expressions for the vibrational wave functions of lower and upper state, Caldwell arrives at a rather general, but very complicated equation for the band shape of the circular dichroism.

Sometimes chemical equilibria may be held responsible for the occurrence of bisignate Cotton effects. Suppose in an ensemble of chiral molecules of given absolute configuration an equilibrium exists between the two conformers A and A'. If with A is associated a positive CD curve which has its peak at a given wavelength, while A' exhibits at a slightly different wavelength a Cotton effect of similar shape but opposite sign, the resultant CD curve will be bisignate. A change of temperature will cause a shift of the equilibrium and consequently a different CD spectrum. Temperature dependent CD measurements in such cases therefore often provide an easy entrance to the study of these equilibria. However, as the ketones in the bicycloheptanone series are very rigid, it is not likely that in these compounds the bisignate Cotton effects are brought about by conformational equilibria.

Another chemical explanation for CD curves of mixed sign was put forward by various authors<sup>18)</sup>. Apparently based on the conviction that bisignate circular dichroism curves ought to result from the presence of two different species, it was suggested that there is in solution an equilibrium between on the one hand solvated molecules which have e.g. a positive CD, and on the other hand molecules which are not solvated and exhibit an opposite Cotton effect at longer wavelengths. In a polar medium this equilibrium will shift towards the solvated molecules and as a result the absolute value of the extremum in the CD at long wavelengths will decrease (while that at short wavelengths increases); this is indeed observed when n-heptane as a solvent is replaced by methanol (see figures 7 and 8). Full use was made of the implications of this theory,

for in attempts to relate the sign of the rotational strength to molecular structure only the long wavelength branch of the bisignate CD curve was appreciated. For instance by Rassat<sup>19</sup>, who constructed from the acquired data on bicycloheptanones a sector rule for this type of compounds. However, from the results of the most appropriate experiment to test this theory on bisignate Cotton effects, it follows that it is incapable to explain them: gas phase CD measurements on camphenilone and isofenchone reveal that the bisignate curves persist when no solvent molecules are present<sup>20</sup>.

## 5. Band shapes of CD and CPL

### 5a. General

From §4a we recall that, in the Born-Oppenheimer approximation, the rotational strength and dipole strength of a transition between the vibronic ground state  $O_0$  and an excited vibronic state  $N\bar{n}$  are given by

$$R_{O_0 \rightarrow N\bar{n}} = \text{Im} \left( \langle O_0 | \vec{r}_{ON}(Q_1, Q_2, \dots, Q_{3M-6}) | N\bar{n} \rangle \cdot \langle N\bar{n} | \vec{\mu}_{NO}(Q_1, Q_2, \dots, Q_{3M-6}) | O_0 \rangle \right) \quad (11a)$$

and

$$D_{O_0 \rightarrow N\bar{n}} = \left| \langle O_0 | \vec{r}_{ON}(Q_1, Q_2, \dots, Q_{3M-6}) | N\bar{n} \rangle \right|^2 \quad (12a)$$

The matrix elements  $\vec{r}_{ON}$  and  $\vec{\mu}_{NO}$  in (11a) and (12a) are functions in a  $(3M-6)$  dimensional space of nuclear coordinates ( $M$  is the number of nuclei in the molecule).

Analogously, if in emission the initial state is denoted by  $N\bar{n}$  and the final one by  $O_n$ , it is convenient to define<sup>6)6a)</sup> the rotational strength in this transition as

$$\begin{aligned} R_{N\bar{n} \rightarrow O_n} &= \text{Im} \left( \langle O_n | \vec{r} | N\bar{n} \rangle \cdot \langle N\bar{n} | \vec{\mu} | O_n \rangle \right) = \\ &= \text{Im} \left( \langle n | \vec{r}_{ON}(Q_1, Q_2, \dots, Q_{3M-6}) | \bar{n} \rangle \cdot \langle \bar{n} | \vec{\mu}_{NO}(Q_1, Q_2, \dots, Q_{3M-6}) | n \rangle \right) \end{aligned} \quad (28)$$

whereas we have for its dipole strength

$$D_{N\bar{n} \rightarrow O_n} = \left| \langle \bar{n} | \vec{r}_{NO}(Q_1, Q_2, \dots, Q_{3M-6}) | n \rangle \right|^2 \quad (29)$$

From the above equations, which hold quite generally, one can draw some important conclusions.

Firstly, from a comparison of (11a) and (28) it follows that the rotatory strength of the  $(o, o)$  transition in absorption is identical to that in the  $(o, o)$  emission band and a similar conclusion is reached for the dipole

strengths of both transitions

$$R_{O_o \rightarrow N_o^-} = R_{N_o^- \rightarrow O_o} \quad (30)$$

$$D_{O_o \rightarrow N_o^-} = D_{N_o^- \rightarrow O_o} \quad (31)$$

These relations, which are rather trivial for a molecule in the gas phase, do not necessarily hold if between the absorption process and emission process the nature of the species changes - e.g. because of a different solvation in the excited state. In that case namely, the initial and final states of the absorbing species are no longer identical with the final and initial states of the fluorescent species and relations (30) and (31) may break down. Later on in this paragraph we shall briefly refer to this point.

Secondly, application of the quantum mechanical sum rule to (11a), (12a), (28) and (29) yields the expressions for the total rotational and dipole strengths in absorption and emission.

$$R^{abs} = \sum_n R_{O_o \rightarrow N_n^-} = \text{Im} \langle o | \vec{r}_{ON}(Q_1, \dots) \cdot \vec{\mu}_{NO}(Q_1, \dots) | o \rangle = \langle o | R_{ON}(Q_1, \dots) | o \rangle \quad (32)$$

$$D^{abs} = \sum_n D_{O_o \rightarrow N_n^-} = \langle o | D_{ON}(Q_1, \dots) | o \rangle \quad (33)$$

$$R^{em} = \sum_n R_{N_n^- \rightarrow O_n} = \langle \bar{o} | R_{NO}(Q_1, \dots) | \bar{o} \rangle \quad (34)$$

$$D^{em} = \sum_n D_{N_n^- \rightarrow O_n} = \langle \bar{o} | D_{NO}(Q_1, \dots) | \bar{o} \rangle \quad (35)$$

The variables  $Q_r$  in the electronic matrix elements  $\vec{r}_{ON}(\dots Q_r \dots)$  and  $\vec{\mu}_{NO}(\dots Q_r \dots)$  refer to the nuclear normal coordinates in the ground state in (32) and (33), and to the normal coordinates of the excited state in (34) and (35). The vibrational wave functions of the ground state,  $o$  and  $n$ , are taken to be products of one-dimensional vibrational wave functions in the variables  $Q_r - Q_r^o$ , where  $Q_r^o$  is the expectation value of  $Q_r$  in the vibronic ground state  $O_o$ . That is

$$o = o_1(Q_1 - Q_1^o) o_2(Q_2 - Q_2^o) \dots o_r(Q_r - Q_r^o) \quad (36)$$

and the form of  $n$  is similar, but with one or more elementary vibrations excited. Likewise the vibrational wave functions of the excited state consist of a product of 3M-6 1-dimensional vibrations in the normal coordinates of the upper state. When neglecting mode-mixing, the normal coordinates of ground and excited state are equal whence we have

$$\bar{o} = \bar{o}_1(Q_1 - Q_1^0) \bar{o}_2(Q_2 - Q_2^0) \dots \bar{o}_r(Q_r - Q_r^0) \quad (37)$$

and an analogous expression for  $\bar{n}$ . The bars in  $\bar{o}_r$  and  $\bar{Q}_r^0$  indicate that both shape and center of the vibrational wave functions in the upper state differ from those in the ground state. It will appear later that the large value of  $Q_r^0 - \bar{Q}_r^0$  in ketones gives us a clue for a better understanding of their optical activity. To illustrate this, we assume for a moment that  $R_{ON}$  depends on one  $Q_r$ . The total rotational strength in absorption is given by

$$R^{abs} = \langle o | R(Q) | o \rangle = \langle o_1 | o_1 \rangle \langle o_2 | o_2 \rangle \dots \langle o_r | R(Q_r) | o_r \rangle \dots = \langle o_r | R(Q_r) | o_r \rangle \quad (38)$$

meaning that  $R(Q_r)$  has to be averaged with the distribution function  $o_r^2$ . Similarly  $R^{em}$  is found from the rotational strength function by weighting it with  $\bar{o}_r^2$ . In the situation, represented by figure 14, both rotational strengths are therefore negative, the absolute value of  $R^{abs}$  being larger than that of  $R^{em}$ . It also follows that, generally,  $R^{abs}$  will be equal to  $R^{em}$  only if the vibrational functions  $o$  and  $\bar{o}$  are identical, or if  $R$  does not depend on  $Q_r$ .

Before elaborating the equations (30)-(35) further we first discuss

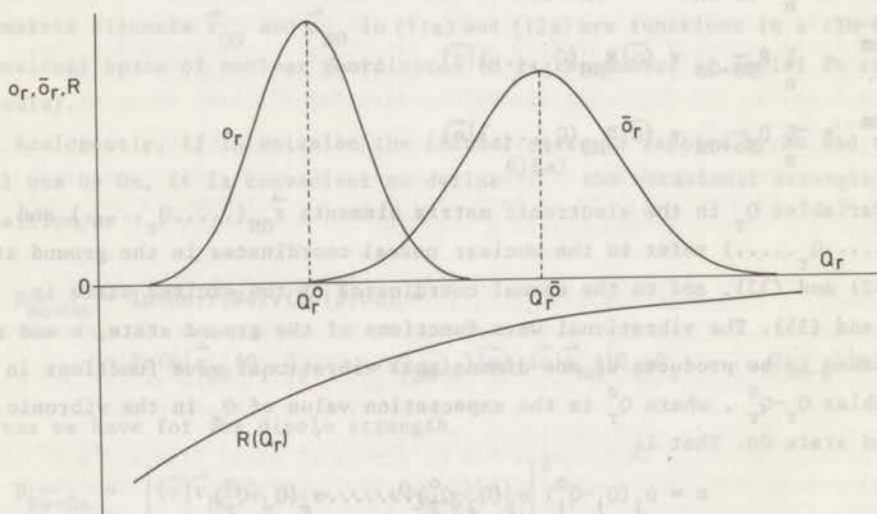


Figure 14. One-dimensional zero point vibrational wave functions in ground- and excited state. Variation of electronic rotational strength with  $Q_r$ .

where a confrontation of these basic equations with experiment leads to. We recall that the quantum mechanical quantities  $R^{abs}$  and  $D^{abs}$  are accessible from experiment through the relations (1) and (2), but that from an actual CPL measurement only the value of  $4R^{em}/D^{em}$  is found, not those of  $R^{em}$  and  $D^{em}$  separately (cf (8)-(10)). This means, that in order to be able to compare the magnitudes of  $R^{abs}$  and  $R^{em}$ , we first have to know  $D^{em}$ . However, if the signs of  $g$  and  $g_{lum}$  are opposite, we immediately can conclude - without knowing the exact value of  $D^{em}$  - that the rotational strengths in absorption and fluorescence are quite different. A situation which actually occurs for camphor (figure 6), camphenilone (figure 7) and epi-androsterone (figure 13).

As regards the experimental values of the rotational strengths in the (o,o) bands of absorption and fluorescence the following may be remarked. Although in chiral ketones the (o,o) transition is never symmetry-forbidden, its intensity is still weak because of a small Franck-Condon factor. Besides, were it not for this reason, the (o,o) band would not be easily observable as such because of the lack of fine structure in the spectra. However, with the assumption that on the one hand the sign of the CD at the extreme long wavelength side of the absorption band agrees with that in the (o,o) transition and on the other hand the sign of  $\Delta I$  near the intersection region of the fluorescence and absorption curves corresponds with that in the (o,o) emission band, the signs of the rotational strengths of the (o,o) bands in absorption and emission are available. From the experimental spectra it then follows that indeed the signs of the optical activities of the (o,o) transitions in fluorescence and absorption are identical, one possible exception being constituted by isofenchone in methanol solution, where the CPL value at short wavelengths is zero (see figure 8). However, in view of the extremely large solvent dependence of the total rotational strength of this compound (compare in figure 8 the CD curves in n-heptane and methanol), we here probably encounter a case in which the role of the solvent molecules in the generation of optical activity may not be neglected.

Having found no indication (except isofenchone) that the solvent enters the rotational strength in a decisive way, we can now consider in more detail the rotational strength of the individual vibronic transitions. Before doing this we notice that a negative ratio  $R^{abs}/R^{em}$  has a very interesting implication. Suppose that for a given ketone  $R^{abs}$  (i.e. the integrated CD) is positive and  $R^{em}$  (the integrated CPL) negative. Then the mere fact that the rotational strength in the (o,o) transition in absorption and emission must have equal sign, requires a change of sign to occur in the CD or in the CPL spectrum.

At this stage however, we do neither know where in the frequency scale the change of sign takes place, nor do we know whether there is only one such change. To answer these questions we shall design in the next section a formalism to describe the rotational strengths in vibronic transitions, which will allow us to draw in §5c more pertinent conclusions about the band shapes of CD and CPL. In these discussions we shall lean heavily on the fact that the equilibrium geometry of ketones in ground and  ${}^1n\pi^*$ -states is quite different (which may be concluded from the large discrepancies between the observed values of  $R^{abs}$  and  $R^{em}$ ).

### 5b. The rotational strength in vibronic transitions

We assume that the quantities  $\vec{r}_{ON}(Q)$  and  $\vec{\mu}_{NO}(Q)$  vary at most linearly with the  $Q_r$ . This implies that we may cut off their expansions around some fixed point  $\check{Q} = (\check{Q}_1, \check{Q}_2, \dots, \check{Q}_{3M-6})$  after the second term.

$$\langle o | \vec{r}_{ON}(Q) | \bar{n} \rangle = \langle o | \vec{r}_{ON}(\check{Q}) | \bar{n} \rangle + \langle o | \sum_r (Q_r - \check{Q}_r) \vec{r}_{ON}^{(1)r} | \bar{n} \rangle \quad (39)$$

$$\langle \bar{n} | \vec{\mu}_{NO}(Q) | o \rangle = \langle \bar{n} | \vec{\mu}_{NO}(\check{Q}) | o \rangle + \langle \bar{n} | \sum_r (Q_r - \check{Q}_r) \vec{\mu}_{NO}^{(1)r} | o \rangle \quad (40)$$

where

$$\vec{r}_{ON}^{(1)r} = \left. \frac{\partial \vec{r}_{ON}(Q)}{\partial Q_r} \right|_{Q=\check{Q}} \quad (41)$$

and

$$\vec{\mu}_{NO}^{(1)r} = \left. \frac{\partial \vec{\mu}_{NO}(Q)}{\partial Q_r} \right|_{Q=\check{Q}} \quad (42)$$

Previously, in (13)-(18) we chose  $Q$  equal to  $Q^0$ , the equilibrium geometry in the vibronic ground state. In view however of the large difference in equilibrium geometry in ground and  ${}^1n\pi^*$ -state of ketones, the following alternative may be fruitful. Consider an integral such as  $\langle o | \vec{r}_{ON}(Q) | \bar{n} \rangle$ . The integrand of this matrix element, consisting of a product of the function  $\vec{r}_{ON}(Q)$  and the vibrational transition density  $o(Q)\bar{n}(Q)$ , can have appreciable values only at those points  $Q$  where the product  $\bar{n}$  is different from zero. This immediately suggests an expansion of  $\vec{r}_{ON}(Q)$  at a point in  $Q$ -space where  $\bar{n}$  is peaked. Therefore we shall take  $Q$  equal to  $Q^{on}$ , where  $Q^{on}$  is obtained by weighting the nuclear position vector with the distribution function  $\bar{n}$ .

$$Q_r^{on} = \frac{\langle o | Q_r | \bar{n} \rangle}{\langle o | \bar{n} \rangle} \quad (43)$$

where  $r=1,2,\dots,3M-6$ . Note that different  $n$  give rise to different values of  $Q^{\text{on}}$ . \*) With (43) the expansions (39) and (40) transform to

$$\langle o | \vec{r}_{\text{ON}}(Q) | \bar{n} \rangle = \vec{r}_{\text{ON}}(Q^{\text{on}}) \langle o | \bar{n} \rangle \quad (44)$$

$$\langle \bar{n} | \vec{\mu}_{\text{NO}}(Q) | o \rangle = \vec{\mu}_{\text{NO}}(Q^{\text{on}}) \langle \bar{n} | o \rangle \quad (45)$$

whereas the expression for the rotational strength in the transition  $0o \rightarrow \bar{N}\bar{n}$  takes the form

$$\begin{aligned} R_{0o \rightarrow \bar{N}\bar{n}} &= \text{Im} \vec{r}_{\text{ON}}(Q^{\text{on}}) \cdot \vec{\mu}_{\text{NO}}(Q^{\text{on}}) \langle o | \bar{n} \rangle \langle \bar{n} | o \rangle = \\ &= R_{\text{ON}}(Q^{\text{on}}) \langle o | \bar{n} \rangle^2 \end{aligned} \quad (46)$$

From (46) we see that the vibronic rotatory strength is equal to the electronic rotational strength evaluated at the point  $Q^{\text{on}}$ , times a Franck-Condon factor.

Before using (46) to study the band shapes of CD and CPL, we emphasize that the expansion leading to (44)-(46) is not always warranted. It is obvious that its utility depends heavily on the shape of the vibrational overlap density  $\bar{o}$ . If  $\bar{o}$  is a capricious function consisting of many large peaks at various positions on the  $Q$ -scale, the value of an integrand such as  $\langle o(Q) | \vec{r}_{\text{ON}}(Q) | \bar{n}(Q) \rangle$  is not predominantly determined by its value in a restricted region around one point  $Q$ . In this case, which would arise if  $o$  and  $\bar{n}$  were centered around the same point  $Q$ , there is no advantage in expanding the matrix element  $\langle o | \vec{r}_{\text{ON}}(Q) | \bar{n} \rangle$  around  $Q^{\text{on}}$ . With ketones however, there is a large separation between the centers of  $o$  and  $\bar{n}$ , and one may expect that to a good approximation  $\bar{o}$  has one dominating peak in  $Q$ -space.

There is still another argument which underlines the relevance of (46) in the interpretation of the experimental spectra of ketones: when upon excitation the molecule is distorted in the direction  $Q_r$ , one will observe in the spectrum particularly progressions in the vibrations that are based on the normal coordinate  $Q_r$ .

\*) The definition (43) is used also in theories on the spectral intensities of diatomic molecules, where it is a starting point for the so-called  $r$ -centroid approximation<sup>21)</sup>.

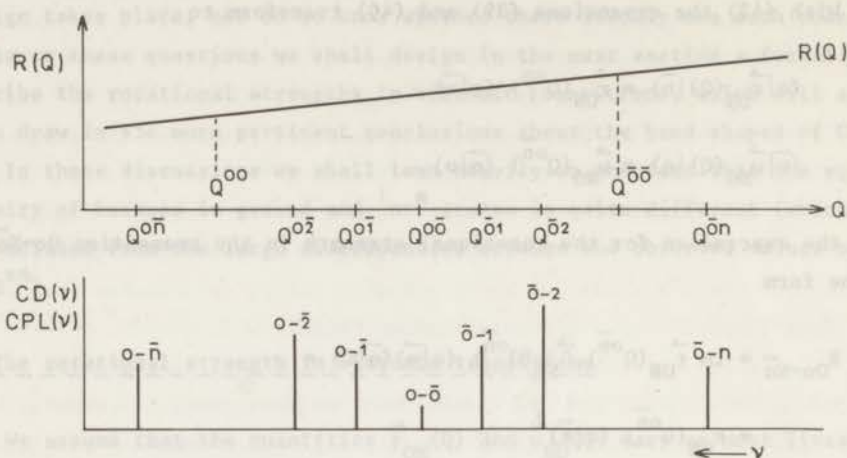


Figure 15. Correlation of the rotational strength as a function of  $Q$  and optical activity as a function of frequency.

### 5c. Band shapes of CD and CPL

We assume that the electronic rotational strength (46) depends on one normal coordinate  $Q_r$  and moreover that the experimental CD and CPL spectra arise predominantly from progressions in normal modes corresponding to this  $Q_r$ . Then a transparent connection may be laid between  $R$  as a function of  $Q$  and the experimental CD and CPL as a function of frequency. This is illustrated in figure 15. The rotational strength in the  $(o,o)$  transition is  $R(Q^{oo})(o|\bar{o})^2$ . In vibrational transitions  $o \rightarrow \bar{n}$  one proceeds towards the left on the  $Q$ -scale as  $\bar{n}$  increases and to higher frequencies in the CD spectrum. In emission one deals with transitions  $\bar{o} \rightarrow n$ . The higher  $n$ , the lower the frequency and the larger the value of  $Q^{on}$ . Since in the construction of figure 15 the necessary Franck-Condon factors are guessed and the relation of  $Q$  and  $\nu$  of course is not linear, the figure expresses a qualitative relationship only between  $R(Q)$  and the magnitude of the CD and CPL as a function of frequency.

We are now ready for a comparison of experimental data and theory. As mentioned, the determination of the absolute magnitude of  $R^{em}$  is hampered by not knowing the value of  $D^{em}$ . From the ratio  $g/g_{lum}$  which is obtainable from



the observed spectra, however, we can deduce the value of  $R^{abs}/R^{em}$  when we assume that  $D^{em} = cD^{abs}$ , where  $c$  is a constant for all ketones. The latter approximation probably is not that unrealistic: the highly localized nature of the  $n \rightarrow \pi^*$  transition causes transition energies, bandwidths and extinction coefficients for aliphatic ketones to be very similar and it is conceivable that a similar argument holds for the reverse transition as well. Since it can be argued that for hydrindanone  $R^{abs} \approx R^{em}$  (cf §3b), implying that here  $D^{em} \approx 5D^{abs}$ , we tentatively take for all ketones  $c=5$ . Then the compounds we have measured, when classified according to their  $R^{abs}/R^{em}$  values, can be divided into the following four groups\*).

- (a)  $\frac{4}{5} < R^{abs}/R^{em} < 2$ . This applies for most compounds: hydrindanone, 3-methylcyclopentanone, 2,2,3-trimethylcyclopentanone, 5-ketoborneol, 5-ketobornylacetate and 6-ketobornylacetate.
- (b)  $R^{abs}/R^{em} \approx 4$  for  $\alpha$ -fenchocampherone
- (c)  $R^{abs}/R^{em} < -10$  for camphor and epi-androsterone
- (d)  $R^{abs}/R^{em} \approx -2$  for camphenilone.

In obtaining the above classification use has been made of the various spectra in n-heptane, except for epi-androsterone which was measured in methanol only.

When we assume that  $R(Q)$  is a linear function of  $Q$  and that the shift of origin  $Q^{00} - Q^{oo}$  is equal for all compounds studied, the knowledge of  $R^{abs}/R^{em}$  allows the construction of the shapes of the functions  $R(Q)$  for the cases (a)-(d). They are displayed in figure 16, where for convenience all  $R^{abs}$  are taken equal. At the bottom of the same figure the predicted qualitative band shapes of CD and CPL are given. In case (a)  $R(Q)$  invariably is positive in the entire region where the vibrational transition densities  $\bar{o}_n$  and  $\bar{o}_n$  can have nonvanishing values. Therefore no changes of sign are expected for the optical activity, neither in the CD nor in the CPL. In (b) the quantities  $R^{abs}$ ,  $R^{em}$  and  $R(Q^{oo})$  are all positive, but for large  $n$  the CPL curve crosses the zero-line. With (c) the integrated CD is large and positive, the integrated CPL has a small negative value and the optical activity in the (o,o) band is positive, resulting in a change of sign near the central frequency of the emission curve. In case (d) the larger negative value of  $R^{em}$  as compared to (c) causes a shift of the zero-point of the optical activity towards the  $Q^{oo}$

\*) Isofenchone was discussed earlier.

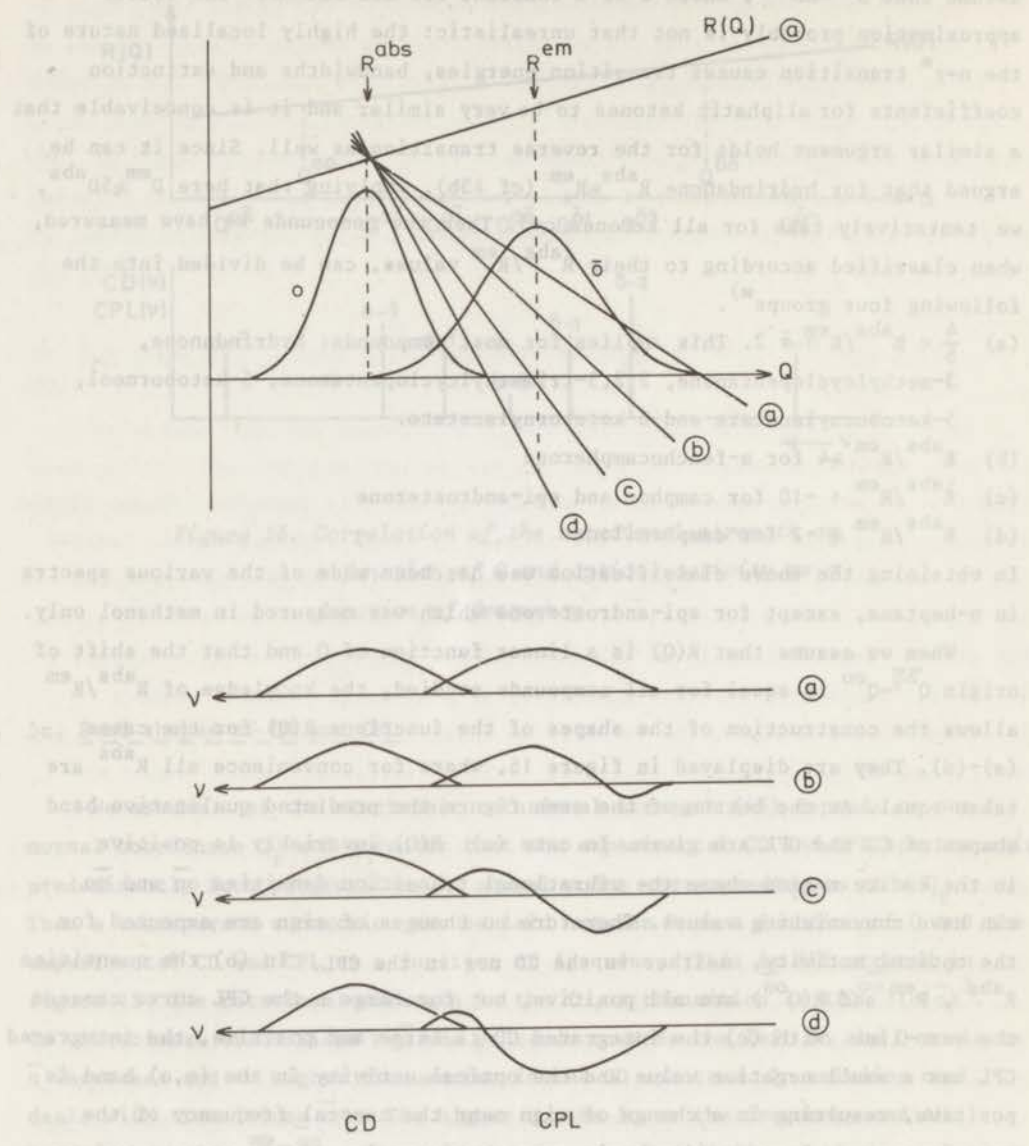


Figure 16. Top half: Zero point vibrational wave functions in the ground state ( $o$ ) and  $1n\pi^{\#}$ -state ( $\bar{o}$ ), Electronic rotational strength as a function of  $Q$  for the cases (a)-(d), see text. Lower half: Corresponding band shapes of CD and CPL.

region. In the figure this results in a bisignate CPL curve but a bisignate CD could have been obtained as well, e.g. if somewhat different shapes of  $\sigma$  and  $\bar{\sigma}$  were taken.

From a comparison of the experimental spectra (cf. figure 3,5-13) with figure 16 it appears that the agreement of the observed and predicted bandshapes is quite good. We take this as an indication that our model, notwithstanding its simplicity, is essentially correct.

#### 5d. Discussion

The discussion in the preceding section is a further elaboration of the observation made in §5a that the large difference which exists between the values of the integrated CD (i.e.  $R^{abs}$ ) and the integrated CPL ( $R^{em}$ ) has to be of consequence for the CD and CPL as a function of frequency. In §5c it is shown that it is possible to predict qualitatively the band shape of the optical activity in absorption and emission on the basis of a simple model. The success of the model in accounting for the observed phenomena not only contributes to a better understanding of bisignate Cotton effects as such, it also has some important implications.

The first pertains to the general description of the optical activity in the  $n-\pi^*$  transition of ketones. We find that a linear relationship of  $R$  and  $Q$  satisfactorily explains for our ketones the observed band shapes in CD and CPL. Therefore we see no reasons why higher order terms should be indispensable for the description of the lion's share of the optical activity of ketones in their  $n-\pi^*$  transition. This implies that probably the convenient framework of Case II of Moffitt and Moscovitz is still adequate to describe the optical activity of ketones, even if they exhibit bisignate Cotton effects. We arrive at this conclusion because the first order dependence of  $R$  on  $Q$  more likely originates in a variation of  $\vec{r}_{ON}$  with  $Q$  than in a dependence of the large magnetic dipole transition moment on the normal coordinates.

It is perhaps illuminating to discuss briefly the competition of vibrations and upper state geometry in the generation of optical activity. Of course, both factors play their part but with different success: although the value of  $Q^{on}$  is determined by a product of vibrational wave functions, the variation with  $\bar{n}$  of  $Q^{on}$  (and thus of  $R(Oo \rightarrow N\bar{n})$ ) is primarily due to the shift of origin,  $Q^{oo} - Q^{\bar{o}\bar{o}}$ . In a way of speaking, the difference in equilibrium geometry between lower and upper state enables the vibrations to exhibit in the experimental CD spectrum the variation of  $R$  in a certain region of  $Q$ -space. Whereas thus in the

CD (CPL) spectrum a large variation of  $R$  may be reflected, summing over all vibrational structure yields the rotational strength which pertains to the equilibrium configuration of the molecule in its ground (excited) state. This favourable circumstance permits to draw a practical conclusion. In correlating a bisignate circular dichroism with ground state structure it will be wise, generally, to consider the entire CD and not just one of the two branches. This answers the question at the end of section 2.

In his explanation of bisignate CD curves of ketones, Weigang underrates the importance of the upper state's geometry. This deficiency is not present in the treatment of bisignate circular dichroism by Caldwell but his theory, although rather general, is very complex. That bisignate Cotton effects can be explained from a simple linear relationship of  $R$  and  $Q$  has not been noted prior to our investigation.

So far we did not deal with the question which specific vibrations could be operative in the structuring of the CD and CPL spectra of ketones. From calculations<sup>22)</sup> it follows that the geometry of the  ${}^1n\pi^*$ -state of formaldehyde differs in two important respects from that of the ground state. Firstly the carbonyl bond is lengthened by  $+0.29 \text{ \AA}$  (experimental value  $+0.12 \text{ \AA}$ )<sup>23)</sup> and secondly the configuration around the carbon atom no longer is planar but pyramidal, the calculated out-of-plane angle being  $32.7^\circ$  (experiment:  $33.6^\circ$ )<sup>23)</sup> Completely in accord with these data the  $n\pi^*$  transition of formaldehyde shows long progressions in the carbonyl stretch and out-of-plane bending frequencies. These two geometry changes in the parent compound being so prominent, it is plausible that they are also present - although perhaps modified to some extent - in the low-symmetry ketones. In this respect we recall that for a proper understanding of the spectral properties of hydrindanone (§3b) particularly the geometry change along the carbonyl out-of-plane bending normal coordinate has to be taken into account. However, whereas for the latter compound the energy of the upper state, as a function of the out-of-plane angle, is a double minimum potential because of symmetry reasons, this is no longer the case for low-symmetry ketones. There we presumably encounter for the excited state at most a skew energy curve whose minimum is either above or below the original carbonyl plane. And we think it should be interesting to try and decide from the CD and CPL data in which direction the oxygen atom moves upon excitation. Using models which correlate rotational strength with structure (cf. §2) we are in the process of doing this. Furthermore, from high resolution measurements on ketones, at low temperatures or in the gas phase, we hope to obtain more detailed information on vibronic rotational strengths which,

hopefully, will provide us with the means for a more exacting comparison of theory and experiment. Perhaps at that stage it will be possible also to make more pertinent statements about the nature of the active modes which are involved in the vibronic optical activity.

## 6. Conclusion

A comparison of the experimental CD and CPL spectrum reveals marked differences between the two: both the magnitude of the integrated optical activity and the band shape may be utterly different in absorption and emission. In this chapter a relation is laid between these phenomena. The often large discrepancy between the value of the rotational strength in absorption and fluorescence (for some compounds up to sign) points to a large distortion of the  $^1n\pi^*$ -state of ketones with respect to their ground state. On the other hand it is shown from general principles that a negative value of the ratio  $R^{abs}/R^{em}$  requires a change of sign in either the CD or the CPL curve, i.e. can cause a bisignate Cotton effect. To get a better insight in the observed phenomena, a model is constructed to predict the qualitative band forms of the CD and CPL. Based on the large shift in equilibrium geometry between ground and excited state, this model makes use of an expansion of the electronic rotational strength in those points of normal coordinate space where the Franck-Condon overlap for a particular vibronic transition is peaked. When a linear relationship between the rotational strength and one normal coordinate is assumed, the observed band shapes of CD and CPL of our ketones can be successfully explained. Apart from a better understanding of the origins of bisignate Cotton effects, a main result of this work is the conclusion that the optical activity in the  $n\pi^*$  transition of ketones still can be understood with the relatively simple theory of Moffitt and Moscovitz, provided proper allowance is made for a legitimate role of the excited state. The latter conclusion may add considerably to the value of optical activity data as a source for structural information.

## References

1. C.A.Emeis and L.J.Oosterhoff, 1967, Chem.Phys.Letters 1, 129
2. W.C.M.C.Kokke and L.J.Oosterhoff, 1972, J.Am.Chem.Soc. 94, 7583
3. O.E.Weigang, Jr, 1965, J.Chem.Phys. 42, 2244; 43, 3609  
O.E.Weigang, Jr, 1968, *ibid.* 48, 4332
4. W.Moffitt and A.Moscowitz, 1959, J.Chem.Phys. 30, 648
5. W.Klyne and D.N.Kirk in "Fundamental Aspects and Recent Developments in Optical Rotatory Dispersion and Circular Dichroism", Eds F.Ciardelli and P.Salvadori, Heyden & Son Ltd, London 1973
6. C.A.Emeis and L.J.Oosterhoff, 1971, J.Chem.Phys. 54, 4809
- 6a. C.A.Emeis, Thesis Leiden, 1968
7. W.J.Kauzmann, J.E.Walter and H.Eyring, 1940, Chem.Rev. 26, 339
8. M.V.Volkenstein and M.P.Kruchek, 1960, Opt.Spect. 9, 243
9. W.Moffitt, R.B.Woodward, A.Moscowitz, W.Klyne and C.Djerassi, 1961, J.Am.Chem.Soc. 83, 4013
10. I.Tinoco, 1962, Adv.Chem.Phys. 4, 113
11. O.E.Weigang, Jr, and E.G.Höhn, 1966, J.Am.Chem.Soc. 88, 3673
12. E.G.Höhn and O.E.Weigang, Jr, 1968, J.Chem.Phys. 74, 4543
13. F.S.Richardson, 1971, J.Phys.Chem. 75, 2466
14. K.M.Wellman, E.Bunnenberg and C.Djerassi, 1963, J.Am.Chem.Soc. 85, 1870
15. R.T.Klingbiel and H.Eyring, 1970, J.Phys.Chem. 74, 4543
16. See e.g. G.Snatzke and G.Eckhardt, 1968, Tetrahedron 24, 4543
17. D.J.Caldwell, 1969, J.Chem.Phys. 51, 984  
D.J.Caldwell and H.Eyring, The Theory of Optical Activity, Wiley-Interscience, New York, 1971
18. H.P.Gervais and A.Rassat, 1961, Bull.Soc.Chim.France 743  
See also:  
C.Coulombeau and A.Rassat, 1963, Bull.Soc.Chim.France 2673  
P.Witz and G.Ourisson, 1964, Bull.Soc.Chim.France 627  
A.Moscowitz, K.M.Wellman and C.Djerassi, 1963, Proc.Nat.Acad.Sci. 50, 799  
K.M.Wellman, R.Records, E.Bunnenberg and C.Djerassi, 1964, J.Am.Chem.Soc. 86, 492  
K.M.Wellman, P.H.A.Laur, W.S.Briggs, A.Moscowitz and C.Djerassi 1965, J.Am.Chem.Soc. 87, 66  
D.E.Bays, G.W.Cannon and R.C.Cookson, 1966, J.Chem.Soc. B 885
19. A.Rassat, 1966, Bull.Soc.Chim.France 3752

- C.Coulombeau and A.Rassat, 1971, *ibid.* 516
20. H.P.J.M.Dekkers, unpublished observation
21. P.A.Fraser, 1954, *Can.J.Phys.* 32, 515
22. R.J.Buenker and S.D.Peyerimhoff, 1970, *J.Chem.Phys.* 53, 1368
23. V.T.Jones and J.B.Coon, 1969, *J.Mol.Spectrosc.* 31, 137

A P P E N D I X

A P P A R A T U S

The apparatus used in this experiment is shown in Figure 1. It consists of a laser, a sample, a detector, and a photometer. The laser beam is directed through the sample and the detector. The photometer measures the intensity of the light passing through the sample. The intensity of the light is measured as a function of the angle of incidence. The results are shown in Figure 2.

A P P E N D I X

1. INTRODUCTION

The purpose of this experiment is to determine the intensity of the light passing through a sample. The intensity of the light is measured as a function of the angle of incidence. The results are shown in Figure 2.

The intensity of the light passing through a sample is given by the equation  $I = I_0 e^{-\mu x}$ , where  $I_0$  is the initial intensity,  $\mu$  is the absorption coefficient, and  $x$  is the thickness of the sample. The intensity of the light is measured as a function of the angle of incidence. The results are shown in Figure 2.

The circular dichroism of the sample is found from the difference of both

References

1. C. Couillard and A. Szwarc, *Bull. Soc. Chim. France*, 1971, 1144-1148.

2. R. L. M. Jeffrey, *Journal of Polymer Science*, 1971, 55-60.

3. W. M. C. Kaita and L. J. Fetters, *J. Polym. Sci. A-1*, 1970, 8-13.

4. R. L. M. Jeffrey and J. D. Hoffman, *J. Polym. Sci. A-1*, 1970, 14-19.

5. R. T. Jones and J. B. Conant, *J. Polym. Sci. A-1*, 1971, 1011-1016.

6. W. Ruffin and A. Benisek, 1970, *J. Chem. Phys.*, 52, 444.

7. W. Ruffin and D. K. Rice in "Fundamental Aspects and Recent Developments in Optical Rotatory Dispersion and Circular Dichroism", *Advances in Chemical Physics*, Vol. 12, Wiley-Interscience, New York-London, 1970.

8. C. Couillard and L. J. Fetters, *APPENDIX Phys.*, 25, 4609.

9. C. E. Sroog, *Thesis*, 1969.

APPARATUS

1. W. J. Karman, J. E. Miller and J. D. Hoffman, *J. Polym. Sci. A-1*, 1970, 1011-1016.

2. M. V. Ballal and M. F. Grubb, 1970, *Opt. Spectr.*, 5, 243.

3. M. Hoffert, M. B. Woodruff, K. Nevozhin, W. Ruffin and C. Djerassi, 1971, *J. Am. Chem. Soc.*, 93, 4013.

We shall outline here the main features of the MCD-spectrometer and CPL-apparatus we have constructed to obtain the spectra described in this thesis.

4. F. J. Richards, 1971, *J. Phys. Chem.*, 75, 2444.

5. C. Couillard and C. Djerassi, 1971, *J. Am. Chem. Soc.*, 93, 1970.

6. R. T. Christian and R. Xyrias, 1970, *J. Phys. Chem.*, 74, 6343.

When a sample exhibits (magnetic) circular dichroism, left and right circularly polarized light are absorbed to a different extent. Suppose a left circularly polarized light beam with intensity  $I_L$  hits such a sample. After passage through the sample the intensity of the light, according to the law of Lambert and Beer, is given by

$$I'_L = I_L 10^{-\epsilon_L cd}$$

Here  $\epsilon_L$  is the molar extinction coefficient in L-light,  $c$  is the concentration of the absorbing molecules and  $d$  the path-length of the light in the sample. When we repeat the measurement with R-light (intensity  $I_R$ ), the light which reaches the photomultiplier has an intensity  $I'_R$ .

$$I'_R = I_R 10^{-\epsilon_R cd}$$

The circular dichroism of the sample is found from the difference of both



signals, divided by their average value

$$\frac{I'_L - I'_R}{\frac{1}{2}(I'_L + I'_R)} = 2 \frac{10^{-\epsilon_L cd} - 10^{-\epsilon_R cd}}{10^{-\epsilon_L cd} + 10^{-\epsilon_R cd}} = 2 \frac{1 - 10^{(\epsilon_L - \epsilon_R) cd}}{1 + 10^{(\epsilon_L - \epsilon_R) cd}} = (\log_e 10) \Delta \epsilon cd$$

where we have assumed  $I_L = I_R$  and used the fact that in practice always  $\Delta \epsilon cd \ll 1$ .

In the actually experiment the circular polarization state of the light is modulated between L and R with a frequency  $\omega$  and the CD of the sample will give rise to an AC signal of frequency  $\omega$  on the DC current of the photomultiplier.

$$\Delta \epsilon cd \sim \frac{AC}{DC}$$

By adapting the gain of the photomultiplier tube via a feed-back system, the DC is made constant. Then the AC-signal, which is phase-sensitive detected, is directly proportional to the circular dichroism.

With our dichrograph, which covers the region 230-700 nm, (magnetic) circular dichroisms as low as  $3 \cdot 10^{-6}$  units  $\Delta OD$  may be detected.

### Measurement of optical density

The part of the MCD-spectrometer indicated in figure 1 by Q, A and PM-2 allows the simultaneous measurement of OD and  $\Delta OD$  of the sample.

After the beam splitter Q a fraction  $q$  of the total light intensity  $I$  reaches the attenuator A (attenuation factor  $a$ ). If the gain of PM-2 is  $G'$ , the photocurrent from PM-2 is

$$IqaG'$$

The fraction  $(1-q)$  passes through the sample (optical density  $OD = \epsilon cd$ ) and reaches PM-1. When the gain of the latter is  $G$ , the DC photocurrent is  $(1-q) I 10^{-\epsilon cd} G$ . As mentioned,  $G$  is such that the DC-signal is constant, i.e.

$$(1-q) I 10^{-\epsilon cd} G = p$$

When both photomultipliers are operating with the same high voltage and we assume that their performance is identical,  $G' = G = \frac{p}{(1-q)I} 10^{\epsilon cd}$  and the signal from PM-2 is

$$\frac{qap}{1-q} 10^{\epsilon cd}$$

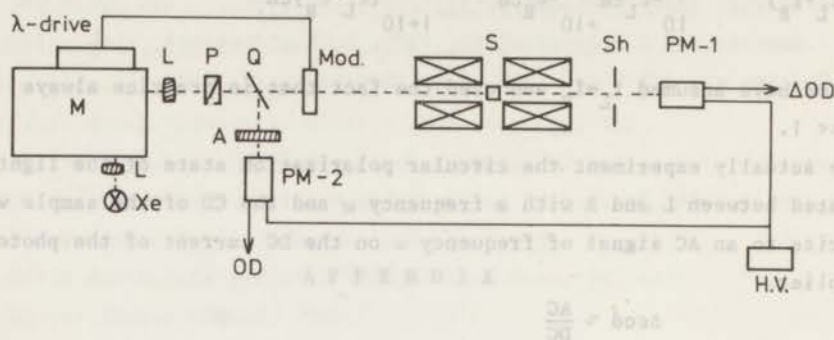


Figure 1. Diagram of the optical part of the MCD-spectrometer.

- Xe Xenon-arc (XBO 900 W, Osram)  
 L lenses  
 M monochromator (Glan, calcite)  
 Q suprasil plate  
 Mod electro-optic modulator (Pockels cell, Jouan). The frequency of the driving voltage (380 Hz) determines the modulation frequency, its amplitude is varied with the wavelength  $\lambda$  to ensure a phase shift of  $\lambda/4$ .  
 s sample placed inside an electro-magnet (4"-magnet, Varian)  
 Sh magnetic shielding  
 PM-1,2 photomultipliers (EMI D-224). PM-1 detects the circular dichroism  $\Delta OD$ , PM-2 the optical density OD of the sample (see text).  
 HV High voltage supply for PM-1 and PM-2.  
 A light attenuator

The logarithm of this signal yields the optical density of the sample, since it appears that  $qa/(1-q)$  is sufficiently independent of wavelength.

## 2. CPL-spectrometer

The sample, which contains a collection of chiral molecules, is irradiated by (unpolarized) excitation light. As a result a stationary concentration of excited chiral molecules is built up. In emission the amounts of left and right

circularly polarized photons are different. Their difference divided by their mean is equal to  $g_{lum}$  (cf Chapter V).

$$g_{lum} = \frac{I_L - I_R}{\frac{1}{2}(I_L + I_R)}$$

The circular polarization of the luminescence,  $I_L - I_R$ , is modulated at a frequency of 50 kHz and detected as AC-photocurrent, the unpolarized luminescence  $\frac{1}{2}(I_L + I_R)$  is measured as DC-current.

Depending on the intensity of the emission available, our spectrometer may detect  $g_{lum}$ -values of  $10^{-3} - 10^{-4}$ .

The circular polarizer (P,  $\frac{\lambda}{4}$ ) in the excitation channel is not needed in normal CPL measurements. It is used when the optical activity of a racemic mixture has to be determined.

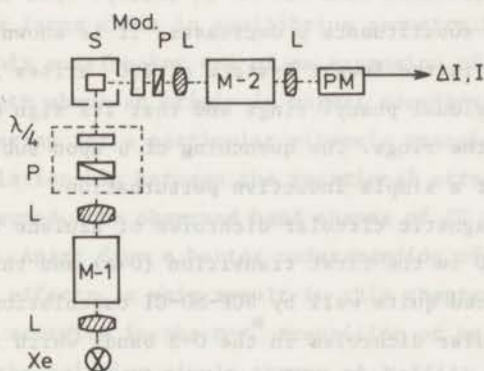


Figure 2. Optical scheme of the CPL-spectrometer.

- |             |  |
|-------------|--|
| Xe          | Xenon-arc (XBO 900 Watt, Osram)  |
| L           | lenses   |
| M-1 and M-2 | excitation and emission monochromators ("high intensity monochromator", Bausch and Lomb) |
| p           | linear polarizer (Glan, calcite)   |
| $\lambda/4$ | quarter-wave plate (quartz or mica)  |
| s           | sample   |
| Mod         | photo-elastic modulator (Morvue)   |
|             | The linear polarizer p after the modulator is a sheet polarizer (Polacoat)               |
| PM          | photomultiplier (EMI 6256Q, 9558 QB)   |

## SUMMARY

The experiments which form the basis of this thesis pertain firstly to the determination of the magnetic circular dichroism of some rather divergent organic molecules and secondly to the measurement of the optical activities in absorption and fluorescence of a series of ketones.

1. After a discussion on some characteristic features of MCD spectroscopy (Chapter I), the MCD spectra of the triphenylcarbenium ion and some of its symmetrically para-substituted analogues are reported in Chapter II. Along with polarization measurements the MCD spectrum indicates that in solution the triphenylcarbenium ion has  $D_3$  symmetry. The magnetic moment  $\mu$  in the lowest excited singlet state of  $\phi_3C^+$ , which is of E-symmetry, is large and positive. Its sign is opposite to that in other aromatic systems of high symmetry and at variance with predictions from SCF-MO-CI theory. Upon the introduction of three identical para-substituents  $\mu$  decreases. It is shown in Chapter II that the large value of  $\mu$  in the lowest E-state of  $\phi_3C^+$  arises from the high local symmetry of the individual phenyl rings and that its sign obtains from the interaction between the rings. The quenching of  $\mu$  upon substitution is described in terms of a simple inductive perturbation.

In Chapter III the magnetic circular dichroism of azulene is discussed. It is shown that the MCD in the first transition (O $\rightarrow$ A) and third transition (O $\rightarrow$ C) can be reproduced quite well by SCF-MO-CI calculations. From an analysis of the magnetic circular dichroism in the O $\rightarrow$ B band, which in contrast to that of the other bands has a very peculiar shape, it is demonstrated that the amount of Franck-Condon intensity in this transition is only 20% of the total intensity: 80% of the absorption is induced by vibronic coupling via totally symmetric modes. In addition, this analysis yields the detailed distribution of allowed and forbidden intensity throughout the entire O $\rightarrow$ B absorption system. The relevance of these data - which cannot be obtained that easily by means of other techniques - to some earlier explanations of the O $\rightarrow$ B transition, is discussed.

Chapter IV deals with singlet-triplet transitions. It is shown that in molecules which lack orbitally degenerate states, singlet-triplet transitions often can be recognized as such from the characteristic shape of their MCD. The magnitude of this MCD appears to be a sensitive measure for small spin-orbit couplings next to large ones. In two thioketones the observed MCD allows the assignment of a weak absorption band in the spectrum to a singlet-

triplet transition.

2. In Chapter V the optical activity in absorption and emission of a series of ketones is studied. For a number of ketones the comparison of the observed CD and CPL spectra reveals marked differences between the two: both the magnitude of the integrated optical activity and the band shape differ drastically in absorption and emission. In Chapter V a relation is laid between these phenomena. The often large discrepancy between the values of the rotational strength in absorption and fluorescence (for some compounds up to sign) points to a large distortion in the  $^1n\pi^*$  state of ketones as compared with the ground state. On the other hand it is shown from general principles that opposite rotational strengths in absorption and emission require a change of sign in either the CD or the CPL curve, i.e. can cause a bisignate Cotton effect. To get a better insight in the observed phenomena a model is constructed to predict the qualitative band forms of the CD and CPL. Based on the large shift in equilibrium geometry between ground and excited state, this model makes use of an expansion of the electronic rotational strength about an origin in normal coordinate space where the Franck-Condon overlap for a particular vibronic transition is peaked. When a linear relationship between the rotational strength and one normal coordinate is assumed, the observed band shapes of CD and CPL of our ketones can be explained. Apart from a better understanding of the origins of bisignate Cotton effects, a main result in this chapter is the conclusion that the optical activity in the  $n\pi^*$  transition of ketones still can be understood with the relative simple theory of Moffitt and Moscovitz, provided proper allowance is made for a legitimate role of the excited state. The latter conclusion may add considerably to the value of optical activity data as a source for structural information.

De experimenten die aan dit proefschrift ten grondslag liggen hebben betrekking op 1. de meting van het magnetisch circulair dichroïsme van een aantal uiteenlopende organische moleculen en 2. op de bepaling van de optische activiteit van een reeks ketonen in absorptie en emissie.

1. Na een discussie van enkele karakteristieke aspecten van de MCD spectroscopie (Hoofdstuk I), worden in Hoofdstuk II de MCD spectra van het trifenylcarbenium ion en enkele van zijn symmetrisch para-gesubstitueerde derivaten besproken. Tezamen met lineaire polarisatie metingen wijst het MCD spectrum van het trifenylcarbenium ion erop, dat dit ion ook in oplossing  $D_3$  symmetrie heeft. In zijn laagste aangeslagen singulet toestand - die E-symmetrie heeft - is de waarde van het magnetische moment  $\mu$  groot en positief. Het teken van  $\mu$  verschilt van dat in andere aromatische systemen met hoge symmetrie en contrasteert met resultaten van berekeningen van het SCF-MO-CI type. Bij het invoeren van drie gelijke para-substituenten daalt de waarde van het magnetische moment. In Hoofdstuk II wordt aangetoond dat de hoge waarde van  $\mu$  in de laagste aangeslagen singulet toestand van  $\Phi_3C^+$  een gevolg is van de hoge locale symmetrie van de afzonderlijke fenylingen, maar dat het teken van het magnetische moment bepaald wordt door de wisselwerking tussen de ringen. Dat bij substitutie de waarde van  $\mu$  afneemt, kan verklaard worden door de substituenten als eenvoudige inductieve storingen op te vatten.

In Hoofdstuk III wordt het MCD spectrum van azuleen besproken. Het blijkt dat het magnetisch circulair dichroïsme in de eerste en de derde absorptie band O+A resp. O+C goed beschreven kan worden met SCF-MO-CI berekeningen. In tegenstelling tot de O+A en O+C band heeft het MCD van de tweede overgang O+B een zeer eigenaardige vorm. Uit een analyse ervan blijkt, dat de hoeveelheid Franck-Condon intensiteit in deze band slechts 20% van het totaal bedraagt: 80% van de absorptie wordt teweeggebracht door vibronische koppeling via totaal-symmetrische vibraties. Verder wordt uit deze analyse de gedetailleerde verdeling van toegestane en verboden intensiteit over de gehele absorptieband gevonden. Het laatste gedeelte van dit hoofdstuk is gewijd aan een bespreking van de gevolgen van de verkregen resultaten voor vroeger gegeven verklaringen van de O+B band.

Hoofdstuk IV handelt over singulet-triplet overgangen. Er wordt aangetoond dat, in moleculen zonder baan-ontaarding, singulet-triplet overgangen vaak als zodanig herkend kunnen worden dank zij de karakteristieke vorm van hun



## CURRICULUM VITAE

Na het behalen van het eindexamen HBS B aan de toenmalige Sint-Paulus-HBS te Tilburg begon ik in september 1958 mijn studie aan de Rijksuniversiteit te Leiden. Het kandidaatsexamen in de chemie (letter f) werd in juli 1962 afgelegd. De studie werd voortgezet op de Afdeling Theoretisch Organische Chemie van wijlen Prof. dr. L.J. Oosterhoff. Onder leiding van dr. H.M. Buck werkte ik hier mee aan een onderzoek over reacties in sterk zure media. In mei 1966 werd het doctoraalexamen afgelegd in de theoretisch organische scheikunde met de bijvakken theoretische natuurkunde en wiskunde. Daarna begon ik onder leiding van Prof. dr. L.J. Oosterhoff aan onderzoekingen over natuurlijke en magneto-optische activiteit.

Sinds 1964 ben ik verbonden aan de afdeling theoretisch organische chemie, aanvankelijk als assistent en sinds 1968 als wetenschappelijk medewerker. In 1972 volgde de benoeming tot wetenschappelijk medewerker 1e klas. Van 1961 tot 1973 ben ik voor een beperkt aantal uren als leraar werkzaam geweest aan achtereenvolgens het Sint-Pauluslyceum te Tilburg, de R.K. Avondopleiding N.O. Akten te Tilburg en het Fioreticollege te Lisse.



Ik stel er prijs op mijn erkentelijkheid te betuigen aan Professor J.H. van der Waals, die na het overlijden van Professor L.J. Oosterhoff bereid was als promotor op te treden.

De verhelderende en stimulerende gesprekken met de andere leden van de Afdeling Theoretisch Organische Chemie en de vaak daadwerkelijke hulp van vooral drs. E.J.J. Groenen, dr. W.J. van der Hart en drs. A.H. Huizer zijn voor mij een belangrijke steun geweest. Verscheidene studenten leverden door hun enthousiaste medewerking een belangrijke bijdrage tot het onderzoek.

Goede herinneringen blijf ik bewaren aan discussies over optische activiteit met dr. C.A. Emeis en dr. H.J.C. Jacobs. Mevr. drs. E.C.M. Kielman- van Luijt heeft mij op effectieve wijze geholpen bij het gereed maken van het manuscript voor dit proefschrift.

De Technische en Administratieve Staf van de Gorlaeus Laboratoria ben ik erkentelijk voor hun bijdrage tot het onderzoek. In het bijzonder denk ik hierbij aan de medewerkers van de Instrumentmakerij (onder de leiding van de Heer W.C. Bauer), van de Electronische Afdeling (onder de leiding van de Heer J.D. van Gelder) en van de Glasinstrumentmakerij (onder de leiding van de Heer C.J. van der Poel). De Heren M. Pison, J.J. Pot en A.G. Huygen verzorgden de tekeningen in dit proefschrift.

CURRICULUM VITAE

De wetenschappelijke carrière van de heer J. H. van der Meer begon in 1925 met zijn aanstelling als assistent van de heer J. H. van der Meer aan de Universiteit van Amsterdam. Hij werd in 1930 benoemd tot eerste assistent van de heer J. H. van der Meer en in 1935 tot tweede assistent van de heer J. H. van der Meer. In 1940 werd hij benoemd tot eerste assistent van de heer J. H. van der Meer en in 1945 tot tweede assistent van de heer J. H. van der Meer. In 1950 werd hij benoemd tot eerste assistent van de heer J. H. van der Meer en in 1955 tot tweede assistent van de heer J. H. van der Meer. In 1960 werd hij benoemd tot eerste assistent van de heer J. H. van der Meer en in 1965 tot tweede assistent van de heer J. H. van der Meer. In 1970 werd hij benoemd tot eerste assistent van de heer J. H. van der Meer en in 1975 tot tweede assistent van de heer J. H. van der Meer. In 1980 werd hij benoemd tot eerste assistent van de heer J. H. van der Meer en in 1985 tot tweede assistent van de heer J. H. van der Meer. In 1990 werd hij benoemd tot eerste assistent van de heer J. H. van der Meer en in 1995 tot tweede assistent van de heer J. H. van der Meer. In 2000 werd hij benoemd tot eerste assistent van de heer J. H. van der Meer en in 2005 tot tweede assistent van de heer J. H. van der Meer. In 2010 werd hij benoemd tot eerste assistent van de heer J. H. van der Meer en in 2015 tot tweede assistent van de heer J. H. van der Meer. In 2020 werd hij benoemd tot eerste assistent van de heer J. H. van der Meer en in 2025 tot tweede assistent van de heer J. H. van der Meer.

